PROCESS-PROPERTY RELATION OF PREPREG TRIM WASTE COMPOSITES VIA SHEET MOLDING COMPOUND (SMC)

A Dissertation
Presented to
The Academic Faculty

by

Sanzida Sultana

In Partial Fulfillment
of the Requirements for the Degree
Doctor of Philosophy in the
GEORGE W. WOODRUFF SCHOOL OF MECHANICAL ENGINEERING

Georgia Institute of Technology
MAY 2019

PROCESS-PROPERTY RELATION OF PREPREG TRIM WASTE COMPOSITES VIA SHEET MOLDING COMPOUND (SMC)

Approved by:

Dr. Kyriaki Kalaitzidou, Advisor
School of Mechanical Engineering
Georgia Institute of Technology

Dr. Jonathan S. Colton, Co-advisor
School of Mechanical Engineering
Georgia Institute of Technology

Dr. Suresh Sitaraman
School of Mechanical Engineering
Georgia Institute of Technology

Dr. Ben Wang
School of Material Science and Engineering
Georgia Institute of Technology

Dr. Satish Kumar
School of Material Science and Engineering
Georgia Institute of Technology

Date Approved: December 11, 2018

ACKNOWLEDGEMENTS

I would like to express my utmost gratefulness to my advisor Dr. Kyriaki Kalaitzidou for her guidance, support, and encouragement throughout my thesis. I sincerely appreciate her thought-provoking direction in every step of my graduate study at Georgia Tech. Her patience and perseverance to achieve a goal will always enlighten me in my career. I am very fortunate to have Dr. Jonathan Colton as my Co-advisor who is truly a problem solver. It has been a privilege to work with him as a team. I want to present my sincere gratitude to him for being accessible for help at any time, and his continuous support during my thesis preparation.

I would like to thank my other committee members, Dr. Suresh Sitaraman, Dr. Satish Kumar and Dr. Ben Wang for serving as my committee members and for providing me with insightful comments during my PhD proposal presentation. Their questions and suggestions have been very helpful to improve the experiments and analyses performed to complete this dissertation.

I also would like to thank Ms. Glenda Johnson and Ms. Ann Lamb for all their support during my stay at Georgia Tech. My sincere gratitude goes to all my former and present lab mates for their support to complete my research in a timely manner. I am also very grateful to my former roommates and student community of Bangladesh at GT for their support and friendship to make my journey an enjoyable one.

I acknowledge the financial support from the Boeing Company to accomplish this work. The support with the post-industrial prepregs is greatly appreciated. I sincerely thank Mr. Pete E. George, Material Engineer at Boeing Engineering and Operations

Technologies, for his comments and suggestions in our weekly meetings, which helped me to solve real life problems. I would also like to thank Dr. Asegun Henry for giving me the opportunity to work with him on the fabrication of high thermal conductivity polymer composites supported by Intel Corp. in the first two years of my PhD studies at Georgia Tech.

Most importantly, I thank Almighty for blessing me with a strong support system of my parents, siblings, nephews and nieces. Lastly, I owe a special thanks to my husband for his persistent support. It would not be possible to make it here without the sacrifices you all have made.

TABLE OF CONTENTS

LIST OF TABLES

LIST OF FIGURES

LIST OF SYMBOLS AND ABBREVIATIONS

ANOVA	Analysis of variance
AR	Aspect ratio
ASTM	American Society for Testing Materials
CAFE	Corporate average fuel economy
CF	Carbon fiber
CFRP	Carbon fiber reinforced polymer
CMC	Ceramic matrix composites
COV	Coefficient of variation
DMA	Dynamic mechanical analysis
DOC	Degree of cure
DSC	Differential scanning calorimetry
EOL	End of life
FEA	Finite element analysis
GF	Glass fiber
HVAC	Heating, ventilation, and air conditioning
ISO	International Organization for Standardization

MDS	Material data sheet
MMC	Metal matrix composites
MRA	Mold release agent
PMC	Polymer matrix composites
PU	Polyurethane
RT	Room temperature
RVE	Representative volume element
SEM	Scanning electron microscopy
SMC	Sheet molding compound
TT	Thermal transition
TGA	Thermogravimetric analysis
UD	Unidirectional
UD_L	In a unidirectional layup testing along the fiber direction
UD_T	In a unidirectional layup testing in the perpendicular to the fiber direction

SUMMARY

Carbon fiber reinforced polymers (CFRP) are used in aerospace industries due to their high strength to weight ratio and increased fuel efficiency. Thus, the increasing demand results in the production of large amount of CF prepreg scrap and CF composites. Both the scrap and the composites at the end of their life are currently disposed in landfills. Disposal of the scrap prepreg is hazardous to the environment, which also incurs cost for landfilling. Recently, automotive industries have shown interest in the use of recycled materials for the manufacture of vehicles. The focus of this research is recycling the post-industrial prepreg waste to produce light weight polymer composites suitable for automotive industries and to understand their process-property relationships. The progression of the research was performed in three stages including employing sheet molding compound (SMC) technique for recycling the prepreg, aging condition assessment of the incoming prepreg waste and mechanical performance analysis of the CF prepreg composite. The SMC technique was used to chop the prepreg tapes and to form a sheet in the SMC line. The standard SMC line was engineered to process the CF prepregs by developing prepreg spool holding system, guiding systems for prepreg tapes, spool-core to shaft friction reduction system, and by introducing the venturi equipment for removing backup film of tapes. Since cutting and SMC preparation of the prepreg wastes depend on their thermal history, a systematic assessment of their aging condition was performed using differential scanning calorimetry (DSC). The DSC analysis revealed that aging advances the cure of the resin in prepregs resulting in non-tacky prepregs which can be cut completely in the SMC line. The non-tacky aged prepregs can be obtained either by oven

aging or room temperature aging. The cure kinetic parameters such as thermal transitions, degree of cure, activation energy etc. were studied to investigate the thermal history of the prepregs. To study the mechanical performance of the recycled prepregs, composites with minimum void contents were fabricated from the tacky and the non-tacky prepregs using compression molding. The mechanical properties of the composites, including tensile modulus, tensile strength and impact strength were determined according to the ASTM standards as a function of the composite's fabrication conditions. The following values were found for the average tensile strength (150 MPa), tensile modulus (40 GPa) and impact strength (144 KJ/m^2) of the fresh (minimum out time) prepreg composites. The composites from the aged prepreg also showed comparable properties to that of the fresh (minimum out time) prepreg composites. A micromechanical model for randomly oriented discontinuous fiber composite system was used to calculate theoretical modulus of the CF prepreg composite. The calculated modulus was 69 GPa. In addition to the manufacturing defects such as voids and resin rich and fiber curled area in the composite, the assumption of discontinuous fibers used for the model, which is different from our discontinuous prepreg chips, might also contribute to the modulus discrepancy. The recycled CF prepreg composites are 18% lighter, and are two times higher in tensile modulus and tensile strength compared to the commercial glass fiber SMC composites which are currently used in automotive industries. Furthermore, failure analysis indicated that the recycled composites retained its integrity upon failure under tensile loading. Thus, this thesis suggests that the post-industrial prepreg composites processed by SMC technique is a promising lightweight material for applications in automotive industries.

CHAPTER 1

INTRODUCTION

Carbon fiber (CF) reinforced polymers (CFRP) are used in aerospace industries for their high strength to weight ratios and increased fuel efficiency. According to a study conducted in 2012, it was predicted that the demand of carbon fibers would be double within the period of 2012 to 2020 [1]. About 50 percent by weight of the total structure of a Boeing 787 is manufactured from CFRP [2]. The current market outlook (2014–2033) of Boeing indicates that there will be addition of 27 to 34k new planes in the world aircraft fleet by 2030. This will increase the volume of scrap prepreg as well as of CF composites. Both the scrap and the composites at the end of their life are currently disposed of in a landfill. The scrap prepreg is toxic to the environment because chemicals leach from the uncured resin into the soil and ground water. Moreover, landfilling is restricted by legislation. The disposal incurs $1.5 to $6 per kg of prepreg waste, which will further increase due to stricter regulations in the future [3]. Additionally, the prepreg contains high value resin and carbon fibers. It is high time to adopt a recycling approach to utilize CFRP. Recently, automotive industries are exploring the use of recycled material for the manufacture of vehicles. Automotive industries demonstrated that replacing steel parts with CFRP can significantly reduce the weight of the vehicles. For example, fenders and roof panels made of CFRP in Corvette Z06 and BMW M6, can save up to a 6 kg of weight [4, 5]. So, in this study, a low-cost manufacturing method will be introduced to reuse CFRP as a solution for both aerospace and automotive industries.

In this chapter the background and motivation of the thesis will be discussed. First, a summary of the life of carbon fiber prepreg from precursor to its end of life will be presented. In the next section, existing light weighting technologies in automotive and other industries will be discussed. This will lead to the next section that presents and justifies glass fiber (GF)/epoxy composites as candidates for lightweight applications. Then, an overview of the sheet molding compound (SMC) technique will be provided. SMC is the third most globally used method for producing polymer composites parts. As a result, the motivation for the CF-SMC as a candidate for replacing metal and GF-SMC in light-weighting application will be clear. Thus, the fabrication of CF-SMC from out-of-spec, aerospace prepreg emerges as an alternative to landfilling with its issues of cost and environmental damage. Finally, the goal and objectives of the thesis will be described.

1.1 Carbon fibers

1.1.1 Manufacturing techniques and properties of carbon fibers

Carbon fibers have gained popularity in industries for their high strength to weight ratios. Petroleum based precursors polyacrylonitrile (PAN) and pitches are used for manufacturing carbon fibers [6]. For PAN based carbon fibers, filaments are wet spun from a PAN based solution and stretched. Then, these are held at elevated temperature in air. The PAN filaments are heated and stretched at 1000-2000^{o}C in an inert atmosphere for 30 minutes [6] . This process is called carbonization and produces low modulus, high strength carbon fibers. The carbonized fibers are then graphitized by heating above 2000^{o}C with or without stretching. Relatively high modulus carbon fibers are obtained via stretching; stretching also provides improved strength. For pitch-based carbon fibers, filaments are melt-spun from mesophase pitch and stretched, followed by heat treatment at 200-300^{o}C

in an oxygenated atmosphere. Pitch filaments are then carbonized and graphitized in a similar procedure as explained for PAN filaments to yield carbon fibers. Carbonization transforms the PAN molecules into an aromatic ring pattern, whereas the pitch molecules have inherent aromatic structures. Graphitization helps the molecular structure to become more ordered and graphitic.

Rayon based carbon fiber has been also studied [7]. However, the carbon yield for rayon is 30% while it is 50% for PAN. Other precursors are heterocyclic heat-resistant organic polymers, such as polyimides [8-10], polybenzimidazole [8, 11], poly-benzimidazonium salt [12]. These precursors have provided high modulus carbon fibers with carbon yields of 90%. However, these approaches are reported to be expensive. Several thermoplastic polymers such as polyethylene, polypropylene [12], polyvinyl chloride [13, 14] have also been investigated as precursors of carbon fibers but the resulting carbon fibers exhibited poor mechanical performance.

Recently, a research team in Oak Ridge National Laboratory manufactured carbon fibers from cheap textile grade acrylic fiber by replacing the PAN based precursor [15]. The textile grade acrylic fiber is half the price of PAN based precursor. This less expensive carbon fiber met the performance criteria of the automotive industries. The tensile strength, modulus, and strain to failure of the fiber surpassed the values required by automotive manufacturer [16]. They have further improved the manufacturing process collaborating with Deaken University. The manufacturing cost has been reduced to half as the energy consumption is 60-80% lower while the process time is about 60 min less than the conventional PAN based one.

Pitch based carbon fibers have higher tensile modulus and lower tensile strength and strain to failure as compared to PAN fibers [6]. The high tensile modulus of pitch fibers results from higher graphitize-ability. However, shear is easier between parallel planes of graphitized fibers, which causes lower strength. PAN carbon fibers have higher compressive strengths than pitch fibers. The lower compressive strengths in pitch fibers result from higher orientation, higher graphitic order, and larger crystal size. However, this structure causes higher thermal and electrical conductivities.

1.1.2 Application of carbon fibers

The structural, thermal, and electrical properties of carbon fibers make them the most suitable reinforcement in composite materials [17]. The fibers are used in applications where strength, stiffness, light weight, and superior fatigue characteristics are necessary. Further applications include composites with high damping capacity, and with high thermal and chemical inertness [18]. Overall, there are two categories of industrial applications of carbon fibers [17, 19]. In aerospace industries, maximum performance and fuel efficiency are required where cost and mass production requirements are not that critical. However, performance is less critical in automotive industries and general engineering applications such as bearing, gears, fan blades, etc. where the low cost and high production rates are important.

Carbon fibers are available in different forms to meet the demand of industries such as long and continuous tows, which are bundles of 1000 to 160000 parallel filaments, chopped (6 to 50mm length), or milled (30 to 3000μm). Carbon fibers are also available in woven or interlaced in two or multi-dimensional architectures. Another form is prepreg

where continuous or woven fibers are pre-impregnated with a thin layer of resin. The major manufacturers of carbon fibers are Hexcel, Toray, SGL, Zoltek, Mistubishi and Toho Tenax. Global market share by each company is shown in Figure 1.1. It has been reported that the global demand of carbon fibers will be double with in the period of 2012 to 2020 for various industrial applications as shown in Figure 1.2 [1, 15].

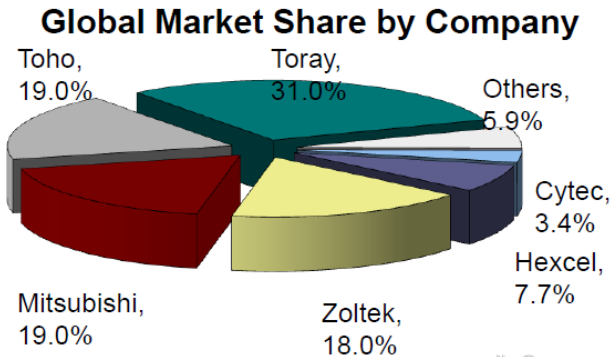

Figure 1.1: Global market share of carbon fiber manufacturer [15].

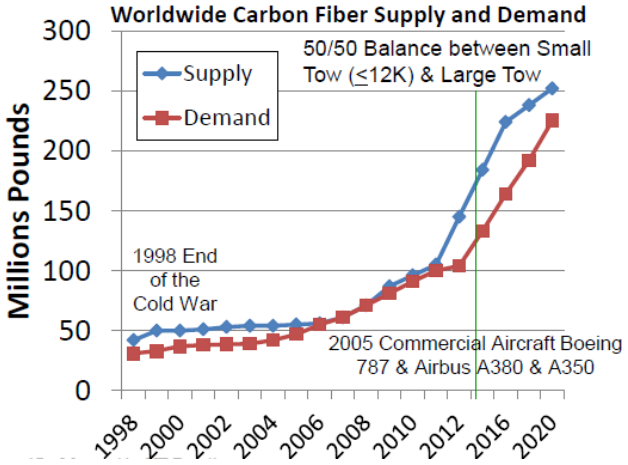

Figure 1.2 : Worldwide carbon fiber supply and demand [15].

As demand increases, it is critical to understand the life cycle of carbon fibers, and consequently, the techniques to reclaim them from the composite for recycling purposes.

The next section will discuss what happens at the end of life of and the recycling methods for carbon fibers.

1.1.3 End of life carbon fiber and recycling

Carbon fibers are expensive. It is noted that disposal at the End of Life (EOL) of composites is required. The amount of composites to be disposed is expected to increase with decommissioning of carbon fiber reinforced polymer (CFRP) based aircraft and automotive vehicles. Furthermore, a large amount of scrap prepregs are produced by aerospace industries. Landfilling is an option for waste management, but it has environmental impact due to the chemicals leaching out of the uncured prepregs into the soil and water. There have already been legislative limitations of landfilling in Europe. It is now time to find an industry-scale alternative solution to landfilling. Landfilling is required at two stages in the life of carbon fibers: first, scrap prepreg produced after cutting the prepreg rolls for making parts in industries; second, the composite at the end of life of aircraft or vehicles.

Both CF prepreg scrap and CF composites are high value materials in the sense that these can be recycled. Recycling composites can provide carbon fibers that are re-useable in secondary applications [1]. The scrap prepregs can be used as well. The cost of virgin carbon fibers is $33 to $66 per kg, while it is $13 to $19 per kg for recycled fibers [3].

There are several techniques available for recycling of post-industrial carbon fibers. The flowchart shown in Figure 1.3 summarizes the techniques of recycling carbon fibers. Many techniques have been studied that highlight the key parameters of environmental impact, efficiency, and commercial viability. Pyrolysis is one of the most developed

thermal processes suitable for carbon fiber reclamation as CF is less prone to temperature. Pyrolysis is performed in an atmosphere with oxygen and/or nitrogen and sometimes in steam [20]. A temperature of 500 to 600^{o}C removes the resin but leaves a char-like material on the fiber which prevents good bonding between fibers and matrix [21]. A post treatment at 1300^{o}C completely removes the char but simultaneously significantly reduces the tensile strength of the fibers [22]. Thus, the fiber properties are greatly influenced by the treatment conditions. Another issue is the wide distribution of properties in industry scale reclaimed fibers resulting from different feedstocks [23]. However, pyrolysis is suitable for EOL composites with painted surfaces, foam cores, metal inserts, etc. In addition to temperature, attrition of the resin might cause extra damage to the fiber [24]. Moreover, the recovery of valuable oil from resin is not possible via this technique. Microwave assisted pyrolysis performed under a nitrogen atmosphere is another technique where the heat transfer is very fast enabling energy saving [25]. The fluidized-bed process is another thermal process where a bed of silica sand is fluidized by hot air. Eltron Research and Development has developed a 'catalytic microwave assisted gasification' technique in lab scale which convert matrix to usable chemicals or fuels without degrading the strength and length of fiber at a lower temperature [26].

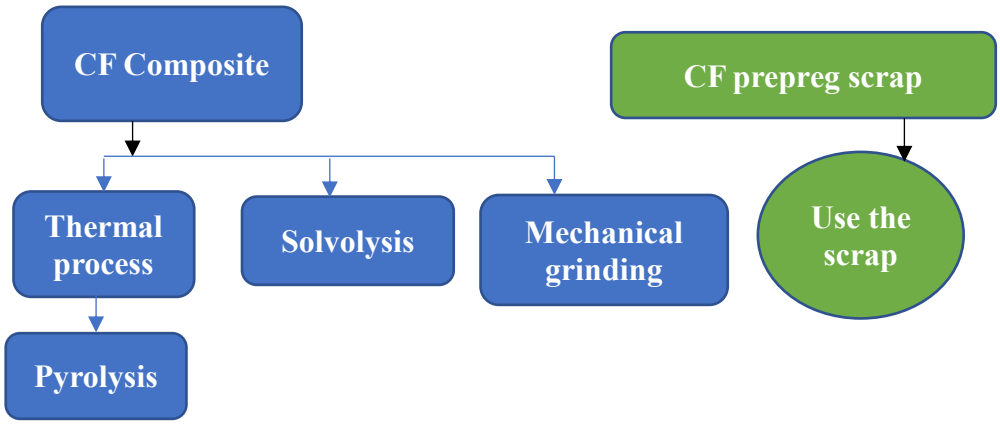

Figure 1.3: Flowchart of recycling techniques for carbon fiber.

While applying temperature helps in recycling used carbon fibers, solvent-based recycling is an alternative method to recover post-industrial carbon fibers. In solvolysis, a solvent is used to degrade the resin. Sometimes co-solvent (alcohols) and catalysts are used. This method requires lower operating temperature. For this technique, less energy is consumed as compared to pyrolysis. There is also a smaller possibility of char formation on the fibers, as the solvent breaks down the bonds in the resin. Thus, the resin's monomer can be obtained as a by-product. But sometimes, the catalysts, solvents, and chemical byproducts are not suitable for disposal. Water is the most commonly used solvent for its tunable properties with temperature and pressure. Efficient temperature and pressure level depend on the type of resin [27-29].

Other than the thermal and solvolysis methods, carbon fibers can also be recycled using mechanical processes. In mechanical recycling techniques, cured CFRP are crushed into small pieces before being grinded. These ground composites are used as fillers and

reinforcements. However, the filler content is limited to less than 10% because of increased viscosity of the compound [30]. Recently, an electro-dynamic fragmentation technique has been reported in which the composite is fragmented in water between two high voltage electrodes [31].

Along with developing various methods for carbon fiber composite recycling at the lab scale, commercialization of these recycling methods has also made some progress. For example, full scale commercial operations of recycling composites have been reported by Material Innovation Technologies, Adherent Technologies in the US, and ELG carbon fiber in the UK.

The above-mentioned methods have been developed for recycling EOL carbon fiber composites. However, there is limited study of the unused prepreg scraps left over from producing composites parts. Large volumes of scrap prepregs are produced by the aerospace and automotive industries. In most cases, the thermal histories of unused prepregs are not tracked before these are thrown away. Recently, scrap prepregs have drawn the attention of the research community which focuses on alternative approaches to landfilling. Moreover, the prepregs still are able to be utilized in suitable applications. There are two main sources of scrap: from ply cutting operations and out of specification materials. Scrap can be obtained in different forms: (a) unopened/ partially opened prepreg out of specification [32], (b) regular cutout forms - pieces large enough to produce regular shaped pieces to be used in vacuum bagging and hot pressing, and (c) loose chip forms - cutting leftover prepreg into rectangular shaped chips. The production of the latter can be automated in a two-stage cutting system. In the reused scrap roll form, loose chip scraps are formed into rolls under specific pressure and temperature. These rolls can be

sandwiched between out-of-spec rolls to improve the aesthetic appearance and can be used in applications with less critical properties at lower costs. Further, the high strength to weight ratio of carbon fiber is always an added benefit of light weighting, suitable for any application. In the next section, importance of light weighting in automotive application and possible techniques for light weighting will be discussed.

1.2 Light weighting in automotive applications

1.2.1 Importance of light weighting

Fuel economy and emission control are the key impetus for light weighting of automotive vehicles. According to US energy policy, the 2012 Corporate Average Fuel Economy (CAFE) standard suggests the average fuel economy of cars and light trucks should increase to 54.4 miles/gallon by 2025; it was 28.5 miles/gallon in 2012 [33]. Many other countries, including Japan and European Union, are also adopting similar policies to improve the fuel economy of automotive vehicles [34]. It may be noted that a 6-8% increase in fuel efficiency is possible by a 10% reduction in vehicle weight [35]. Lighter weight cars result in reduced rolling resistance and are more energy efficient to control speed or acceleration [4]. Moreover, a reduction in the weight of vehicles reduces the net production of greenhouse gases. A vehicle weight reduction of one hundred kg may save up to 12.5 gm of CO_2 emission per kilometer [36]. Furthermore, price of gasoline also motivates people to have light weight cars with better fuel efficiency [5]. Besides, it has been challenging for electric vehicles to travel longer distance without charging while hybrid cars need to have long lasting batteries. Thus, light weight automobiles are the solution to overcome these challenges with better performance.

In recent years, many high-performance cars have incorporated parts made of carbon fiber reinforced epoxy composites for light weighting. For example, the fender of a 2006 Corvette Z06 saves about 6 kg of weight [37], and the roof panel of a BMW M6 saves 5.5 kg replacing conventional steel [36]. In the next section, different approaches for light weighting will be discussed.

1.2.2 Different approaches for light-weighting

Manufacturers follow two main approaches to cope with the light weighting challenges. The first approach is designing to reduce the size and/or number of components and to incorporate efficient lighter structural parts [38]. As the body and chassis share 60% of the total weight of the vehicle, part consolidation may reduce the weight of the body and the chassis component. So, manufacturers have focused on light weighting of these parts [39].

The second approach is to replace heavier parts with lighter materials with higher strength to weight ratios. Recent light weight vehicles are manufactured from a hybrid of different materials such as high strength steel, aluminum, magnesium, titanium alloys and fiber reinforced composites. For example, the passenger chamber of the BMW i3, which is fixed to an aluminum chassis, is made of CFRP, while the roof panel is made of recycled CFRP [40]. Utilization of recycled fibers is reported to be more cost effective.

1.2.3 Materials for light-weighting

Steel has been popular in structural application for its mechanical properties, low cost, and manufacturability [36]. However, steel, which has a density of 7.87 g/cm^3, is

being replaced by other lighter metals such as titanium (4.43 g/cm^3), magnesium (1.74 g/cm^3), and aluminum (2.7 g/cm^3). Although many lighter materials are available for use in automotive and aerospace industries, the main hurdle to the use of these metals and alloys is the cost involved in the innovation of required new process and equipment [41].

Recently, composites have drawn a great deal of attention for their applications in automotive and aerospace industries to reduce the manufacturing cost as well as to make the vehicles lighter to be more energy efficient. In composite materials, the properties can be tailored, and functionality can be added by incorporating fibers and different nano-particles. For example, metal matrix composites (MMC), ceramic matrix composites (CMC), and polymer matrix composites (PMC) have applications in automotive, aerospace, and sports industries [6]. Glass or carbon fiber reinforced polymer (G/CFRP) are being used in automotive industries for the weight reduction replacing conventional materials [42]. In addition to weight reduction, GFRP produce less greenhouse gas according to life cycle assessments. GF/epoxy is one of the most popular GFRP for its mechanical performance, manufacturability, and low cost. For further understanding, GF/epoxy composites will be discussed in detail in the next section.

1.3 GF/epoxy composites

GF/epoxy composites are widely used in electronics, aviation and automotive industries due to the superior properties of epoxy resin and GF reinforcement. Glass fibers are low-cost and have high tensile strengths and moduli, chemical resistance and outstanding insulation properties [6]. On the other hand, many starting materials, compatible curing agents and modifiers are available for epoxy resins, which give the resin

systems a wide variety of properties. This type of resin also has high chemical and corrosion resistance, and low shrinkage on curing. Furthermore, the excellent mechanical performance of GF/epoxy composites is provided by the fiber strength, modulus and chemical stability, matrix strength and interfacial bond strength between the fiber and matrix to transfer the load [43]. To achieve the desired properties of the composites, manufacturing processes play crucial roles. In the next section, commonly used manufacturing techniques for GF/epoxy composites will be discussed.

1.3.1 Manufacturing techniques of GF/epoxy composites

Different forms of GF such as long continuous fiber, woven mat, chopped fiber and chopped mat are used to manufacture composites. To include GF as a reinforcement, the production of the resin-hardener mixture is the first step. Then, the resin mixture is poured on the fibers. Sometimes brushes and rollers are used to apply the resin on the fiber. The composite is cured under heat and pressure to achieve a certain degree of cure. It is also post cured before it is cooled. Woven mat GF reinforced epoxy composites are prepared using the hot-press technique [44]. Another method for composite fabrication is the hand layup method followed by pressing in a hydraulic press [45]. In both cases, the cure cycle varies from four hours to twenty-four hours with applied pressure in the range of 0.35 to 0.5 MPa.

The hot-press technique is also used to prepare unidirectional GF/epoxy laminates with a fiber content of 65 wt% [46]. Woven fabric GF/epoxy composites can also be prepared using a similar method [47]. Generally, a compression molding technique is used to prepare a discontinuous or chopped strand GF/epoxy composite where the fiber content can be varied between 10 to 60% [48, 49]. Sheet molding compound and compression

molding are also used to fabricate the discontinuous GF/epoxy composite [42]. Sometimes, fillers are added to the matrix to facilitate the resin to flow as well as to modify the interfacial strength between the fiber and the matrix.

1.3.2 Characteristics of GF/epoxy composites

Unidirectional continuous GF/ epoxy composites exhibit increases in tensile strength and Young's modulus with an increase in fiber content and decreases with increasing fiber diameter [50]. The tensile strength is strongly dependent on the fiber orientation with respect to the applied load direction [51]. It has been reported that the maximum tensile strength, compressive strength, and tensile modulus of a unidirectional GF/epoxy system, can be as high as 784 MPa, 186.22 MPa and 28.65 GPa respectively, even at -60^{o}C [52]. Another study showed that randomly oriented E-GF reinforced epoxy composites with 50% fiber content provided with a tensile strength of 249.6 MPa and a flexural strength of 368 MPa [53]. Further, the properties of the composites are modified by adding fillers to the composite. For example, the addition of pine bark dust increased the interlaminar shear strength and the addition of SiC improved the impact strength and hardness of the composites [53]. In a recent study, a randomly oriented short GF in epoxy composite containing 65 wt.% fiber showed tensile strength, flexural strength, modulus and impact energy of 250 MPa, 340 MPa, 18 GPa and 200 KJ/m^2, respectively [54]. This composite had a density of 1.85 g/cc^3 and void content of 7 vol.%.

The characteristics of composite materials vary with fiber architecture and laminate structure under impact loading. For example, the impact strength for woven mat type GF/epoxy composite increases with decreasing the weaving angle between the interweaved yarns [44]. The best impact property is obtained in Z-directional stitched GF fabrics among

different fabrics including plain weave, biaxial non-crimp and uniaxial stitched [55]. In the case of unidirectional GF/epoxy systems, impact loading causes a smaller delamination for isotropic stacking sequence such as [0/90/+45/-45]. However, isotropic laminates show temperature effects beyond 20 J of applied impact energy within the temperature range of 20 to -60^{o}C [56]. For discontinuous GF/epoxy composites, the impact strength decreases with the increase in aspect ratio [48].

While the properties of GF/epoxy composite depend on the fiber orientation, the aging conditions also play significant roles on their final properties. For example, the aging conditions of a composite can determine its mechanical performance. The effect of aging on GF/epoxy composites has been observed under different aging media. The effect of water immersion is less significant compared to that of alkali or acid soaking. However, all of these aging conditions deteriorate the mechanical performance depending on the duration and intensity [57]. Water absorption causing weight gain has been reported in a separate study. It shows 0.23 wt.% and 0.29 wt.% weight gain of E-GF/epoxy composite tube by immersion for four months at 20^{o}C and 50^{o}C respectively [58].

1.3.3 Advantages of GF/epoxy composites

GF/epoxy composites are replacing metal and non-metal parts in various applications [59]. The stiffness of the composite is higher than that of aluminum and its weight is four times lighter than steel. Moreover, in GF/epoxy composites, fiber architecture, orientation and fiber content provide the ability to tailor its properties [60]. Another advantage of this composite system is low tooling cost. Furthermore, GF/epoxy structure can even tolerate wind and seismic loads [61]. In addition, it has high thermal stability as well as resistance to cryogenic conditions. Short fiber reinforced composites

are suitable for manufacturing complex shapes along with high wear resistance [62]. Hence, the above-mentioned prominent properties of GF/epoxy composites indicate clearly that these composite materials are suitable for aerospace, automotive, sporting, defense, medical industries and beyond. Light-weighting can be obtained with outstanding mechanical properties at a low cost. One of the most popular manufacturing methods for polymer composites is the Sheet Molding Compounds (SMC) technique [63], which is discussed in the next section.

1.4 Overview of SMC technique

Sheet molding compounds (SMC) are sheets of short and continuous fibers impregnated with thermoset or thermoplastic resin. Typically, a compression molding technique is used to convert the SMC into finished composite parts [6]. Commercially available SMC types include SMC-R, SMC-CR, and XMC, as shown in Figure 1.4. As the names suggest SMC-R contains randomly oriented discontinuous fibers, SMC-CR contains a layer of continuous fibers on top of a layer of randomly oriented discontinuous fibers, and XMC contains continuous fibers arranged in an X pattern. XMC may also contain randomly oriented discontinuous fibers. SMC was first introduced by Charles Fisk in 1950 [63]. Further research was conducted to refine the resin paste formulation, to adapt compound machinery, to enhance the properties of the interfaces between the fibrous reinforcement and the paste, to avoid geometrical defects, and to improve the size formulation. Large scale SMC in automotive industry was first employed in 1980. Recent studies have been conducted on SMC mold flow and rheology, physicochemical, thermo-mechanical, optical, technological, environmental, and safety properties of SMC.

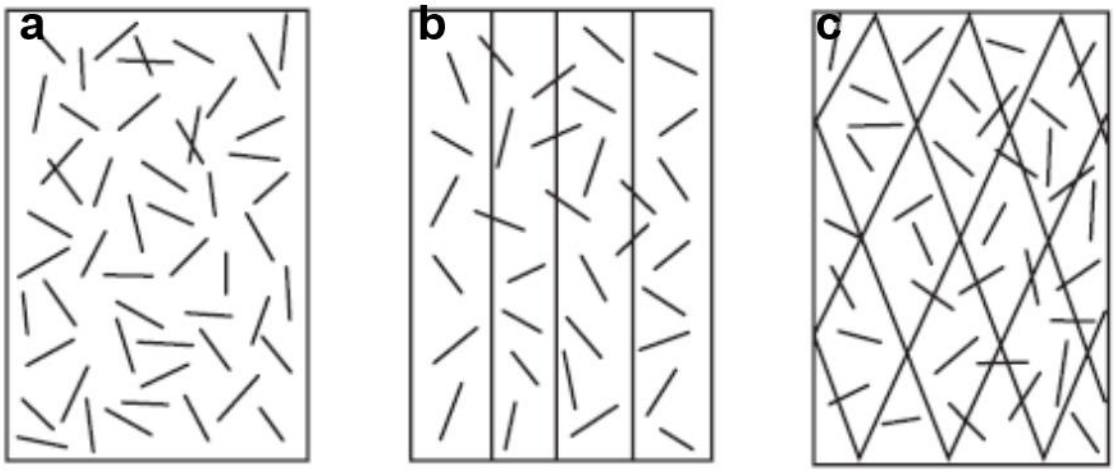

Figure 1.4: Various types of sheet molding compound, a. SMC-R, b. SMC-CR, c. XMC [6].

1.4.1 Materials and processing of SMC

Different types of fibers are used as reinforcement in SMC [63]. The typical fiber length is 25 to 50mm. The most commonly used is the glass fiber strand which consists of multiple filaments. CF are also used in applications with superior property requirements. Other fibers that have been used in making SMC include natural fibers, aramid fibers [36], and basalt fibers [54]. The fiber weight fraction ranges from 25% to 65% [64]. However, higher fiber content makes it harder to wet all the fibers with resin. The fiber content determines the processability, performance and cost of the composite. Higher fiber content generally results in higher mechanical performance in terms of strength and modulus and enhanced density. However, it increases the overall cost of the material and the density of the resulting composite.

The most common matrices for SMC composites are thermoset resins such as polyester, vinyl ester, and epoxy [63]. Thermoset resins generally have lower viscosities than thermoplastic resins. A lower viscosity helps to increase fiber wetting and the ease of removal of trapped air during the compaction stage of SMC preparation. Polyester and vinyl ester resins are also used due to their low cost and shorter cure cycle [36]. However, moisture resistance and higher mechanical performance make epoxy suitable for high performance applications such as aerospace industries [65].

To further modify the properties, other additives such as filler, initiator, inhibitor, thickener, releasing agent are added to the resin [63]. The addition of filler sometimes enhances the viscosity of the resin. Moreover, the resin paste viscosity is increased as the curing reaction proceeds with time, which makes the paste a putty like material. This allows the SMC sheet to be handled easily with good flow of resin and fiber during compression molding.

The SMC composite preparation has two major steps: making the SMC and then compression molding the part. Initially, chopped fibers and resin are introduced as per the desired composition of the composite. The fibers are sandwiched between two layers of resin, which are supported by backing plastic films. The fibers are wetted by the resin as the whole sandwich structure passes through the compaction zone, which consists of a series of rollers. Then, the sheet is collected in rolls that are kept in a controlled environment. Once the SMC sheet becomes viscous enough and similar to putty, it is cut into sheets, the backing films are peeled off and the sheets are stacked up in a mold to be compression molded under pressure and heat. A detailed discussion of the SMC process will be presented in section 2.2.

1.4.2 Opportunities and challenges of SMC

Continuous thickening of the paste results in variation of the rheological properties, which impact the curing reaction. Proper control is required during mold cooling to avoid dimensional distortion. Parts fabricated from SMC are coated with thermoplastic to improve surface finish [63]. The near net shape type of manufacturing process makes SMC popular in automotive, aerospace and entertainment industries.

The key advantages of SMC are high mechanical performance, inherent design flexibility, and improved damage resistance [42]. Further, SMC is cost effective as it is not labor intensive and produces little scrap. Moreover, SMC formulation can be adjusted and tailored based on the necessary functionality of the composite [63]. Another prominent advantage of SMC is that compression molding of SMC allows the fabrication of complex and large shapes with a rapid cycle time, in which features such as ribs, inserts, bosses, attachments can be molded. Little mold preparation as well as good surface finishes are obtainable. Finally, the process can be automated. Thus, it is economically efficient.

1.4.3 Applications of SMC

Compression molding of SMC is one of the most popular techniques for polymer composite fabrication worldwide [63]. SMC has applications in various fields, such as the automotive industry. However, SMC is used in agricultural and marine industries, as well as for electrical applications.

GF SMC applications include low and medium voltage energy systems, fuses, switch gear, cabinet, junction boxes, encapsulation for wiring for its electrical insulation

properties. SMC is also used to fabricate parts for wind turbines and solar power systems, domestic appliances like heating, ventilation and HVAC systems for its light weight properties with higher mechanical performance and thermal stability. In the automotive industries, bumpers, fenders, trunk dividers, hood and door assemblies, desk lids, body panels, roof panels, spoilers, step assists, back panels, wheelhouses, firewalls, grillers, tailboards, cargo lids, stowage tubs, headlamp housings and supports are manufactured from both GF and CF SMC. The performance of CF SMC is in between conventional GF SMC and quasi-isotropic laminate structures. CF SMC have been used in aerospace industries for aircraft window frames, secondary structures, and interiors. It is also used in sporting and leisure goods. The aforementioned applications for both GF and CF SMC provide tremendous motivation to look deeper into the possibilities for CF prepreg scrap introducing SMC manufacturing method. In the next section existing CF-SMC systems will be discussed.

1.4.4 CF SMC composites

Considering that CF are stronger and lighter than glass fibers (GF), and that prepreg trim waste produced by aerospace industry can be available to the automotive industry at very low cost, replacing traditional GF SMC composites with ones made from CF prepreg trim waste will be a “win-win” solution for both the aerospace and automotive industries. CF composites, if affordable at large scale, can either replace standard GF SMC composites or metal structural parts used in automotive industry [35].

It has been reported that mechanical properties for SMC with carbon fibers are better than conventional GF SMC. Anisotropy has been reported for both CF-SMC and GF-SMC composite systems. Specially for CF-SMC, heterogeneity has been reported to

be an inherent material property for both Hexmc [62] and randomly oriented strand based thermoplastic prepreg composites [66]; these differ from GF-SMC because they are are meso-structures of chips. Their heterogeneity has been described in terms of the size of the chip (a chip is a rectangular piece of prepreg tapes) or strands rather than the constitutive fiber and matrix. Material inhomogeneity of the composites results in variability of their mechanical properties [62]. Feraboli et el. found that the chip aspect ratio influences strength but not modulus [67]. Similar behavior was observed for both thermoset and thermoplastic resin systems. Chen and Tucker showed that SMC has planar isotropy for a charge covering 100% of the mold surface prior to molding while there is planar anisotropy for 33% initial mold coverage [68].

Short CF reinforced polymer composites, which are in between aerospace grade and traditional SMC composites, are suitable for compression molding and were first introduced to the aerospace community by Halpin and Pagano [69-72]. Discontinuous systems have drawn the attention for their high performance that is suitable for primary and secondary applications in airframes [73, 74]. Hexmc and Lytex are the two most commonly used commercial short fiber composites systems prepared from unidirectional (UD) prepreg tapes. In a typical Hexmc, AS4/ Hexply 8552 UD prepreg tape, a chip dimension of 50 mm by 8 mm is used. Each layer is 2 mm thick. Hexmc is formulated with an internal release agent [75]. The performance is superior due to the high-performance resin and fiber constituents. It is costlier than UD prepreg from which it is prepared; but its lower manufacturing cost, higher rate of production, ability to be molded in complex shapes, and reduction in overall part acquisition cost make it acceptable in the aerospace industry. Labor cost is also reduced as individual ply layup is not required. It has been

reported that the specific tensile modulus of Hexmc is better than other typically used structural materials such as steel, aluminum, glass fiber SMC systems, etc. [75].

In this work, the SMC technique will be used as a scalable approach to recycle post-industrial CFRP prepreg thereby eliminating the need for landfilling. Further, the mechanical performance study will open doors for automotive and other applications. The next section will state the goal and objectives of the thesis.

1.5 Thesis Goal and Objectives

The goal of the research is to utilize the unique properties of fibers and resin in prepreg trim waste to produce light weight polymer composites as a solution to existing engineering problems and to understand the corresponding process-property relationships.

1.5.1 Objectives

To investigate the possibilities for utilizing prepreg trim waste as an alternative for light weighting SMC composites and as a solution for land filling of the scrap prepreg, three primary objectives are set. Each objective will be accomplished through specific tasks that outline the progression of the research. Figure 1.5 shows a flow diagram of the advancement of the research structured according to the goal and objectives.

Objective 1: Employ sheet molding compound (SMC) technique to utilize the post-industrial CF-epoxy prepreg trim waste

To utilize the CF-epoxy prepreg trim waste, it is necessary to choose a low-cost manufacturing method that already exists. Hence, the SMC technique is employed to produce randomly oriented short fiber composites suitable for fabrication from prepreg

tapes with random widths, which are available as post-industrial material. Thus, it becomes essential to modify existing SMC equipment to cut and make SMC sheet using prepreg trim waste, and to optimize the parameters of SMC setup and the process of composite manufacturing.

Objective 2: Develop techniques to assess the quality of the incoming post-industrial prepreg

To utilize the SMC technique for recycling the post-industrial prepreg wastes, these materials need to be studied thoroughly using thermal analysis characterization techniques. To accomplish this, the incoming prepreg will be categorized by Differential Scanning Calorimetry (DSC) to determine the effects of aging on the cure kinetics. To predict the thermal history of the prepreg tapes, the behavior of the heat of curing reaction, thermal transitions, degree of cure, and activation energy will be focused. In addition, a further study will be performed to cut the tapes with the SMC machine's cutting head at different prepreg aging conditions to determine the effect of aging on cutting.

Objective 3: Mechanical performance analysis of post-industrial prepreg SMC composites

After characterizing the quality of the prepreg obtained from industry, it is necessary to fabricate and investigate the mechanical performance of the prepreg SMC composites test articles. The mechanical performance analysis will be discussed in Chapter 4. Tensile testing, impact testing, and void content measurement will be performed to investigate the performance of the composites. The mechanical properties of the composite materials fabricated from fresh and aged prepregs will be compared to conventional GF/epoxy SMC composites. Finally, the effects of aspect ratio, anisotropy and aging on

the mechanical performance of the resulting composites will be studied to identify process-property relationships.

Objectives 1, 2 and 3 and the corresponding tasks to achieve the research goal will be described in Chapter 2,3 and 4, respectively. Finally, in Chapter 5 conclusions based on the findings of this thesis and research directions for future will be presented.

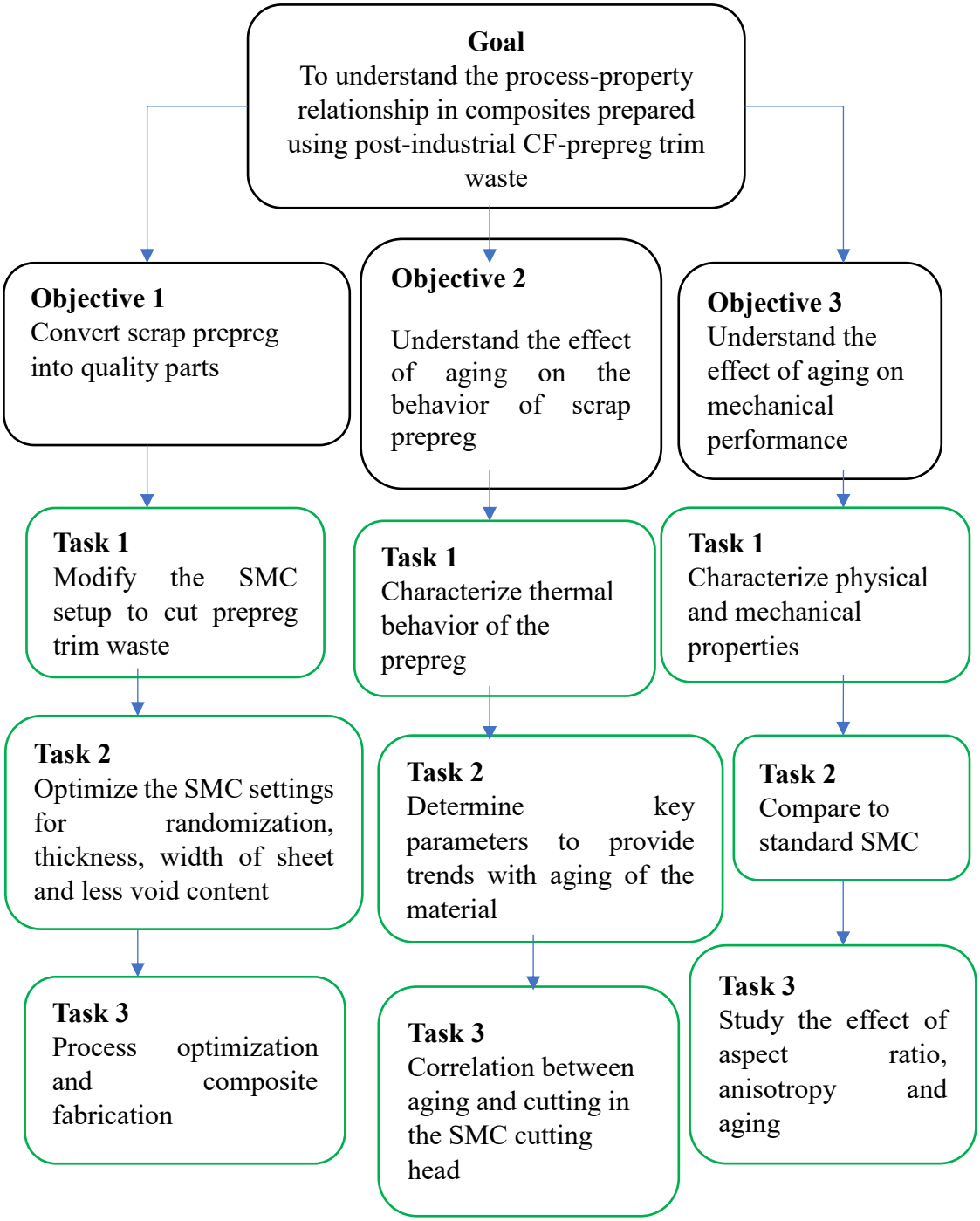

Figure 1.5: Flow diagram of the progression of the research structured according to the goal and objectives of the study.

CHAPTER 2

UTILIZATION OF PREPREG TRIM WASTE USING SHEET MOLDING COMPOUND TECHNOLOGY: CHALLENGES AND POSSIBILITIES

The amount of high value post-industrial CF prepreg scrap material increases proportionally to the amount of carbon fiber prepregs used, as this is the material of choice for lightweight structures especially in aerospace industries. These post-industrial CF prepregs are produced either in the form of tapes of various widths or as discontinuous scrap pieces of various shapes. The properties of these materials, including their ability to be cut and processed, strongly depend on their out-time, which is the time they remain at ambient conditions. The out-time and thus their thermal history can vary significantly and is often not known. The goal of this thesis is to transform this industrial waste into a high-value product using existing technology and minimum energy input.

SMC technology was utilized in this study as a low-cost production technique, which is mainly used for structural composites, to convert the high value CF prepreg trim waste into value-added products. The literature suggests that SMC composites exhibit properties similar to those of quasi-isotropic continuous CF/epoxy systems [75]. In conventional SMC, fibers with large numbers of filaments per tow display low performance due to poor fiber impregnation with resin. This challenge can be overcome by using prepreg tapes instead, which also eliminates the fiber curl that commonly occurs in typical SMC during spreading the fibers on the resin[75]. The compression molding

technique, used with SMC technology, further ensures the scalability of this recycling/reuse initiative. However, due to the nature of the prepreg tapes, as described in the above paragraph, it is expected that there will be challenges in using them as a feedstock for a SMC line and in operating the line. In this chapter, these challenges will be addressed and pathways to overcome them will be demonstrated. The mechanical properties of the resulting composites will be measured in order to demonstrate the potential of this recycling approach and the possible applications of these composites.

2.1 Materials

The material used here was unidirectional (UD) CF reinforced epoxy resin prepreg tapes. This prepreg was manufactured by Toray America Inc and supplied by the Boeing Company. The material can be identified as 'Toray 3900-2B epoxy/T800S carbon fiber' prepreg. The resin content is 35.5 weight % and the carbon fibers used are T800S. The fresh (minimum out-time) prepreg had a glass transition temperature of ~ 6^{o}C and was tacky in nature. The specific prepreg tape used in the work presented in Chapter 2 had a width of 12.7 mm and was tacky as received. However, the thermal history of the prepreg prior to receipt was unknown. It may be noted here that aging causes the prepreg to lose tackiness with time and temperature of storage space. The study on the aged prepreg will be discussed in Chapters 3 and 4.

2.2 SMC production line

An SMC line from Finn and Fram, Inc. was used to prepare the SMC using the aerospace grade CF prereg tape. The basic difference between the SMC line used in this study and the heavy-duty lines used in industry is the width of the SMC produced, which

is 0.3m compared to the 0.9-1.5m width of industrial SMC lines. Figure 2.1 shows the SMC setup used for this research. The key parts of the setup are as follows: the cutting head which allows for control of the cutting pressure and feed pressure, the upper and lower doctor blades which can regulate the resin input, the compaction zone, and the take up roll. The gap between the two guiding plates is crucial for controlling the width and thickness of the SMC.

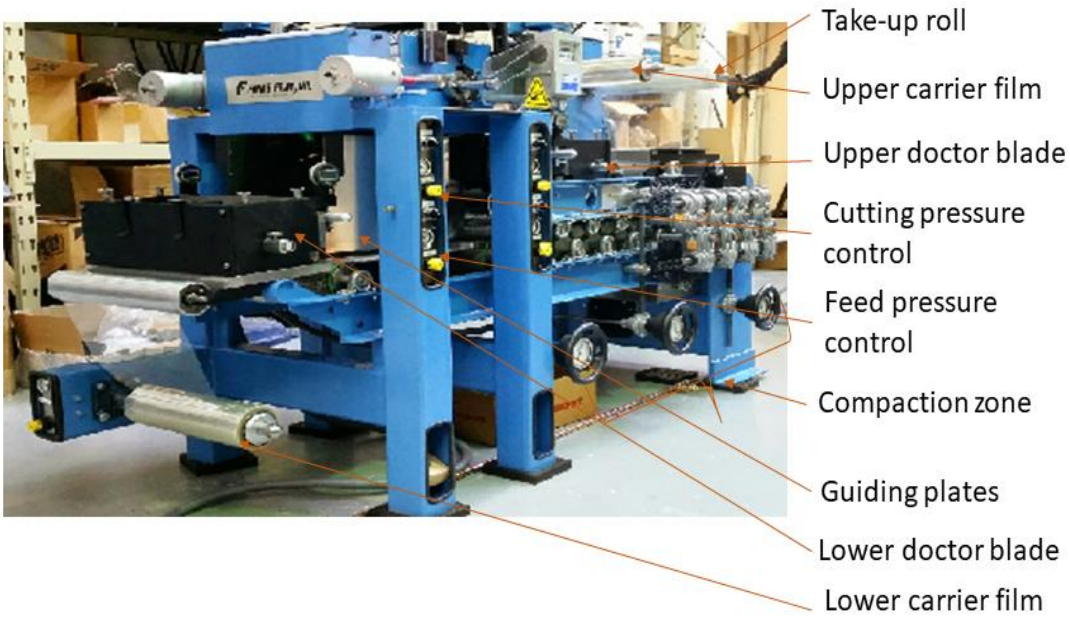

Figure 2.1: SMC setup in the GTMI hi-bay

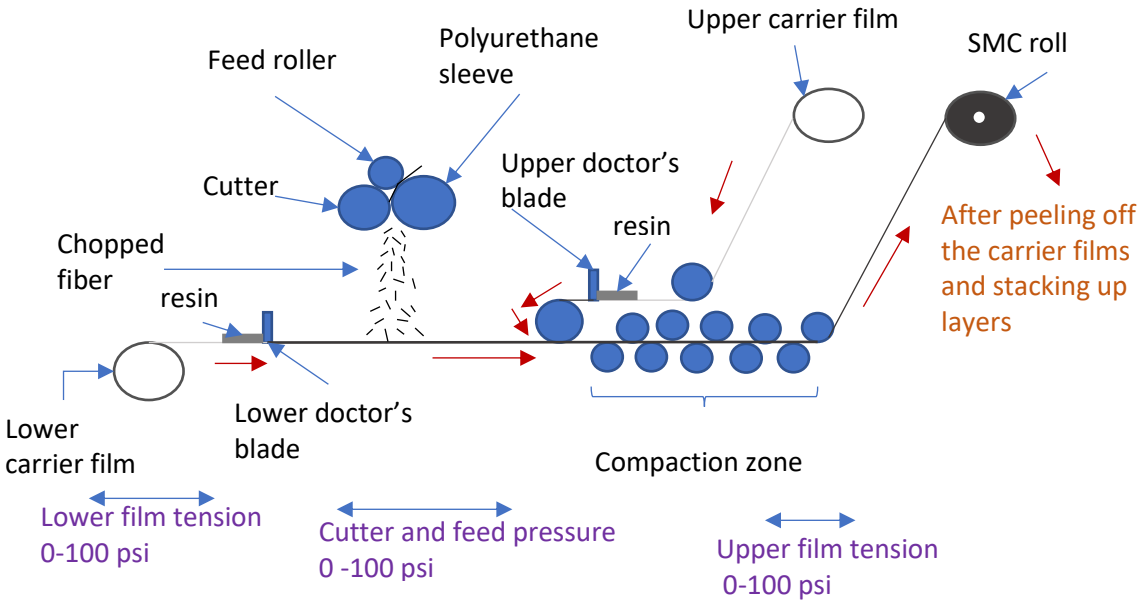

Figure 2.2: Process flow diagram of conventional SMC

Figure 2.2 shows the process flow diagram for the production of conventional (glass fibers roving –polyester system) SMC. As fibers are fed through the cutting head in between the feed roller and the bladed cutting roller, the fibers are pressed against the sleeve roller and chopped. The sleeve roller is generally made of polyurethane of different hardness. Resin is poured on the upper and lower doctor blade reservoirs. The gap in the doctor blade system controls the thickness of the resin layers, which determines the final resin content in the resulting SMC. As the chopped fibers fall randomly on the lower layer of resin, the upper layer of resin is fed simultaneously. Thus, the fiber layer is sandwiched between two resin layers and the sandwich structure passes through the compaction zone where the pressure can be controlled and varied at three different locations (entry, middle and exit of the zone). This compaction ensures resin impregnation and spreading within the fibers. Finally, the SMC is collected on an uptake roll and conditioned properly so that

the resin has the optimum viscosity and tackiness. The rolls of SMC can be either compression molded after the conditioning step or stored in a freezer for later molding.

A detailed feature that needs to be further discussed, as it strongly relates to the ability to convert the CF prepreg tapes in SMC, is the cutting mechanism in the SMC line. A simple observation indicates that the fiber rovings are cut by flexural failure. Specifically, the fiber rovings are pressed against a compliant polymer backing sleeve and sharp knives (the blades on one of the rolls) are plunged into the sleeve. As the knife plunges into the sleeve, the fibers conform to the knife edge curvature and break as the fibers reach their critical radius of curvature. Brittle fibers such as glass and carbon fibers possess a critical radius of curvature. Using the Euler-Bernoulli's beam theory for beams of circular cross-section, the critical radius of curvature can be obtained by Equation 2.1 [76]:

$$r = \frac{Ed}{2\sigma} \tag{2.1}$$

Where E is the fiber modulus, d is the fiber diameter and σ is the flexural stress developed. Thus, the properties of the fibers as well as those of the blades and the sleeve are crucial for maintenance and successful operation of the SMC line including reliability and repeatability of the resulting SMC. The sleeve material is chosen so that it can withstand multiple plunges of the blades while cutting the fibers. If the sleeve is very soft, it will not be able to withstand the plunging of the blades while the blades will be damaged faster if the sleeve is too hard. Generally, low modulus PU sleeves are suggested for SMC cutting head as this makes it easy for the fibers to bend when cutting force is applied by the blades [76].

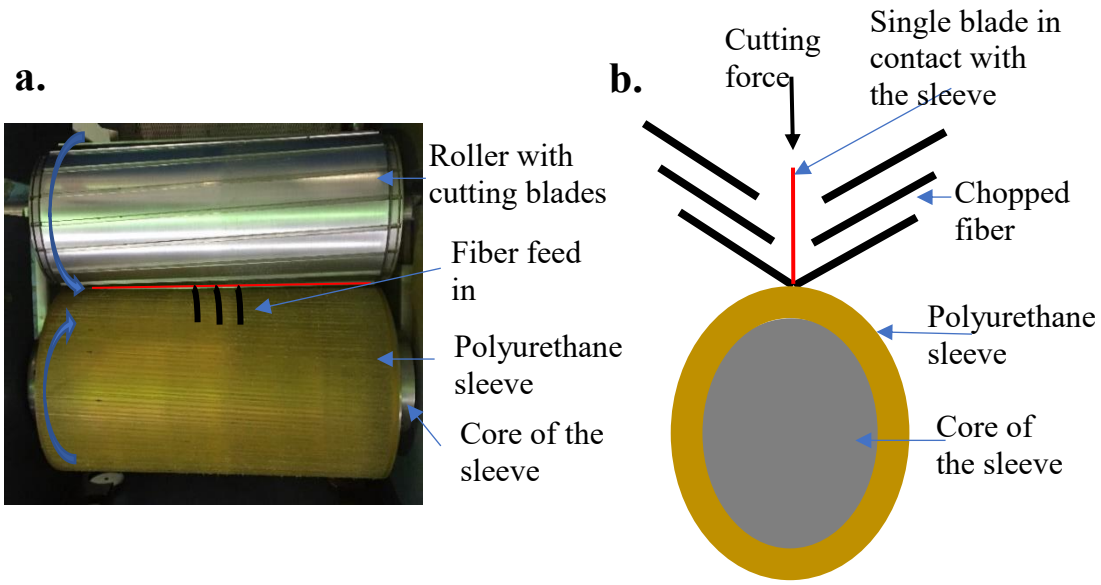

Figure 2.3: Fiber cutting mechanism: a. top view of fiber fed in between roller with cutting blades and roller with polyurethane sleeve (feed roller not shown here), b. simplified schematic of the side view of the cutting of fibers (not drawn to scale).

2.3 Challenges in converting CF prepreg tapes into SMC and corresponding modifications

The fibers used in the form of a roving in a conventional SMC line, such as glass fibers, basalt fibers, and carbon fibers, are brittle in nature and the SMC cutting head is designed for such fibers. The CF prepreg tapes are tacky and more flexible than these fibers and have drastically different dimensions. Based on Equation 2.1, it was clear that cutting the prepreg tapes with the cutting head of the conventional SMC line was expected to be challenging as the tensile strength and modulus are much higher for carbon fiber compared to the glass fiber. A higher load was required to overcome the ultimate strength of carbon fiber.

2.3.1 Challenges associated with cutting the prepregs and the corresponding modifications of the cutting head

The first modification made to the SMC line was to replace the blades in the cutting head with thicker ones made of 1095 carbon steel and thickness of 0.33 mm. In addition, the conventional backing sleeve was initially a neoprene rubber sleeve with a hardness of 60 to 65 Shore A. It was not hard enough to cut the CF prepreg tape. Thus, the softer sleeve was replaced with a polyurethane sleeve with a hardness of 80-85 Shore A so that the CF-prepreg tape could be cut. For the new polyurethane sleeve, the SMC line was initially run without fiber or tapes to create grooves on the sleeve, which helped the tape to reach the required radius of curvature of the fibers for flexural failure. The theoretical radius of curvature was calculated using Equation 2.1, and the properties and dimension from the material data sheet (MDS) for Toray 800S carbon fiber. According to the MDS, the Young's modulus, diameter and tensile strength for the fibers were 294 GPa, 5 μm and 5.88 GPa, respectively. Thus, the critical radius of curvature was calculated to be 125 μm. The blade used in the SMC cutting head had a radius of curvature of 25 μm, obtained from the machine drawings. The literature suggests that the minimum radius of curvature of the blades should be less than the critical radius of curvature for the corresponding fiber [76]. Since the fibers are impregnated with resin in this study, the nature of the material inherits sticking issue which will be discussed shortly. In this case, the cutting head consisting of carbon steel blades and a PU sleeve was suitable for cutting the prepreg, while the critical radius of curvature of the fiber was five times higher than that of the carbon steel blades.

For the tackiness of the fresh (minimum out-time) prepregs, these tapes were prone to sticking to the cutting head especially on the cutting roller and the sleeve upon cutting

into chips because they were tacky. The accumulation of these chips on the cutting head degraded the cutting. Once the prepreg tapes were fed into the cutting head, Frekote ® 700-NC, a mold release agent, was sprayed onto the rollers to prevent the accumulation of prepreg chips. Without the spray, pieces of tapes accumulated, which resulted in poor cutting and consequent stalling of the motor. Spraying at intervals of one minute during the run was helpful. The literature suggests that the molecules of mold release agent (MRA) are smaller than the epoxy molecules of prepreg and thus the MRA molecules may migrate into the polymer and may alter the properties of the cured polymer [77]. A. J. Shields et al. studied the effect of MRA by applying electrical, thermal, mechanical (bending) and radiative stresses on molded epoxy resin. Electrical stresses applied to the parts showed detrimental effects of cracking and crazing on the surface, while the effects of other stresses were insignificant. As this study of recycling of CF prepreg focuses on the mechanical performance of the composite, the effect of MRA on tensile properties was observed and found to be insignificant. However, even with application of MRA, the accumulation of prepreg on the cutting head and roller was observed to be another issue, resulting from incomplete cutting of the prepreg. Buildup of prepreg chips of various lengths was sometimes caused by partial cutting of the tapes. The resulting longer pieces easily stuck to the roller. To produce a complete cut, a cutting pressure of 275 kPa was observed to be sufficient to cleanly cut the tape, in combination with a new set of blades. The cutting pressure discussed here is the pressure to actuate the piston to close the gap between the roller with the blades and the roller with the sleeve.

2.3.2 Challenges in feeding the prepregs and the corresponding modifications of the feeding zone

The feeding set up was needed to be modified too, as the spools of the CF prepreg tapes could not be held vertically but needed to be held horizontally to enable low friction feeding at a constant rate. This was achieved by installing horizontal shafts to support the CF prepreg tape spools as shown in Figure 2.4. As the prepreg tape was pulled for feeding in the cutting head, the tape unwound from the spool, and when it reached the edges of the spool the tape was stuck on the spool holder shaft. This generated a back pressure that resulted in resistance to feeding and consequently the motor stalled. The spool was conical in shape and there was no cover to prevent slipping of the tape at the edge. As shown in Figure 2.4 (left), the tape was pulled at an angle to feed in the cutter setup to support the relative positions.

Figure 2.4: Prepreg tape being drawn from the spool (left), stuck on the shaft (right).

The motor stalled due to the pull of the prepreg tape from its spool, overcoming cutting pressure, feed pressure, and accumulation of chopped tapes on the rollers. The motor also needed to overcome the friction in the feeding system. The cumulative effect caused the drive shaft not to rotate. As a result, it was sometimes necessary to manually

help the drive shaft to start to rotate for certain cutting conditions. Reducing the cutting pressure helped reduce motor work, but that did not result in good cutting of tapes.

Removal of the backup films (yellow films in Figure 2.4) was another concern. The films were added to the tapes so that the fresh tacky tapes did not stick to each other when wound onto a spool. However, these films accumulated and restricted the free pulling of the tape. Sometimes backup films accumulated at the guide-holes for feeding the prepreg. This happened when the rate of pulling the prepreg was not similar to the rate of removal of the backup film by the Venturi device shown in Figure 2.5. As the prepreg was pulled through the guide, the backup film tended to go inside the guide-hole due to inertia. Accumulation of backup film might cause stalling of the motor as explained earlier. Thus, removal of the backup film was necessary. In the setup in Figure 2.5, compressed air was supplied to the inlet to produce a suction pressure to pull in the film into device, rather than through the guide-holes. Controlling the air pressure controls the suction pressure. Hence, regulating the compressed air pressure helped the device keep pace with the speed that the tape was pulled by the SMC machine. Consequently, the SMC line could be run smoothly.

Figure 2.5: Venturi equipment for removal of backup film

Further modification was undertaken to run the SMC line smoothly. A metal structure was added to hold the spools on horizontal shafts from which prepreg tapes were fed to the cutting head. Guides were added at two stages: (1) eyelets were added midway below the spools to prevent the locking of the spool because the prepreg tape stuck on the edge of spool or on the spool holder shaft, as shown in Figure 2.4 and (2) eyelets for feeding into the cutting head were added as shown in Figure 2.8 so that the same distance could be maintained between the tapes. Circular eyelets of galvanized steel with an inner diameter of 16 mm were used as the tapes used for making SMC had the highest width of 12.7 mm. The eyelets came with a shoulder and nut which facilitate their installation. Moreover, these eyelets were cheaper than the ceramic eyelets with rectangular cross-section.

Figure 2.6 shows eyelets were set below /above the spool located in the middle position of the spool. As the tape was in tension as it passed through the eyelets, it did not slip beyond the spool's flat area. An angle, which depended on the placement of the roll relative to the cutting head and on the amount of material removed from the roll, was maintained between the spool surface and tape to avoid slippage. This angle was in the range of $(\pm\Theta)$ to $(\pi-(\pm\Theta))$ degrees, where Θ is an acute angle. Thus, the problem of the tape sticking to the spool holder shaft was resolved.

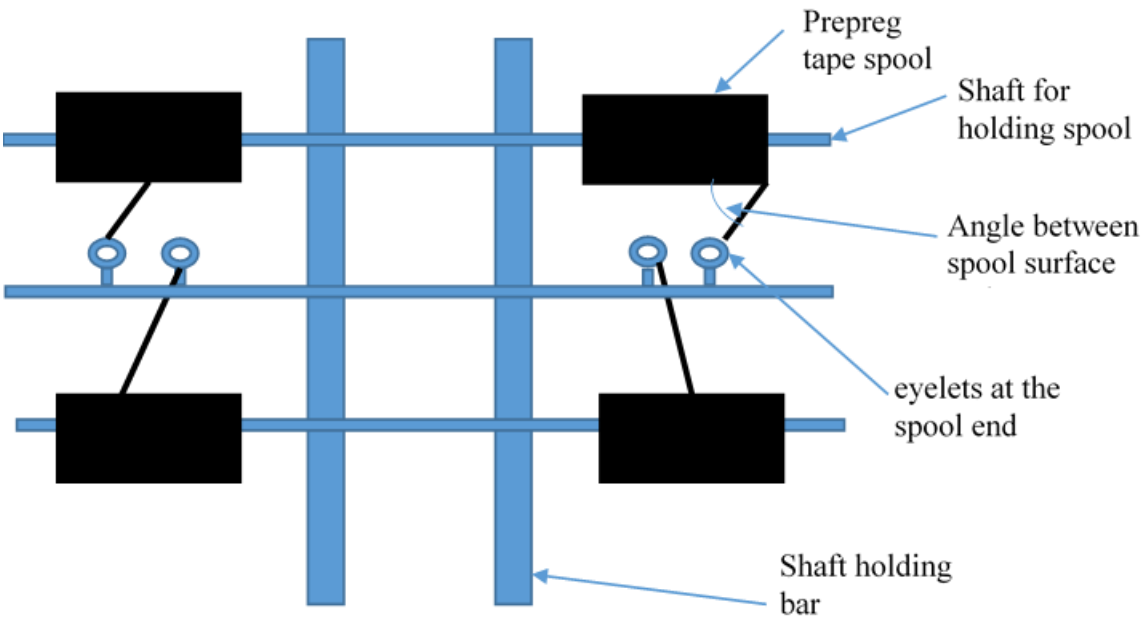

Figure 2.6: Schematic of spool holding setup and eyelets at the spool end

2.3.3 Challenges with maintaining a uniform SMC thickness and the corresponding modifications of the SMC settings

Maintaining the thickness uniformity of the SMC was crucial to achieve uniform thickness of SMC composite parts. Uniformity was examined by areal weight density measurement. A total of nine pieces at three locations were cut along the length of the SMC sheet in the SMC machine direction of travel. For each location, three pieces of 305 mm by 76 mm were cut as shown in Figure 2.7. Weights were 99.85±7.34 grams, 128.39±9.78 grams, 105.03±12.09 grams in the right, center and left locations, respectively for SMC run with four spools. Overall weight was 111.09± 15.72 grams. Thickness uniformity could not be achieved by running the SMC line with four spools. The weight variation also suggested that the central part of the SMC sheet was thicker than the left and right sides of the sheet. The right side was the thinnest. In addition, the SMC motor had difficulty pulling

more than four spools at a time, each weighing about 7 kg. To achieve uniform SMC thickness, the SMC line was run with five spools. However, to reduce the pulling work of the motor lighter spools, each weighing 1 to 2 kg, were used. The main parameters for resolving the thickness issue were as follows: the number of spools fed, the gap between the two guiding plates, the location of the eyelets for tapes at feeding, and the belt speed or conveyor speed for a certain cutting speed. Various combinations were tried.

Figure 2.7: Areal weight density measurement

Running the SMC with five spools and adjusting the eyelet locations at feeding for a certain belt speed and gap between the plate-guides resulted in an improved areal weight density. Table 2.1 shows the weight variation of SMC at different location when SMC was run with four and five spools.

Table 2. 1: Weight variation of SMC at different locations

Number of spools	**Right (grams)**	**Center (grams)**	**Left (grams)**
4	99.85±7.34	128.39±9.78	105.03±12.09
5	132.39±4.32	135.49±5.63	129.33±6.23

Eyelets were added to guide the prepreg tapes at the point of feeding to the cutting head as shown in Figure 2.8. The number of eyelets could be varied as necessary. The gap between the eyelets was adjustable as well. This gap was crucial for thickness uniformity of the SMC sheet prepared from prepreg tapes.

Figure 2.8: Eyelets for guiding the prepreg tapes into the cutting head

2.3.4 Limitations of the motor in terms of its capacity and corresponding modifications of the SMC line

The motor had to overcome friction while pulling the tapes or else it stalled. Friction could be reduced by installing endcaps and bearings on the spool-holding shaft as shown in Figure 2.9. However, adding the bearing reduced friction too much, which resulted in the tape unraveling at a speed greater than the speed of removal of backing up film. This caused accumulation of backup film, jamming the tape and finally stalling the motor. So, for friction reduction, a spool end cap without bearings was a sufficient modification.

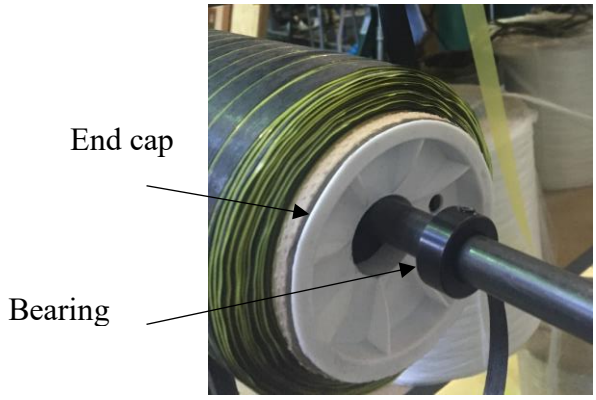

Figure 2.9: Spool end cap and bearing added for friction reduction

After all the modifications mentioned above, the SMC settings needed to be optimized to prepare a sheet of SMC that has a uniform thickness and its production is reproducible. Each parameter was determined by changing them one at a time and observing the SMC operation. The settings' parameters are listed in Table 2.2. The next discussion will clarify the parameters in detail. In the SMC line, the motor is coupled to the core of the sleeve roller. So, the driving roller is the sleeve roller. The feed roller and the roller with cutting blades are pressed against the sleeve roller with air pressure applied by air pistons. The two applied pressures are termed feed pressure and cutting pressure, respectively, as one is applied to the feed roller and the other to the cutting roller. Once the sleeve roller starts rotating, the other two rollers rotate as long as these are engaged by the feed pressure and cutting pressure. Feed pressure did not directly influence the cutting of the prepreg tape. However, it controlled the feed rate, which was influenced by the set speed of the driving roller and the feed pressure. Cutting speed was set by the speed at which the sleeve roller turns. However, the production rate of chips depends on the gap between the blades on cutting roller as well as the cutting speed. Further study with

changing feed pressure, cutting pressure and cutting speed revealed that the cutting speed and cutting pressure were crucial parameters to produce a good cut. If the cutting pressure was increased greater than 345 kPa, the motor could not achieve the torque to rotate the three rollers of the cutting head. However, below 207 kPa the cut was neither good nor complete. The best cutting pressure was found to be 275 kPa to achieve a complete cut and smooth running of the SMC.

The number of spools also played an important role for the SMC preparation. For 280 mm wide SMC made with four spools, there were holes in the SMC which also exhibited non-uniform thickness. Use of more than five spools would increase the thickness of the SMC. The mold could be used to prepare samples as thick as 11 mm. However, the tensile testing grip had an upper limit of 7 mm. Therefore, the use of five spools was the best option to obtain a uniform and reproducible SMC sheet within the capacity of the motor. The distance between two eyelets had a similar effect on the SMC. The distance should be such that the tapes were uniformly distributed at feeding and not so far apart that there would be gaps or holes in the SMC. The conveyor settings controlled the translational motion of the conveyor belt. A higher conveyor speed might cause less accumulation of chips resulting in gaps or holes in the SMC sheet, while a lower conveyor speed might result in thicker SMC sheet. Parameters such as belt tension and winder tension were kept unchanged as default settings from the SMC line manufacturer.

Table 2. 2: Final SMC settings used to prepare the SMC sheet

SMC parameters	Set value	Range
Feed pressure	200 kPa	0 to 690 kPa
Cutting pressure	275 kPa	0 to 690 kPa
Upper belt tension	415 kPa	0 to 690 kPa
Lower belt tension	480 kPa	0 to 690 kPa
Speed of cutting	25 revolutions per second	0 to 60
Conveyor settings	15	0 to 60
Winder tension	480 kPa	0 to 690 kPa
No of spools	5	-
Distance between two eyelets at feeding	57 mm	355 mm between two eyelets' extreme position
Distance between guiding plates	300 mm	355 mm

2.4 Manufacture of SMC sheet and fabrication of composite plate

Using the parameters in Table 2.2, the tapes were cut into chips of predetermined length as per the blade settings and dropped randomly on the carrier film on the conveyor belt. The belt carried the chopped, 'fresh' tacky chips through the compression zone, then a continuous sheet was formed and collected in the form of a roll, as shown in Figure 2.10. Compression was applied by two sets of rollers- upper and lower. The relative position of the two sets of rollers was used to control the applied pressure. The distances between the two sets of rollers were maintained at 232 mm at entry, 204 mm in the middle and minimum possible at the exit of the compression zone. The resulting SMC was ~ 4 mm thick and 300 mm wide. The CF SMC rolls were stored in a freezer at 0^{o}C until it was time for compression molding.

Figure 2.10: SMC sheet prepared from “fresh” prepreg trim waste tapes. The width of tape used was 12.7 mm and it was cut in 25.4 mm long chips. The sheet shown here is approximately 300 mm wide.

A closed mold was used to fabricate the composite plate in a Wabash V-50-1818-2TMX hot-press under vacuum. Once the charge was placed in the mold, the mold was closed and placed in the press, the temperature was increased to 195ºC, and then pressure was applied for 15 minutes. The applied pressure was either 1 MPa, 2 MPa or 4.7 MPa.

2.5 Characterization techniques

The degree of cure (DOC) of the SMC composites was measured using a DSC Q2000 (TA Instruments). Each DOC value presented in Table 2.3 is the average of at least three measurements. To obtain the enthalpy of cure, ~6 mg samples were heated from 25°C to 300°C at 10°C/min. From the curing exotherm, the total enthalpy was calculated, which was normalized for resin mass content assuming the prepreg contains 64.5 wt.% carbon fibers that are not taking part in the curing reaction. After SMC composites were prepared to study the flow behavior of prepreg tape in the mold and finally for investigating the mechanical performance, cured resin was collected. Then, DSC was performed on the as-received prepreg just before making composite panels and on cured resin from the final SMC composite panels in order to determine the total and residual enthalpies. The DOC

was calculated as the ratio of the heat of reaction of the of cured resin to the heat of reaction of the resin in the unaged and unreacted prepreg tape.

The composite fabrication will be discussed in detail in Section 2.6.1. SMC composite plates with dimensions of 280 mm x 280 mm x ~5mm were kept at ambient temperature for 24 hours prior to cutting and testing to prevent any potential plastic deformation during handling/testing. The thickness profile of each plate was measured along three different cross sections, as shown in Figure 2.11 by the XX', X1X1' and YY' lines, using a Mitutoyo micrometer. The test coupons were cut out from the plates using a waterjet cutter (MAXIEM 1515).

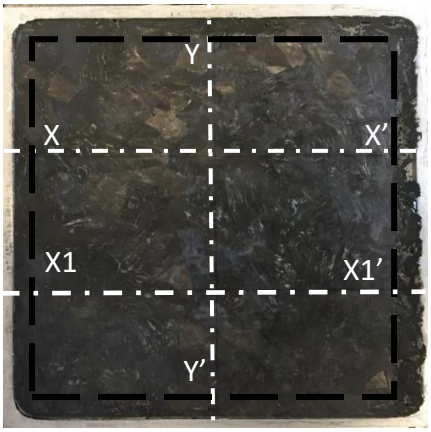

Figure 2.11: A composite plate made of SMC of 12.7 mm wide and 25.4 mm long chips of prepreg trim waste tape. The white dotted lines are the three cross sections along which the thickness profile was recorded, and the black dotted line indicates the original size and location of the charge. This panel measures 280 by 280 mm.

The density and the void content of the composites were determined using the water displacement technique and polymer digestion using acids, respectively. Specifically, a Mettler Toledo scale model number AG245 was used following ASTM D792 to obtain the density. Each data point for density and void content shown in Figure 2.16 is an average of three measurements. Each sample was weighed in air and water at ambient temperature to calculate density per Archimedes' principle. The void content was determined according to ASTM D 3171 by acid digestion. Each sample of ~2 grams was immersed in nitric acid

and heated at 80°C for 2 hours followed by rinsing the fiber with distilled water to remove any resin residue. The fiber was then heated for 5 hours at 115°C and cooled overnight before it was weighed. The void content was calculated using Equations 2.2 and 2.3:

$$V_V = 1 - \rho_e/\rho_t \tag{2.2}$$

$$\rho_t = W_c/[(K_f W_f/\rho_f) + (W_m/\rho_m)] \tag{2.3}$$

where ρ_e = experimental density of composite, ρ_t =theoretical density, ρ_f = density of fiber, ρ_m= density of matrix; K_f = correction factor (ratio of final weight to initial weight of fiber); W_c= weight of composite, W_m= weight of matrix; and W_f= weight of fiber. The theoretical density was calculated using the rule of mixtures.

The tensile properties of the SMC prepreg composites were determined per ASTM D638 using an Instron testing machine model number 33R 4466 equipped with 100 kN load cell for dog bone samples with a gauge length of 57 mm, width of 13.1 mm and thickness of 5 mm. An extensometer, Instron 2630-106, with a gauge length of 25 mm was used to record the axial strain. The modulus was calculated between the axial strain values of 0.05% and 0.2%. The impact energy was measured using Charpy test with an Instron SI series pendulum impact tester with a maximum impact head of 406.7 J (300 ft-lbf) according to ISO179 with a support span of 43 mm, for 12.7 mm wide and ~5 mm thick without notch rectangular samples. Each data point reported in Figure 2.15 was an average of at least seven tests.

A Phenom G2 Pro (Phenom-World BV) scanning electron microscope (SEM) at an acceleration of 5 kV was used to study the fracture surfaces of the SMC composites. A plasma sputterer (Ted Pella Inc.) was used to apply gold coatings on the surfaces of the samples prior to SEM imaging to minimize charging. Through thickness microstructure, prior to fracture, was observed as well. A sample cross-section of 9 mm by 5 mm was set in an epoxy mold and polished in an Allied Hightech Metprep 3 polisher. Then a Leica DM 2500P optical microscope was used to obtain images.

In the next section, the charge characteristics of CF-prepreg SMC in the mold will be discussed. After fabricating composites from SMC, both physical properties and mechanical performance will be investigated.

2.6 Results and discussion

2.6.1 Optimum charge characteristics for fully filling the mold

In order to determine the charge size and its optimum location and surface coverage of the mold in order to fully flow and fill the mold during compression molding, the SMC sheet was cut into squares of various dimensions smaller than or equal to the dimensions of the square mold. Various number of layers were stacked on top of each other on the mold. The mass of the charge was kept the same for all composites plates by adjusting the number and the dimensions of the layers used. The area of the square shaped charges varied from 140 mm x 140 mm to 260 mm x 260 mm. The charges were placed in the middle of the 280 mm x 280 mm square mold shown in Figure 2.12. The masses of the charges are reported in Table 2.3. The table also reveals that the thickness of the composite plates was dictated by the number of SMC layers used.

Figure 2.12: Bottom (left) and top (right) part of a closed mold made of aluminum. The area of the mold cavity is 280 mm x 280 mm

The characteristics of the plates made for the flow study are presented in Table 2.3. The temperature in the press was set to 195^{o}C, which resulted in a targeted DOC of 70-80%. A pressure of 1 MPa was applied for 15 minutes once the temperature reached 195^{o}C. The charge area and location in the mold prior to molding (black dashed lines) and the resultant plate are shown in Figure 2.13. The area of the internal mold cavity was 280 mm X 280 mm. So, the length scale of the mold cavity for each plate in Figure 2.13 can be used as a reference length.

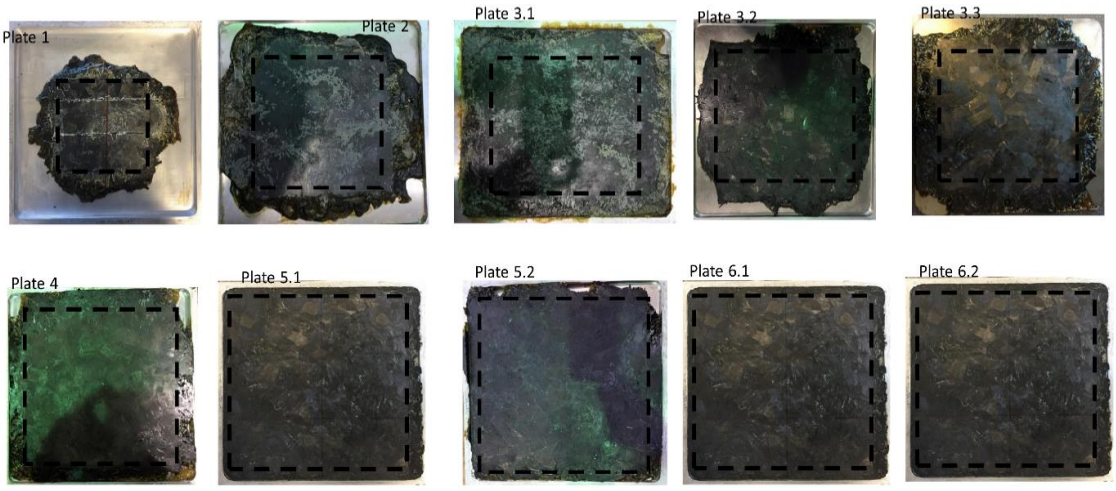

Figure 2.13: The charge size and its location in the mold before and after molding for plates P1-P6 indicating the ability of the charge to flow and fill the mold

For constant mass of initial charge, as the charge lateral size was increased, the dimensions of the resulting plate also increased but still were smaller than those of the mold indicating incomplete mold filling. Even in the case of plates P5.1 and P5.2 where a 254 mm x 254 mm charge was used, the flow was not sufficient to fully cover the mold surface. Thus, when the mass of the charge was increased from 486g to 595g, the size was increased to 260 mm X 260 mm, then the charge flowed to fully cover the mold, i.e., P6.1. It was observed that mold filling depends on both the initial charge size and mass. The major difference between plates P3.1 and P3.2 was the time between the fabrication of the SMC and making of the plate by compression molding. Although the SMC was properly stored in a freezer, the resin's ability to flow decreased significantly in the case of P3.2 where the areal change of the charge was only 56% compared to 87% in case of P3.1. The difference between P5.1 and P5.2 is also the time the SMC was kept in freezer before it was used. But in this case, there was no obvious effect on the resin's ability to flow, maybe because the

initial area of the charge for both plates was significantly larger (254 mm x 254 mm for P5.1 and P5.2 vs 203 mm x 203 mm for P3.1 and P3.2).

The thickness profiles along the three sections for plates P1-P6 are presented in Table 2.3. Each data point reported is an average of at least 30-40 measurements along each section. The thickness of the SMC layers used to make these plates, dictated by the speeds of the conveyor belt and the cutting rolls, varied from 4 to 5 mm. As was expected, a smaller charge area resulted in a thicker plate due to limited flow of the resin within the charge. It was also found that thicker charges produced larger variations in the thickness of the plate along the three sections XX', X1X1' and YY'.

Table 2. 3: Plates fabricated to determine the optimum charge to completely fill the mold

Plate ID	Charge area (mm^2)	# of SMC Layers	Mass of charge (g)	Charge area change (%)	DOC (%)	Days SMC was stored prior to compression molding	Thickness along section XX' (mm)	Thickness along section X1X1' (mm)	Thickness along section YY' (mm)
P1	140 x140	7	485	96	85±3	1	9.87±3.13	9.81±2.87	10.31±2.81
P2	178 x 178	4	518	58	75±2	6	7.25±1.25	7.35±1.07	7.19±1.62
P3.1	203 x 203	3	486	87	78±3	30	5.06±0.24	4.37±0.26	4.87±0.7
P3.2	203 x 203	3	486	56	78±3	140	6.02±0.32	5.88±0.52	5.88±0.82
P3.3	203 x 203	4	486	72	78±3	23	5.29±0.87	5.64±0.75	5.47±0.59
P4	229 x 229	2	486	32	83±3	7	5.03±0.54	5.14±0.03	5.12±0.13
P5.1	254 x 254	2	486	20	75±2	75	3.91±0.15	3.93±0.19	3.9±0.10
P5.2	254 x 254	2	486	21	82±3	9	4.54±0.16	5.11±0.22	4.67±0.45
P6.1	260 x 260	2	595	21	75±2	4	5.22±0.25	5.27±0.24	5.08±0.29

2.6.2 Mechanical performance of the prepreg composites based on the tensile properties and impact strength

The literature suggests planar isotropy develops in SMC composites when mold coverage approaches 100% [78]. However, incomplete mold coverage might result in planar anisotropy induced by flow [68, 78, 79] because resin flow might cause alignment of fibers along the flow. This behavior is reported to be dominant near the boundaries of the mold cavity [68]. Based on the results presented in Table 2.3 and Figure 2.13, the charge size was kept at 260 mm x 260 mm and mass of 600 grams, i.e., close to the area of the mold cavity to reduce planar anisotropy [80] and to fully fill the mold. Two layers of SMC were used to fabricate each plate. Each SMC layer was 4 mm thick. The average thickness of the plate was 5 mm. As expected, there was a decreasing trend of thickness with increasing compression molding pressure. The details of the plates prepared for this study are shown in Table 2.4. The aging of the SMC, i.e. the time from when the SMC was made to when it was used, was recorded and is shown in Table 2.4. The as-received prepreg spools and the prepared SMC rolls were stored in the freezer at 0^{o}C. Before making the composite plates from SMC sheets, the rolls were thawed at room temperature for two hours.

Table 2. 4: Plates prepared from tacky tapes to determine the effect of pressure and anisotropy on the tensile and impact properties

Plate ID	DOC (%)	Pressure (MPa)	Time (days) between SMC fabrication and compression molding
P6.1	75±2	1	3
P6.2	75±2	1	1
P6.3	75±2	1	7
P7.1	73±2	2	18
P7.2	74±2	2	30
P7.3	73±2	2	85
P8.1	75±2	4.7	55
P8.2	75±2	4.7	55

2.6.2.1 Tensile properties of CF prepreg SMC composites

The tensile strength and modulus of the plates as a function of the applied pressure, the age of the SMC, and the planar anisotropy are shown in Figure 2.14 and Figure 2.15 respectively. The comparison of plates P6.1, P6.2 and P6.3 showed an inherent variability, as all three plates were made from the same material using the same processing conditions. The strength was in the range of 138-190 MPa and the modulus varied between 35 and 47 GPa. The effect of the SMC's age and the in-plane anisotropy (parallel or perpendicular to the machine direction) were demonstrated through comparison of plates P7.1, P7.2, and P7.3. As shown in Table 2.4, the SMC used in P7.3 was 85 days old and the tensile coupons were cut parallel to the SMC machine direction. Plate P7.3 exhibited an average strength of 106 MPa, which was lower than the strength of P7.1 and P7.2 by 42% and 55%, respectively. As reported in Table 2.4, the SMC age for plates P7.1 and P7.2 was 18 and 30 days respectively and the coupons in these two plates were perpendicular to the SMC machine direction, as with the case of P6.1-6.3. No effect of SMC age on the tensile modulus was observed. In isolating the effect of the in-plane anisotropy, plate 8 was

prepared and reported as P8.1 for perpendicular to SMC machine direction and P8.2 for parallel to SMC direction coupons, respectively. Planar anisotropy was observed in samples P8.1 and P8.2. However, for the SMC machine direction, samples were cut from a zone closer to the mold edge of plate 8, which represents the high flow zone. This resulted in lower tensile strength for P8.2SMC as shown in Figure 2.14. The literature also suggests that strength is reduced in the high flow zone for substantial fiber-chip distortion [67]. Therefore, plate P7.3SMC was fabricated to varify the effect of planar anisotropy. In this case, samples were cut in the SMC machine direction from the center portion of the plate (not from high flow zone of the edge) to explain there is no planar anisotropy. In other words, tensile strengths in both the SMC machine direction and perpendicular to SMC machine direction were observed to be similar, taking into account the error bars as the Figure 2.14 suggests.

For tensile modulus as shown in Figure 2.15, there was no significant effect of the anisotropy. The tensile modulus was dictated by the through thickness chip structure and orientation. However, a higher tensile modulus for plate P8.2 SMC was observed, which might result from flow induced fiber alignment [68, 79]. Figure 2.14 and 2.15 shows tensile strength and modulus for GF70/epoxy SMC composite with fiber content of 70 wt.% [54], since in SMC for automotive industries GF content varies between 25 to 65 wt.% [64]. To compare the lightweight, it is important to know the density of the composites. GF70/epoxy composite is reported to have an average density of 1.67 g/cc while the density of CF prepreg SMC composites was found to be 1.53 g/cc. Acid digestion tests revealed an average fiber content of 72 wt.% for CF prepreg SMC. Thus, CF prepreg SMC can provide 8% weight saving.

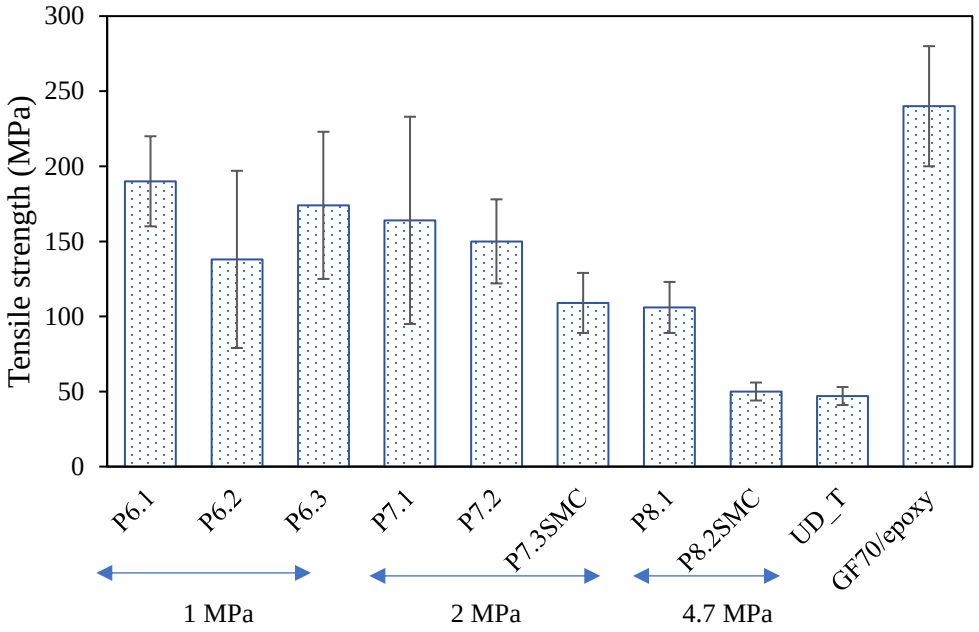

Figure 2.14: Tensile strength as a function of applied pressure, age of SMC and planar anisotropy

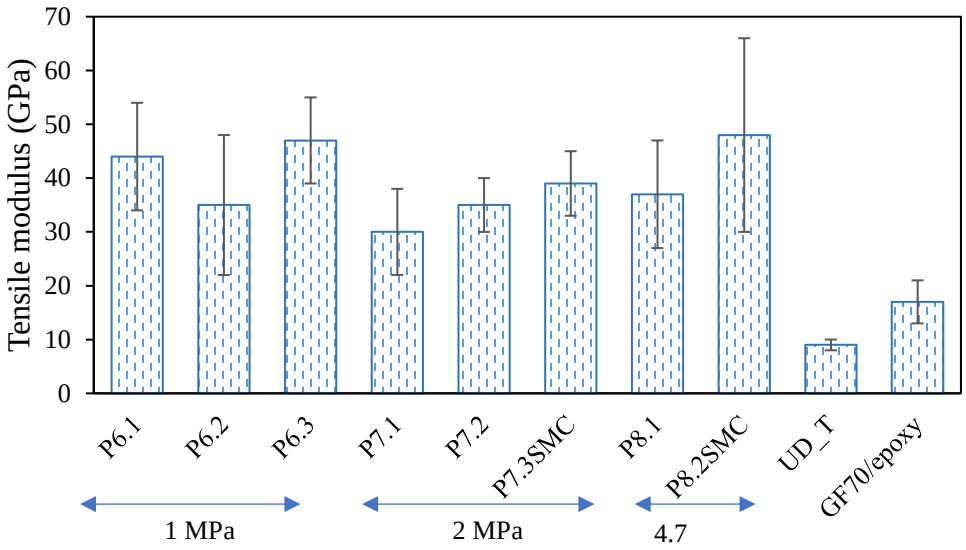

Figure 2.15: Tensile modulus as a function of applied pressure, age of SMC and planar anisotropy

In order to further understand the effect of the CF orientation within the testing coupons, a 152 mm wide prepreg tape consisting of unidirectionally aligned and continuous CF was used to make plates by hand lay-up of 25 tape layers and employing a consolidation pressure of 2 MPa. The average thickness of the plate is 3.9 mm and the experimental density is 1.61 g/cc which is very close to theoretical density of 1.6 g/cc. As expected, both the modulus and the strength of Unidirectional Transverse (UD_T) (the sample was a unidirectional layup tested in the perpendicular to the fiber direction) and Unidirectional Longitudinal (UD_L) (the sample was a unidirectional layup tested in the fiber direction) plates provide the lower and upper limits for the tensile strength and modulus and a qualitative measure of the degree of planar orientation of the CF. This is because the UD_L samples were cut along the fiber direction while UD_T sample were cut perpendicular to the fiber direction. UD_L samples were prepared and tested. The modulus (reported in Table 2.7) was 154 GPa. However, the tensile strength could not be measured as the measurement of the ultimate tensile strength was beyond the capacity of the uniaxial tension test machine. A 100 kN load cell was used and the maximum load that could be applied was 70 kN before the test was stopped. There also was slippage in the grip of UD_L samples. Finally, for comparison purposes the strength and modulus of typical GF/epoxy composites made by SMC are provided in Figure 2.14 and Figure 2.15 respectively. The glass fiber content was reported to be 70 wt.% [54]. The average strength of the GF70/epoxy composite was 240 MPa, which was higher than the average strength of the CF-prepreg composites of 150 MPa. However, the upper bound of the error bars for the tensile strength of CF prepreg SMC overlaps with the lower bound error bars of GF70/epoxy. The most important thing to note here is the tensile modulus. The average

tensile modulus for the CF-prepreg composites was 40 GPa, while it was only 17 GPa for the GF70/epoxy composites. The tensile properties of CF-prepreg SMC composites suggests that the composite can be useful in high stiffness application with less strength-critical parts. Table 2.5 shows comparison of tensile properties among GF SMC composites used in automotive industries with CF prepreg SMC. The table also includes the density of the composites to show the light weighting candidacy of CF prepreg SMC.

Table 2. 5: Tensile properties and densities for GF SMCs and CF prepreg SMC

Properties of composites	**GF25/epoxy[54]**	**GF70/epoxy[54]**	**CF prepreg SMC**
Fiber content (wt%)	25	70	72
Tensile strength (MPa)	72	240	150
Tensile modulus (GPa)	6.2	17	40
Density, ρ_{exp} ($\rho_{theoretical}$) (g/cc)	1.25 (1.31)	1.67 (1.81)	1.53 (1.6)
Void content (vol.%)	5	9	5 (at 2MPa)

2.6.2.2 Tensile modulus of CF prepreg SMC composites: theoretical vs experimental values

In this section, theoretical tensile modulus is calculated for the randomly oriented discontinuous CF-prepreg SMC composite and compared with the experimental tensile modulus. For the calculation of theoretical modulus, micro-mechanical model developed for short fiber reinforced composite is used as shown in Equation 2.4 [6].

$$E_c = \frac{3}{8}E_{11} + \frac{5}{8}E_{22} \tag{2.4}$$

Where,

$$E_{11} = \frac{1+2\left(\frac{l_f}{d_f}\right)\eta_L V_f}{1-\eta_L V_f} E_m \quad (2.5)$$

$$E_{22} = \frac{1+2\eta_T V_f}{1-\eta_T V_f} E_m \quad (2.6)$$

$$\eta_L = \frac{\left(\frac{E_f}{E_m}\right)-1}{\frac{E_f}{E_m}+2\frac{l_f}{d_f}} \quad (2.6)$$

$$\eta_T = \frac{\frac{E_f}{E_m}-1}{\frac{E_f}{E_m}+2} \quad (2.7)$$

Here, E_f is the fiber modulus, E_m is the matrix modulus, d_f is the fiber diameter, l_f is the chopped fiber/tape length, v_f is the fiber volume fraction. v_f is calculated using Equation 2.8.

$$V_f = \frac{\frac{W_f}{\rho_f}}{\left(\frac{W_f}{\rho_f}\right)+\left(\frac{W_m}{\rho_m}\right)} \quad (2.8)$$

To perform this calculation, the required values such as tensile modulus of T800S CF and epoxy resin of the prepreg, chopped fiber length, fiber diameter, resin content, density of fiber and resin are reported in Table 2.6. The values were obtained from data sheets provided by the manufacturer with an exception of resin modulus, which was taken from textbooks on composite materials [6, 81, 82]. The calculated values of η_L, η_T are also reported in Table 2.6, whereas the calculation is shown in Appendix section A2.

Table 2. 6: Parameters for calculation of tensile modulus in Table 2.7

Parameters to calculate modulus	**Unit**
Modulus of epoxy matrix, E_m	3.4 GPa [6]
Modulus of T800s CF, E_f	294 GPa [81]
Chopped fiber length, l_f	25400 µm
CF fiber diameter, d_f	5 µm [81]
Epoxy resin content, V_m	35.5 wt.% [82]
Density of CF, ρ_f	1.81 g/cc [81]
Density of epoxy, ρ_m	1.3 g/cc [82]
Fiber volume fraction, V_f	56.7%
Coefficient, η_L	0.008
Coefficient, η_T	0.966

From Table 2.7, it can be observed that the measured tensile modulus of E_{11} and E_{22} for unidirectional continuous composites are 154 and 9 GPa respectively, which match very well with the corresponding value of 148 and 8.3 GPa as per the data sheet. Using the values of E_{22} and E_{11} for unidirectional discontinuous material were obtained as 169 and 14.5 GPa respectively using Equations 2.6 and 2.5. Using these values of E_{11} and E_{22} of discontinuous unidirectional material in Equation 2.4, the modulus for randomly oriented short fiber composite E_c is obtained. The calculated value of E_c is 68.97 GPa. The detail calculation is reported in Appendix section A2.

Table 2. 7: Theoretical tensile modulus versus experimentally obtained tensile modulus for composites of different configurations

Tensile modulus type	**Theoretical modulus (GPa)**	**Experimental modulus (GPa)**
E_{11} UD continuous	148[81] (from data sheet)	154
E_{22} UD continuous	8.3[81] (from data sheet)	9
E_{11} UD discontinuous	169 (from calculation)	-
E_{22} UD discontinuous	16 (from calculation)	-
E_c discontinuous random	69 (from calculation)	40

Theoretical calculation assumes that the composite could achieve a modulus of 69 GPa when the chips are randomly distributed for discontinuous fiber composite system. However, for the composite prepared in this research, the average modulus obtained was 40 GPa. The theoretical calculation is performed on the assumption that the matrix is void free. However, the CF prepreg composite was not void free. The average void content was measured to be 5 vol.%. A study for CF prepreg unidirectional continuous laminate composites showed a 14% decrease in tensile modulus for a void content of about 8 vol.% [83]. However, the relationship between void content and tensile modulus for randomly oriented prepreg chip composite systems has not been reported in the literature.

Another important point to note is that the data sheet provided by the prepreg manufacturer suggested a cure cycle of 180^{o}C for at least 120 minutes to obtain the calculated modulus of 68.97 GPa [82]. In this research, the cure cycle was much shorter with a 15 minutes hold at 195^{o}C. A longer cure cycle might result in better resin flow and a higher degree of cure, which might improve the measured tensile modulus.

2.6.2.3 Impact properties of the composites

The results of the impact strength tests are shown in Figure 2.16. The average impact strength was greater than 130 KJ/m^2. The overall variation was 11 to 36%. However, the pressure of compression molding did not produce any significant change in impact strength, as the impact strength of P8.1 was similar to those plates prepared under intermediate and low pressure. The average impact strength for UD_L samples was as high as 250 KJ/m^2 and that of UD_T samples was as low as 10 KJ/m^2 which was expected. For UD_T samples the crack was parallel to the fibers and the samples were broken into two

pieces. UD_L samples did not break into two pieces. In this case, two modes of failure could be observed; flexural failure by fiber fracture and fiber pullout, and shear failure by delamination. Although delamination was not observed for all UD_L samples. The average impact strength was 33% higher for GF70/epoxy SMC composite as reported in literature compared to that of CF-prepreg composites [54]. Since GF content varies in SMCs for automotive industries from 25 wt.% to 65 wt.%, the comparison of impact strength of CF prepreg SMC with conventional SMCs are shown in Table 2.8. The densities are also reported here to show the suitability of CF prepreg SMC in light weighting applications.

Table 2. 8: Impact strength and densities for GF SMCs and CF prepreg SMC

Properties of composites	**GF25/epoxy [54]**	**GF70/epoxy [54]**	**CF prepreg SMC**
Fiber content (wt.%)	25	70	72
Impact strength (KJ/m^2)	68	200	144
Density, ρ_{exp} ($\rho_{theoretical}$) (g/cc)	1.25 (1.31)	1.67 (1.81)	1.53 (1.6)

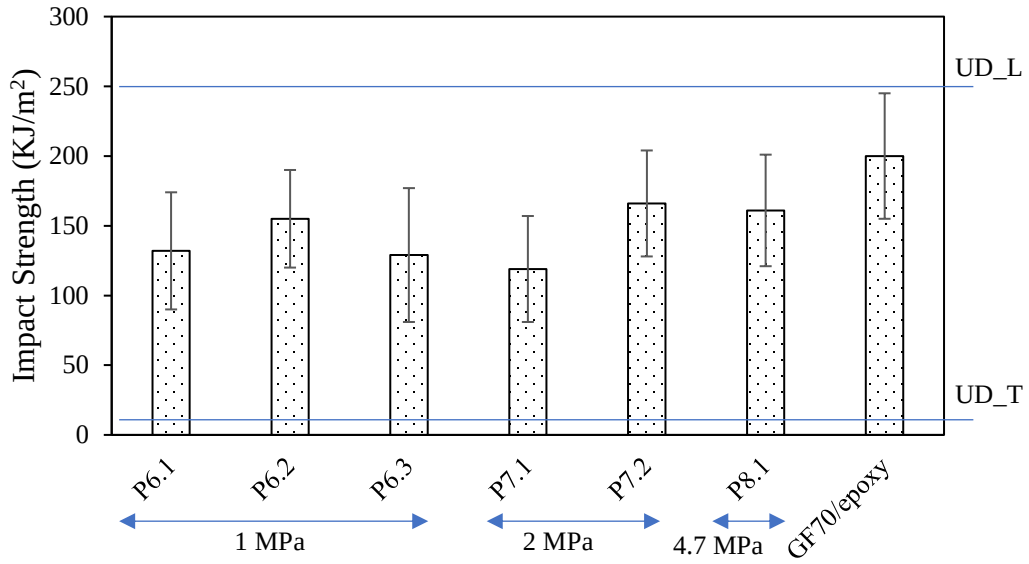

Figure 2.16: Impact Strength of the composite plates

However, the standard deviation of the impact strength was comparable for both CF-prepreg and GF70/epoxy composites.

2.6.2.4 Effect of microstructure on tensile and impact properties

Considering the large standard deviations observed for both the tensile and impact properties, the effects of the compression molding pressure and of the other variables investigated on the properties of the composites are not very clear. Studying the microstructure of the composites might provide an insight into the material behavior. Thus, density, void content, and through thickness fiber orientation of the composites were studied. Figure 2.17 shows that the average density of the plates was 1.5 to 1.6 g/cc. The void content for plates prepared at 1 MPa was approximately 8 vol.% or higher. For higher pressures, a reduction of void content was visible in the Figure 2.17.

Increasing the pressure to 4.7 MPa did not reduce the void content further. It might be assumed that 2 MPa was enough pressure to obtain a compact structure of fiber reinforced resin. Further increasing the pressure might have undesirable effects such as fiber breakage or less resin flow in the fiber network due to a short cure cycle. A decreasing trend of strength for plate P8.1 with increased pressure was observed, which further emphasized this fact. So, a pressure of 2 MPa was considered as the optimal pressure for compression molding. However, no direct correlation was observed between applied pressure and void content. For the UD plate, the void content was about 3 vol.%. In conclusion, a decrease in void content at 2 MPa did not cause any improvement in the modulus and strength, which emphasizes the dominant effect of anisotropy.

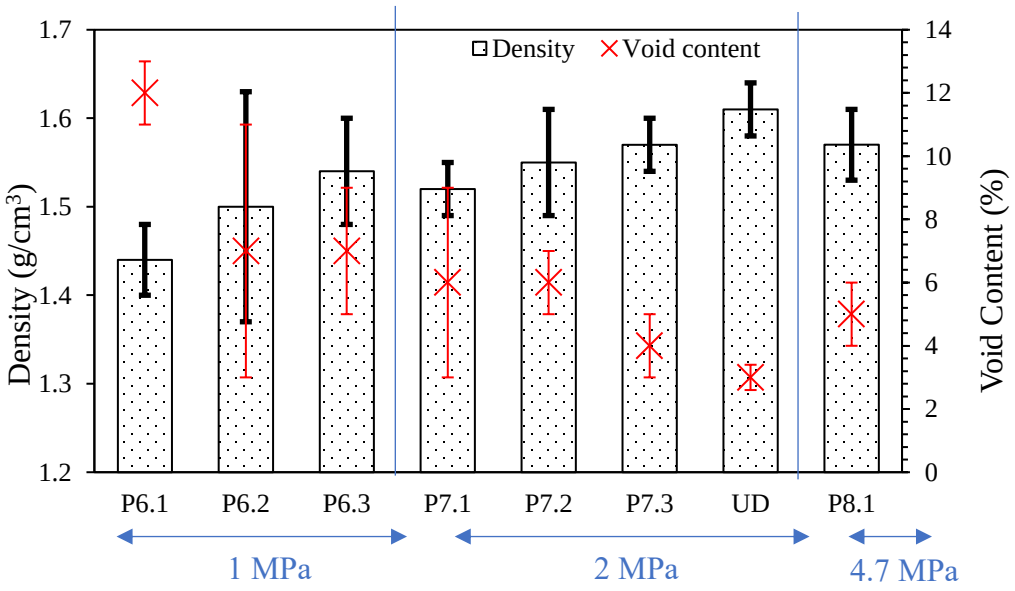

Figure 2.17: Density and void content for plates prepared at different pressure

The average void content for CF prepreg SMC composites prepared under 2 MPa pressure was 5 vol%. Same void content was reported for GF25/epoxy composite, while it was 9 vol% for GF70/epoxy composite [54]. Tensile and impact properties did not show direct correlation with void content for the CF prepreg composites. Inherent heterogeneity might overwhelm the effect of void content. However, low void content is desirable.

In Figure 2.18 (left), fifteen layers of chips can be seen in the cross-section. Each layer had a different fiber orientation. On the right, a magnified view shows circular and elliptical cross-sections of fibers. For all samples, there were different through thickness fiber orientation. The random fiber orientation contributes to the inherent inhomogeneity. There also were voids. Voids might be caused by the lack of resin flow under curing pressure with shorter cure cycle, missing chips in the SMC, and entrapped air [84, 85]. This implies that the distribution of voids was also arbitrary. Thus, random chip and void distributions resulted in point to point variations in the properties.

Modifying the cure cycle specially a longer cure cycle and/or slower cooling rate might be useful to reduce void content[85]. Chip missing might be resolved by optimizing the distance between the eyelets, conveyor settings. Aging might influence the viscosity and gel time of the resin. Since, it is necessary to understand the behavior of viscosity and gel time [86], and adjust the cure cycle accordingly.

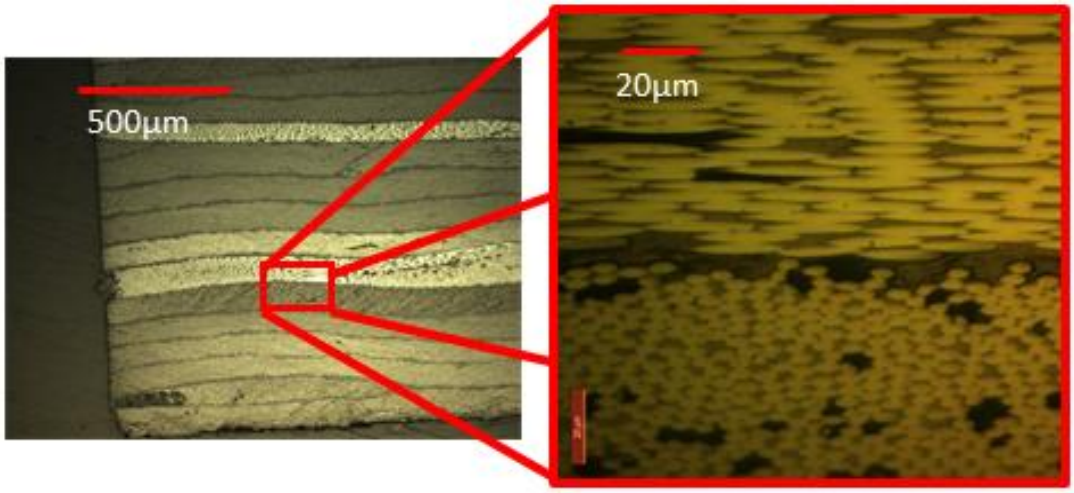

Figure 2.18: Optical micrograph of partial cross-section (left), magnified view showing fiber orientation and voids (right).

In general, the tensile strength of the plates varied by 20 to 40%. This scatter might result from the local microstructure. The preferential orientation of fibers might be influenced by the flow. During the SMC preparation, the chips fell in a random manner. Thus, through thickness fiber orientation was varied. Tensile failure occurred along the shear plane of loading, specifically, along the ends of chips or the curved portions of chips. The random distribution of these weakest links also played a role in the tensile strength. Thus, there was an overall heterogeneity in the material system. This type of variation has been reported previously for the HexMc prepreg material system [68].

Statistical analysis by JMP Pro software revealed that for the CF prepreg SMC plates, tensile strength, modulus and impact strength showed dependency on the age of the SMC and compression molding pressure. The analyses are shown in Appendix A2.1. It was found that impact strength and tensile modulus followed a decreasing trend while tensile strength followed an increasing trend as the compression molding pressure was

increased. However, it is hard to draw any conclusions because the prepregs were not of similar thermal histories. It is unknown how long prepreg was on the shop floor or was thawed before it was received at GT. In addition, a decrease in void content with increasing compression molding pressure did not improve the tensile strength, modulus and impact strength, which emphasizes the dominant effect of through thickness inhomogeneity.

2.6 Conclusions

The SMC equipment was modified to allow cutting of post-industrial CF prepreg tapes using the SMC technique. Initially, the SMC setup was designed for fabricating glass fiber systems. As the properties of carbon fibers in a CF-prepreg are very different than that of the GF systems, the SMC line could not be utilized to prepare SMC material from CF-prepregs. Hence, the existing SMC system was modified to process CF-prepreg wastes successfully; in particular, the blades and supporting sleeve were replaced with carbon steel blades and a harder PU sleeve. Calculations revealed that fiber cutting is due to flexural failure of the fiber, and that the critical radius of curvature is crucial for cutting the fiber. Furthermore, these calculations showed that the calculated critical radius of curvature for cutting the CF prepreg was five times higher than the actual measured critical radius of the blades.

Mechanical properties such as tensile strength, tensile modulus and impact strength were measured for the CF-prepreg composites and were compared to the properties of GF/epoxy SMC composites with fiber contents of 25 to 70 wt.% that were reported in literature [54]. The results were also compared to the lightweight commercial GF SMC composite. The overall comparison is presented in Table 2.9.

Table 2. 9: Comparison between GF SMC and CF prepreg SMC composites

Properties of composites	**GF25/epoxy [54]**	**GF70/epoxy[54]**	**Commercial GF SMC[75]**	**CF prepreg SMC [this work]**
Fiber content (wt.%)	25	70	50	72
Tensile strength (MPa)	72	240	66	150
Tensile modulus (GPa)	6.2	17	15	40
Impact strength (KJ/m^2)	68	200	-	144
Density, ρ_{exp} ($\rho_{theoretical}$) (g/cc)	1.25 (1.31)	1.67 (1.81)	1.9	1.53 (1.6)
Void content (vol.%)	5	9	-	5 (at 2MPa)

Based on this comparison, the CF prepreg composite is 8% lighter than the GF70/epoxy composite and 18% lighter than the commercial GF SMC composites [54, 75]. The most important thing to note in Table 2.9 is the tensile modulus. The average tensile modulus for the CF-prepreg composites was 40 GPa, while it was only 17 GPa for the GF70/epoxy composites. This result suggests that the prepreg trim waste can be utilized for making lightweight composites for high modulus applications.

The theoretical tensile modulus was also calculated using micro-mechanical model for short fiber reinforced composite, and was found to be 69 GPa. It was higher than the average experimental value of 40 GPa. This discrepancy might result from manufacturing defects such as voids, resin rich areas, and chip curl. These defects might also result from a shorter cure cycle and the ability of the resin to flow.

However, the high average value of the specific tensile strength (98 kPa.m^3/kg, which is 70% higher than GF25/epoxy, 65 % higher than commercial GF SMC , and 31% lower than GF70/epoxy SMC composites) and high specific modulus (more than two times higher than GF70/epoxy and three times higher than commercial GF SMC composites) suggest that CF prepreg SMC will be suitable for light-weighting in automotive applications. Certainly, the recycling of CF prepreg is environmentally friendly and adds value to the economy as an alternative to throwing away the prepreg trim waste with the attendant landfill fees and environmental effects. One would like to utilize post-industrial prepreg regardless of its age or thermal history. Thus, it is necessary to assess the quality of the incoming material to determine appropriate processing conditions. In the next chapter, methods will be developed for the quality assessment of the as-received prepreg trim waste.

CHAPTER 3

DEVELOPMENT OF A METHOD TO ASSESS THE QUALITY OF THE POST-INDUSTRIAL CARBON FIBER PREPREG

The out-time of incoming post-industrial prepreg is hard to track in the process of handling. The prepreg is shipped from Toray, where it is manufactured, to Boeing's facilities, where it undergoes lay-up. During lay-up, some amount of thawing occurs between consecutive uses of material from the same roll of the prepreg and, as a result, more out-time may occur before the material arrives at Georgia Tech. Consequently, it is difficult to categorize the thermal history of the post-industrial prepreg used for this thesis in a systematic way. Yet it is important to predict the behavior of the material based upon the amount of curing that occurs before processing into the final product, i.e., an aging scale that ranges from fresh to aged, because cutting the prepreg and converting it into SMC is affected by its thermal history and aging. Fresh tape can be cut and successfully converted to SMC but, because of its tackiness, it sticks to the cutting blades and requires the use of lubricant. Initial observations indicate that very aged tape is cut successfully by the SMC cutting head into chips that however do not produce a SMC that is well stuck together and hence easily handled. Thus, a question that arises is whether or not there is an optimum aging period for the prepreg, so it can be both cut and made into a good SMC. It is also possible that the prepreg age may affect the final mechanical performance of the resulting composites.

In the literature, various characterization techniques have been reported for aging studies of polymer resins. Dynamic mechanical analysis (DMA) has been performed on the prepreg in the single cantilever beam mode. It has been reported that the gelation and vitrification temperatures are decreased with aging [87]. Rheology has been performed on resin without fibers. This is an effective way to determine the increase in melt viscosity and decrease in gel time with aging [86]. For the prepreg, DMA did not provide conclusive data. Rheology could not be performed because it is hard to extract resin from the prepreg for testing. Cole et al. reported a decrease in interlaminar shear strength (ILSS) with aging of prepreg as measured by short beam testing [88]. However, a recent study showed insignificant aging effects on the ILSS [89]. So, this technique might not be useful to characterize the aging effect. Thermal analysis via Differential Scanning Calorimetry (DSC) has been reported as a helpful technique for aging studies of resin and prepregs [90]. The sub-ambient glass-transition temperature has been a significant indicator of aging. Other key parameters are heat of reaction, peak temperature of exothermic reaction, degree of cure, and activation energy.

In this chapter, a study on thermal analysis via DSC, conducted to categorize the incoming prepreg tapes based on the cure kinetic values with aging, is presented. This study focused on the behavior of heat of curing reaction, thermal transitions, degree of cure, and activation energy to predict the thermal history of the tapes. The evolution of the endothermic peak was of interest as it was not present for all aging conditions. In addition, a further study was performed to cut the tapes in the SMC cutting head for different aging conditions to determine the effect of aging on cutting quality.

3.1 Effect of aging on the ability to cut the prepreg in the SMC cutting head

As mentioned in Chapter 2, SMC was introduced to utilize post-industrial aerospace grade prepreg. It is essential to have a well and completely cut prepreg to make good SMC material. But because fresh prepreg is tacky, sometimes it is hard to cut the prepreg as desired. Fresh prepreg can only be cut with the simultaneous application of mold release agent, which is not desirable. Thus, the aging of the prepreg in an oven was used to resolve the issue. Oven aging advanced the cure of the resin, reduced its tack, and increased its brittleness. It is hypothesized that this leads to a cleaner cut. Indeed, oven aging of prepreg for 36 hours at 70^{o} C resulted in a complete and clean cut with no sticking to the rollers or blades. Less than 36 hours of aging resulted in prepregs that were incompletely cut and stuck to the cutting head rollers, for example, the 24 hours oven aged prepreg, even though it was not as tacky as the fresh, unaged, as-received material. The 48 hours oven aged prepregs were also not tacky, yet longer aging caused spitting of the resulting prepreg chips along the fiber length. In addition, as-received prepreg with increased out-time also offered better cutting; for example, very old prepreg with 16 months room temperature (RT) aging, and prepreg that was oven aged for 36 hours followed by RT aging for four months. Table 3.1 explains the aging conditions for prepreg and the observations with aging. The table also clarifies the reasoning for the aging conditions used in this thesis research.

Table 3. 1: Aging conditions to resolve the sticking issue of tacky prepreg and attain a good cut

Aging condition	**Observation after aging**
Fresh (minimum out-time / no aging at GT)	Sticks to cutting head, lubrication needed to have a complete cut.
12 hours oven aging at 70 ^{o}C	Tackiness-related cutting issue exists.
24 hours oven aging at 70 ^{o}C	Less tacky. However, cutting issue prevails.
36 hours oven aging at 70 ^{o}C	Not tacky. Complete cut.
48 hours oven aging at 70 ^{o}C	Not tacky. Splitting along the fiber length.
16 months RT aged (NA-16)	Not tacky as received. SMC could not be prepared. However, tapes could be cut well. DSC revealed an endothermic peak around 60^{o}C which was uncommon for fresh or prepreg oven aged for up to 48 hours.
36 hours oven aged followed by 4 months of RT aging (OA-RT-4)	Not tacky. Complete cut was attained. Endothermic peak was observed.

For the 16 months RT aged prepreg, DSC thermograms revealed an endothermic peak around 60^{o}C, which was uncommon for fresh or prepreg that was oven aged for up to 48 hours. 36 hours oven aged prepreg was also kept at room temperature for up to 4 months to determine how long it takes to evolve the endothermic peak, if at all. The detail study is described in section 3.3.3. Thus, the endothermic peak might be used to understand the behavior of the prepreg with aging.

However, both 16 months RT aged and 36 hours oven aging followed by 4 months RT aged prepreg chips were not tacky at all. SMC could not be prepared with these dry chips. But these chips could be utilized to make composite plates by manually sprinkling the chips into the mold. Further mechanical performance analysis is required to compare

plates made from aged chips to plates made using conventional SMC material to determine its future application. The fabrication of composite plates from aged chips and corresponding mechanical performance will be discussed in Chapter 4.

At this point, it is necessary to classify the incoming prepreg and aged materials along a general scale of aging. In the next sections, the various parameters obtained from thermal analysis are discussed and used to categorize the material.

3.2 Experimental section

3.2.1 Material and specimen preparation

The prepreg was received in the form of unidirectional carbon fiber reinforced epoxy resin tapes. This prepreg is prepared by Toray America Inc. and supplied by the Boeing Company. The material is Toray 3900-2B epoxy/T800S carbon fiber prepreg. The resin content is 35.5 weight % of the prepreg. T800S carbon fiber is the reinforcement. The prepreg tape used in the thermal analysis was 38 mm wide. The initial material all had the same thermal history. The fresh spools were kept in zip-lock bags in a freezer at 0^{o}C. The tapes were cut using scissors into 1-meter lengths and aged in a convective oven (1602 Hafo series oven manufactured by Sheldon Manufacturing Inc., part number: 9070591) for 12, 24, 36 and 48 hours at 70^{o} C. Hence, there were five main categories of material on which this aging study was performed: fresh (minimum out-time), and oven aged for 12 hours, 24 hours, 36 hours, and 48 hours. Then, these materials were kept in an environment of room temperature (RT) of about 23^{o} C and relative humidity of 55%. Thermal analysis was performed on a weekly basis to determine any thermal behavior trends with time. To be clear, the materials tested were both oven aged and aged at room temperature for various amounts of time. However, the prepreg material termed “fresh” was not oven aged.

For sample preparation, about 8 to 10 mg of prepreg were cut and set into an aluminum hermetic pan and sealed with a lid. For comparison purposes, two types of extremely aged prepreg tapes with unknown thermal histories were analyzed. These two categories of aged prepregs are listed at the end of Table 3.1. The first one was very old, non-tacky prepreg, which was room temperature aged in the Georgia Tech Manufacturing Institute high bay for 16 months. These prepregs are termed as naturally aged (NA-16). The second one was oven aged at 70^{o} C for 36 hours and then RT aged for 4 months. These prepregs can be termed as oven aged-RT aged (OA-RT-4).

3.2.2 Thermal analysis via DSC

Thermal analysis was performed with a DSC Q2000 (TA Instruments). The samples were equilibrated at -10^{o}C for a few minutes. Then, the samples were heated from -10°C to 300°C at 10°C/min to investigate the thermal transitions occurring in this temperature range. Heat flow, heat of reaction, thermal transitions, degree of cure, and activation energy are crucial to understand the behavior of the prepregs with aging.

There are two distinct thermal transitions in the heat flow diagrams for fresh and aged prepregs, which are endothermic and are probably associated with the glass transition of the resin system. However, because the chemistry and formulation of the resin system is not known, only the relative positions of these transitions can be recorded as a function of the prepreg aging. For the same reason the transitions are referred to as TT1 and TT2. The prepregs under longer aging, OA-RT-4 and NA-16 as mentioned in Table 3.1 do not have the TT1transitions. These two categories of aged prepreg show a separately identifiable sharp endothermic peak. These transitions and peaks will be discussed in detail in section 3.3. A heat flow curve in Figure 3.1 is presented to show TT1, TT2 and the

exothermic reaction peak. The exothermic peak is used to calculate the heat of reaction/residual enthalpy by integrating the area under the peak. The heat of reaction is also used to measure the degree of cure.

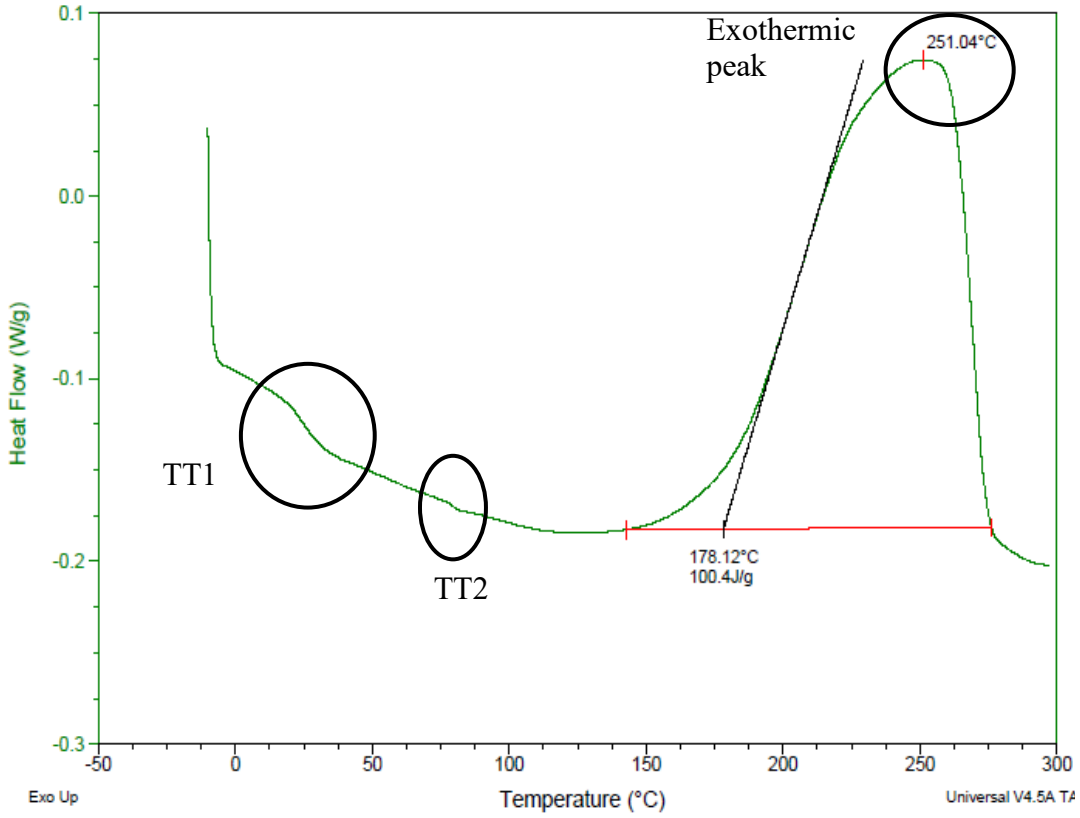

Figure 3.1: Calculation of enthalpy from exothermic peak for an aged prepreg

The degree of cure describes the extent of conversion in a curing reaction. It measures the advancement of the reaction based on the heat of reaction. In this study the degree of cure with aging was calculated using the heat of reaction of as-manufactured fresh material as the total heat of reaction, as shown by Equation 3.1.

$$H_t = \int_0^{t_f} \frac{dQ}{dt}\, dt \tag{3.1}$$

Here, H_t = total heat of reaction.

dQ/dt = rate of heat generation in a dynamic DSC run

t_f = time required to complete the reaction.

The heat evolved in any time, t, at a constant curing temperature, T, is determined from an isothermal experiment. In this study, t is the room temperature aging time. This can be simulated as an isothermal DSC experiment and can be expressed by equation 3.2.

$$H = \int_0^t \frac{dQ}{dt}\, dt \tag{3.2}$$

where

H= instantaneous heat released at any time t

dQ/dt= rate of heat generation in an isothermal experiment at a constant temperature T.

The room temperature aged prepreg had progression of curing at RT while the prepregs were kept at room temperature. DSC was performed on the aged prepreg sample with a heating ramp of 10^{o}C/minute. Thus, a residual heat, H_r, was calculated from the exothermic peak obtained in the dynamic DSC performed on the aged material. H_r can be stated as Equation 3.3.

$$H_r = \int_t^{t_f} \frac{dQ}{dt}\, dt \tag{3.3}$$

Thus, Equation 3.3 can be re-written as $H_{r=}$ H_t-H and the degree of cure (α) can be expressed as a ratio of heat of reaction at any time, H, to the total heat of reaction, H_t. This results in equation 3.4.

$$\alpha = \frac{H}{H_t} = \frac{H_t - H_r}{H_t} \tag{3.4}$$

For calculating α, the value for H_t was provided by the Toray America, Inc. and the value was 158 J/g. H_t was obtained by integrating the exothermic peak from the DSC thermogram of as manufactured prepreg in the manufacturing site. In the GT lab, the value of H_r was measured from the exothermic peak of DSC thermogram on aged prepreg.

An understanding of the curing process activation energy is helpful, because it is an important cure kinetic parameter that changes significantly with aging. Here, ASTM E698 was followed based on the Flynn, Wall and Ozawa method [91]. It is assumed that activation energy (E_a) changes as a function of degree of cure throughout the curing reaction [92, 93]. Three different heating rates (β) 10, 5 and 2°K/min were used for dynamic DSC runs as per the ASTM standard. The temperatures at which the exothermic reaction peaks occurred were plotted as a function of their corresponding heating rates. Using the Arrhenius equation ($\beta = Ae^{\frac{-Ea}{RT}}$), the activation energy (E_a) was calculated from the slope of the logβ versus (1/T) plot.

In the next section, cure kinetic parameters and their behavior with aging will be discussed. Thus, a better understanding will be obtained for categorizing the incoming post-industrial prepreg.

3.3 Results and discussion

3.3.1 Heat flow curve and thermal transitions

The heat flow curve was used to characterize the thermal behavior as a function of the oven aging time and the room temperature aging time. The thermal transitions and heat of reaction were recorded, analyzed and compared in order to identify the key features to assess the quality of the incoming prepreg.

Heat flow curves were studied for five differently aged prepreg samples on a weekly basis to observe any change of thermal behavior with RT aging. The five types include fresh (minimum out-time and no oven aging), 12, 24,36 and 48 hours of oven aging in 70^{o}C. Fresh prepreg and the four oven aged prepregs were then kept at room temperature (RT) for up to 7 weeks. Then DSC was performed on each of the five types of samples weekly. Figure 3.2 presents an overlay plot of DSC thermograms of the five types of aged samples after 3 weeks of RT aging. The black circle shows a thermal transition (TT1) between 9 and 30^{o}C that shifts upward with increasing oven aging time. This transition might be a sub-ambient glass transition temperature, which is a result of physical and chemical factors [86]. TT1 can be seen as a baseline shift in the heat flow curve during the 10^{o}C per minute ramp DSC run. A second thermal transition is marked by the dotted green circle near 80^{o}C. This transition (TT2) remained stable near 80^{o}C with aging even after seven weeks of aging.

Figure 3.3 shows an increasing trend of TT1 with oven aging time from 0 to 48 hours for the five aging conditions. However, TT2 did not show much change with oven aging time. As a result, TT2 might not be useful to categorize the prepreg in terms of aging because it varies little. Table 3.2 summarizes the changes in TT1 and TT2 with RT aging for the five types of prepreg samples during the seven weeks of aging. Each data point represents one DSC run, except for fresh material, for which three runs were performed. The standard deviation for TT1 was 0.06364^{o}C.

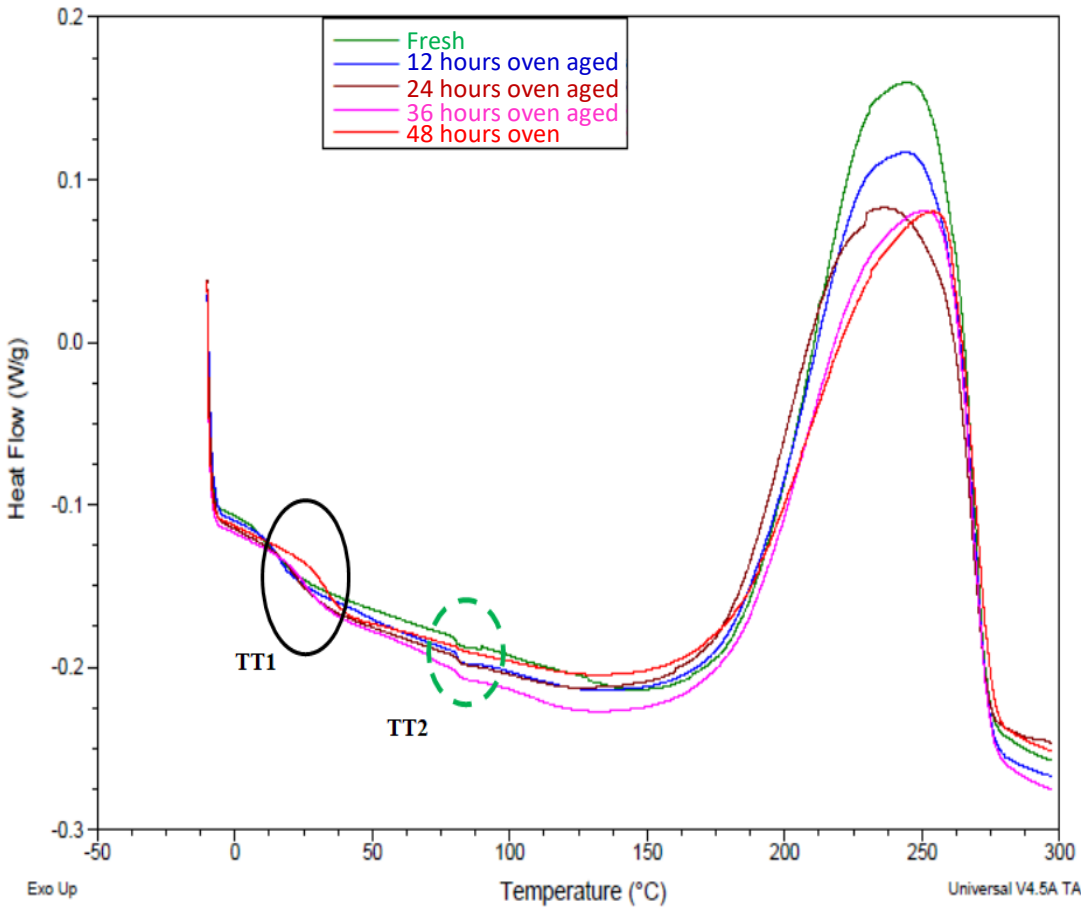

Figure 3.2: Heat flow curves for 5 different types of aged prepregs after 3 weeks of RT aging: Fresh (green),12 hours (blue), 24 hours (maroon), 36 hours (pink) and 48 hours (red) oven aged at 70^{o}C

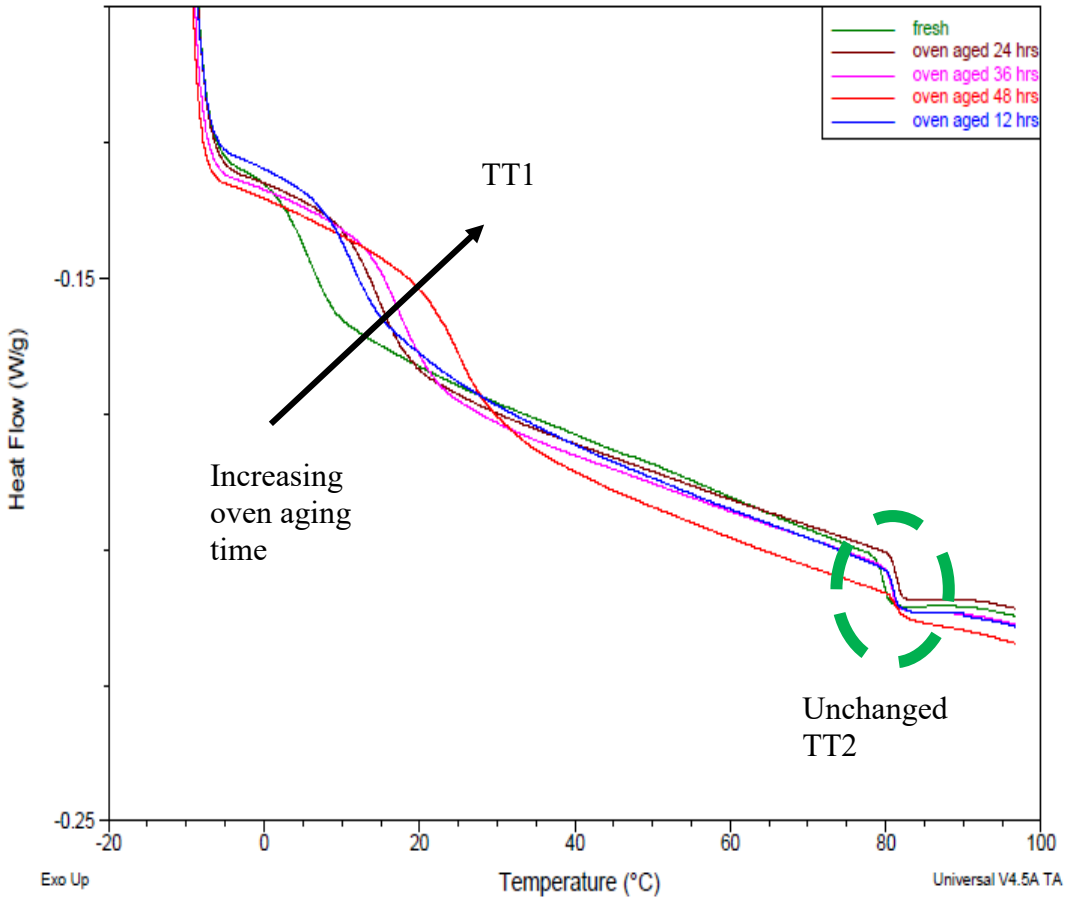

Figure 3.3: Trend of TT1 and TT2 with oven aging time. Oven aging was performed at 70^{o}C.

Table 3. 2: Changes of TT1 and TT2 for seven weeks of RT aging after oven aging at 70^{o}C

Material	**After oven aging (if any)**		**After oven aging + 1 week RT aging**		**After oven aging + 3 weeks RT aging**		**After oven aging + 4 weeks RT aging**		**After oven aging + 5 weeks RT aging**		**After oven aging + 6 weeks RT aging**		**After oven aging + 7 weeks RT aging**	
	TT1 (^{o}C)	TT2 (^{o}C)	TT1 (^{o}C)	TT2 (^{o}C)	TT1 (^{o}C)	TT2 (^{o}C)	TT1 (^{o} C)	TT2 (^{o}C)	TT1 (^{o}C)	TT2 (^{o}C)	TT1 (^{o} C)	TT2 (^{o}C)	TT1 (^{o}C)	TT2 (^{o}C)
Fresh	6.31	79.7	6.08	78.7	9.75	80.9	11	81.9	12	80.1	18	81.1	23	79.5
Aging 12 hours	12.5	80.9	11.9	79.4	14.6	81.1	15.8	78.9	16.4	81.1	24	83.6	25	80
Aging 24 hours	14.5	81.2	14.4	78.8	20.3	81.5	21.1	81.5	24	79.9	30	81.1	31	81
Aging 36 hours	16.5	80.7	16.5	79.4	25.9	81.9	26	80.7	27.3	81.4	33	79.9	38	83
Aging 48 hours	24.4	81.4	23.6	80.1	32.9	81.9	36.2	83.2	36.8	80.1	39.5	81.9	41	82

In addition to the effect of oven aging on TT1 and TT2, the effect of RT aging was also investigated. Figure 3.4 shows the location and shapes of the transitions for fresh prepreg (minimum out time) with increasing RT aging time. For fresh prepreg, TT1 increases with the aging time at RT while TT2 remains at 80^{o}C. The thermal transitions are rapid for the fresh and one-week aged prepregs whereas the three to seven weeks aged prepregs showed more gradual thermal transitions.

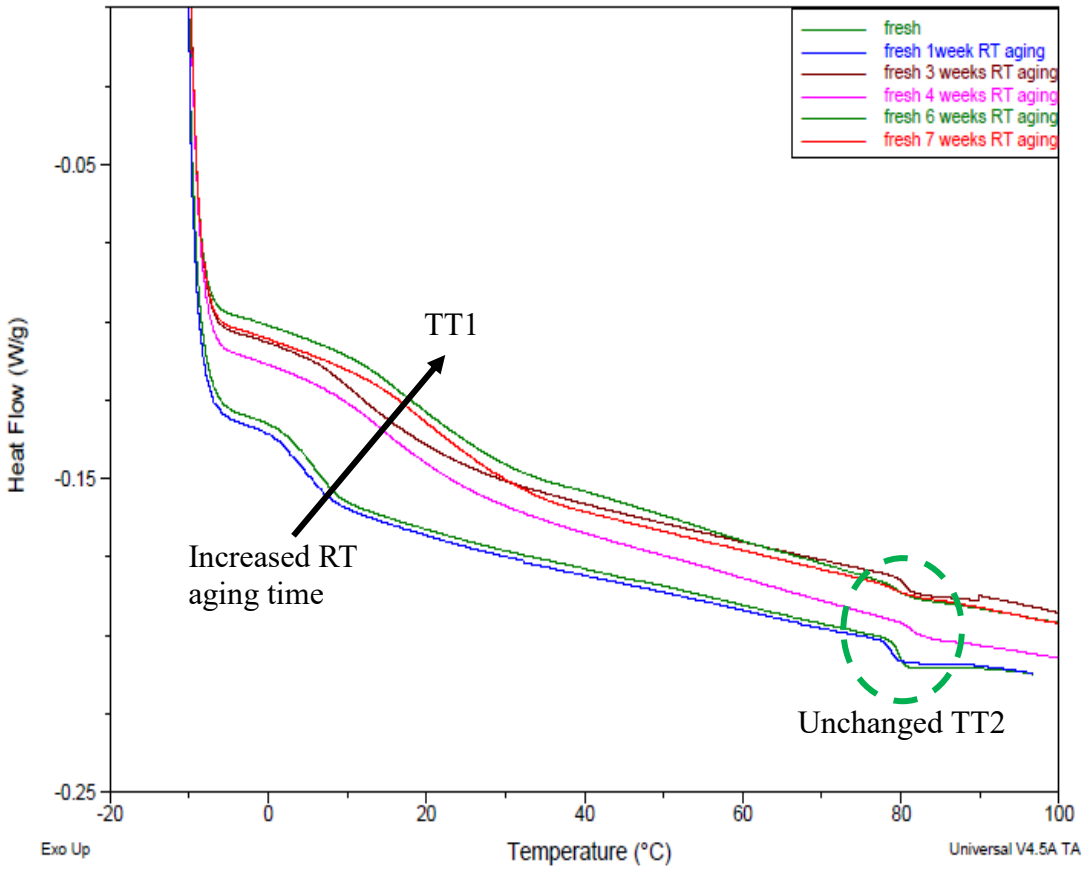

Figure 3.4: TT1 and TT2 with increasing RT aging time for fresh (as received) prepreg (no oven aging)

Since TT1 changes significantly with aging time, the TT1 temperatures of fresh, and oven aged prepregs were plotted against RT aging time to identify a correlation between the transition temperature and the aging time (Figure 3.5). Before aging at room temperature, the transition temperature increased with oven aging time with the lowest value for the fresh prepreg. For example, TT1 was 6.31^{o}C for the fresh prepreg while for the 48 hours oven aged sample, it was 24.4^{o}C. With increasing oven aging time, there might be some advancement of the curing reaction, which causes the transition to occur at a higher temperature. This implies that, with oven aging time, the transition required extra energy to overcome the advancement of curing reaction. When the fresh and the oven aged prepregs were aged at room temperature, the transition temperature increased with the RT aging time. For example, the TT1 temperature for fresh prepreg increased to 23^{o}C from 6.31^{o}C during 7 weeks of RT aging. Hence, it can be observed that RT aging results in an increasing trend of TT1 similar to that of oven aging. To better understand this increasing trend of the transition temperature, the TT1 temperature versus RT aging time was fit with a second order polynomial equation as shown in Equation 3.5.

$$y = ax^2 + bx + c \tag{3.5}$$

Where, y is TT1 and x is the aging time in weeks.

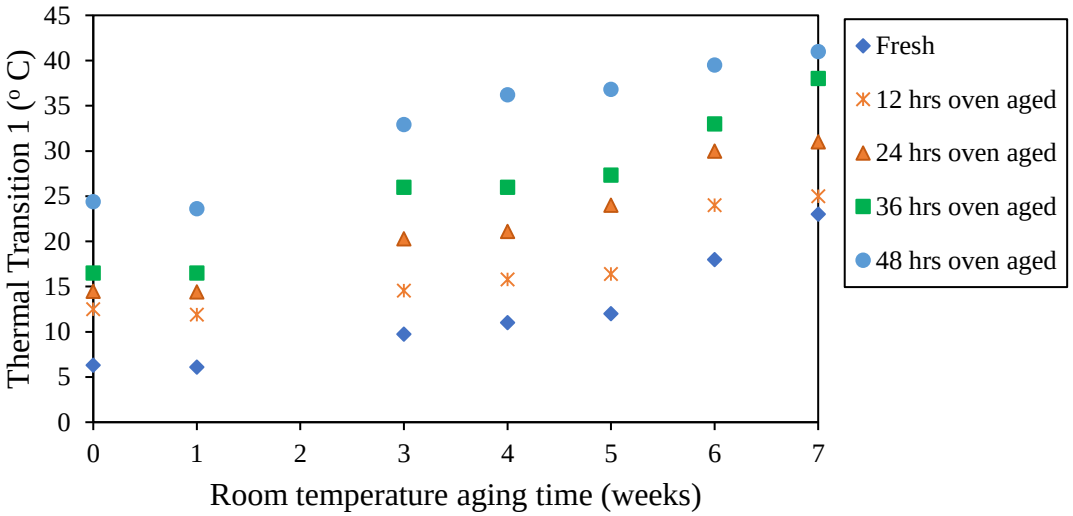

Figure 3.5: Thermal Transition 1 (TT1) versus RT aging time for five RT aged prepregs

The coefficient, constant and R^2 values for fitted equations obtained from TT1 versus RT aging time plots are presented in Table 3.3. These results show that TT1 increases parabolically with RT aging time.

Table 3. 3: Coefficient, constant term and R^2 values for curve fitted equations obtained from TT1 versus RT aging time plots

Sample Thermal History	**A**	**b**	**c**	**R^2**
Fresh prepreg RT aged	0.0083	-0.0804	6.4648	0.98
12 hours oven aged followed by RT aged	0.0072	-0.0809	12.396	0.94
24 hours oven aged followed by RT aged	0.0039	0.1725	13.938	0.97
36 hours oven aged followed by RT aged	0.0034	0.2666	16.056	0.96
48 hours oven aged followed by RT aged	-0.0029	0.5169	22.783	0.96

During the aging process in the oven and at room temperature, samples of the prepregs were obtained to study in the SMC line. It is noted that the fresh material was tacky and difficult to cut whereas aging helps to cut them properly. As the material was aged at 70^{o}C in the oven, it was observed that an aging time of at least 36 hours is necessary to achieve completely cut the prepregs. Similarly, fresh prepreg needs about seven weeks of room temperature aging to reduce the tackiness enough so that it can be cut completely. A TT1 temperature of 16.5^{o}C might be a lower limit that indicates that the prepreg can be successfully cut by the SMC cutting head. Hence to recycle the prepreg tape utilizing SMC, a TT1 temperature above 16.5°C as measured by DSC, must be present before processing. If the TT1 is below 16.5^{o}C the prepreg needs to be further aged to attain that TT1. Prepregs with TT1 higher than TT1 that are oven aged for at least 36 hours or seven weeks of RT aged were non-tacky. Therefore, this type of prepreg could be cut in the SMC cutting head completely. However, SMC sheets that were readily handled could not be formed.

In the next section, heat of reaction, degree of cure and activation energy will be discussed to explain how these kinetic parameters changes with aging. Since, these parameters are inter-dependent.

3.3.2 Heat of reaction, degree of cure and activation energy

The heat of reaction, (H_r) is the enthalpy associated with the exothermic curing reaction of the resin and is calculated by integrating the area under the exothermic peak of heat flow curve obtained from dynamic DSC runs. A linear baseline is used to calculate the area. DSC was performed on one sample of each category of prepreg to obtain the heat of reaction. Figure 3.6 exhibits the decreasing trend of heat of reaction with RT aging time and for oven aging time for each category of prepreg. Samples that were oven aged for 48

hours and then RT aged resulted in 24% of decrease in heat of reaction as compared to those samples that were only RT aged. Similarly, these samples had 19% decreases in heats of reaction during RT aging for four weeks (three to seven weeks). This implies that both room temperature and oven aging had a significant effect on heat of reaction. The decreasing trend of heat of reaction with RT aging has been reported in the literature for IM7-8552 prepreg [90]. Both oven aging and RT aging might provide energy to advance the curing reaction. This agrees with that fact that, during aging, there might have been advancement of curing reaction for the prepreg samples as discussed in section 3.3.1. The plot of degree of cure versus aging time in Figure 3.7 further emphasizes this fact. The degree of cure was calculated using Equation 3.4 for five categories of prepreg samples, while H_t was taken as the enthalpy for as manufactured fresh prepreg (H_t =158 J/g provided by the Toray America, Inc.) and the residual enthalpy (H_r) value was the heat of reaction for each category of prepreg samples. An increasing trend was observed with both oven aging time and room temperature aging time in Figure 3.7. This means there was advancement of reaction with aging.

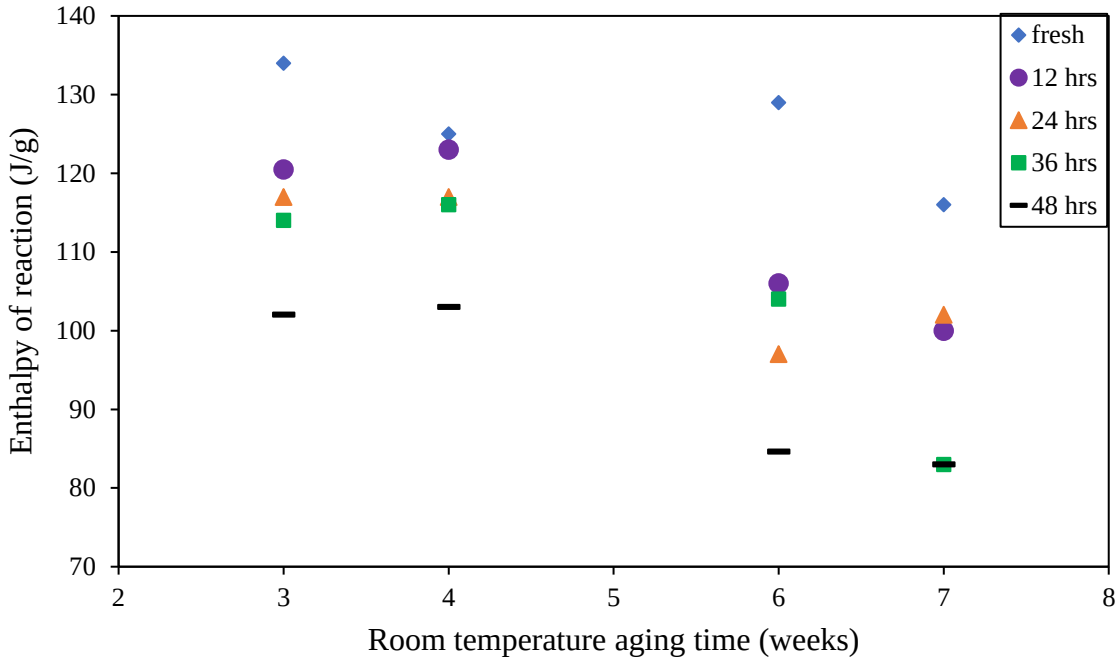

Figure 3.6: Enthalpy of reaction with aging at room temperature

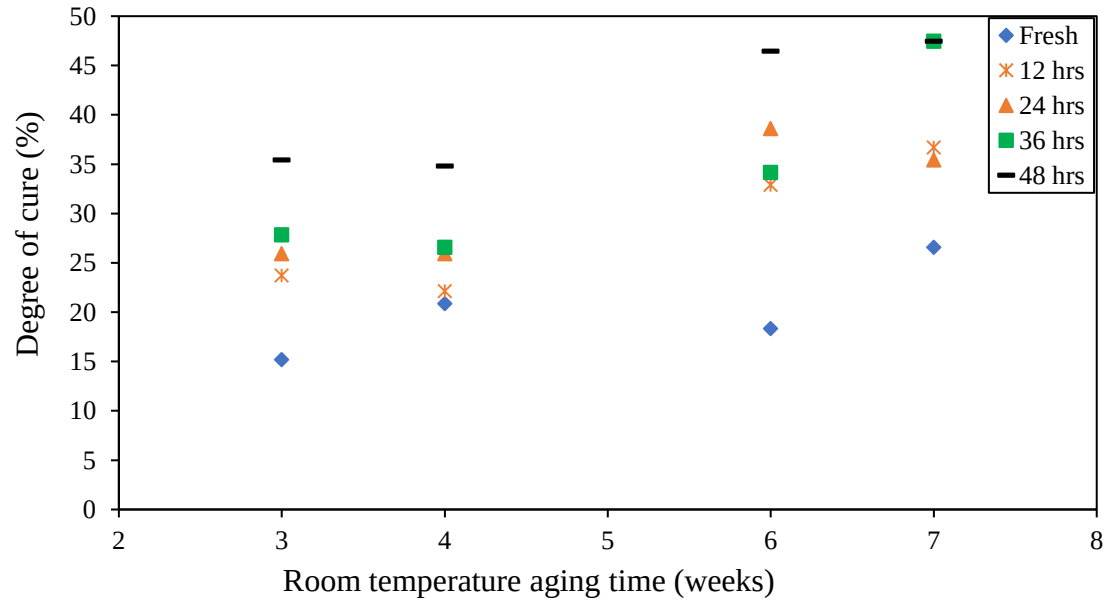

Figure 3.7: Degree of cure with oven aging and room temperature aging

The thermal analysis based on heat of reaction and degree of cure may be helpful in guiding the processing of incoming prepreg from industries. For example, fresh prepreg after RT aging of seven weeks is suitable to be utilized in the SMC line which has a degree of cure of about 27%. Hence, the degree of cure of the incoming prepreg can determine whether it needs further aging before feeding into the SMC line.

The process of curing reaction can also be explained in terms of activation energy of the reaction. To determine the activation energy (E_a) of the prepregs with different aging conditions, a plot of $\log_{10}(\beta)$ versus $1/T_{peak}$ was obtained. T is the reaction exothermic peak temperature in degrees Kelvin. E_a was calculated based on the slope of the curve, assuming an Arrhenius relationship. Figure 3.8 shows a linear trend of y= mx+C equation form for each of the three categories of material. E_a was evaluated for each type of prepreg to observe the trend for three extreme cases of aging. These are fresh, oven aged with room temperature aging for 4 months (OA-RT-4), and naturally aged or room temperature aging for 16 months (NA-16) to simulate a real life prepreg resource.

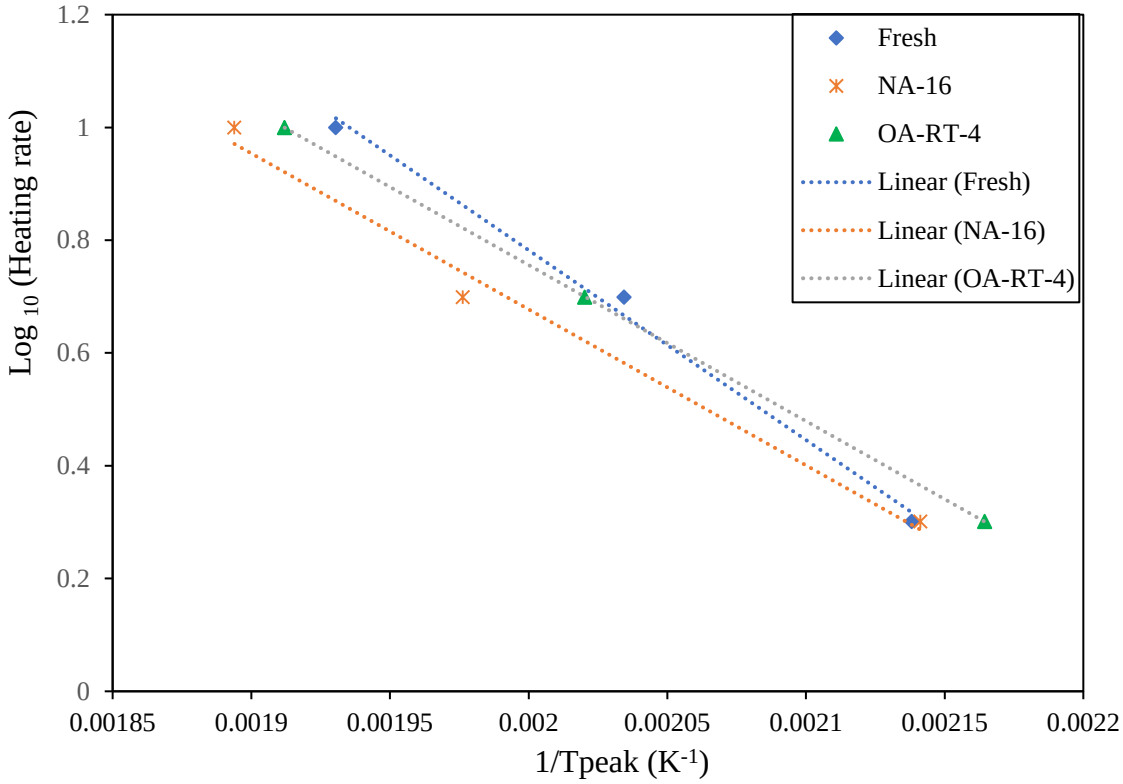

Figure 3.8: Activation energy evaluation for fresh, NA-16 (RT aged for 16 months), OA-RT-4 (oven aged at 70°C for 36 hours followed by RT aged for 4 months) prepreg tapes

Details of the material and the measured activation energies are reported in Table 3.4.

Table 3. 4: Activation energy with aging

Material	**Specification**	**Trendline**	**E_a (KJ/mol)**	**DOC (%)**
Fresh	Kept frozen as received	Y=-3365.8x+7.5, R^2=0.9936	61.3	16.4
OA-RT-4	Oven aged for 36 hours, followed by 4 months RT aging	Y=-2768.1x+6.3, R^2=1	50.4	48.0
NA-16	RT aged for 16 months	Y=-2766x+6.2, R^2=0.9878	50.4	45.8

A decrease in E_a was observed with aging. Long-term room temperature aging had a similar effect as oven aging followed by room temperature aging. It was observed that E_a decreases with increasing degree of cure. The literature suggests that the decrease in E_a with increase in degree of cure might be due to an autocatalytic effect in the curing process [94, 95]. It further emphasizes the fact that cure advancement might occur with aging, which results in lower activation energy for the curing reaction. Hence, the activation energy can be calculated for the incoming post-industrial prepreg and used to determine its behavior on the scale of fresh to very old. Both the OA-RT-4 and NA-16 prepregs could be cut completely in SMC Cutting head. However, aging turned them into non-tacky material and SMC sheet could not be prepared from those prepregs. Thus, an activation energy value of 50 KJ/mol can be used as the lower limit to accept the incoming prepreg for recycling into SMC. The literature also suggested an activation energy of 50 KJ/mol for IM7/977-3 prepreg after 2 months of RT aging, whereas the value was 53 KJ/mol for an unaged sample [87]. To explore the possibilities of the aged prepreg, composite preparation and mechanical performance for non-tacky aged prepreg will be studied in Chapter 4.

Thermal analyses based on heat of reaction and degree of cure show that there was advancement of curing reaction with both oven aging and RT aging. This study revealed that to utilize the incoming prepreg in a SMC line, the desired degree of cure was about 27% to attain a complete cut. The study of the activation energies of fresh to extremely aged prepregs helped to determine a lower limit of E_a for aged prepregs to be recycled. Thus, a combination of cure kinetic parameters will be helpful to better understand the appropriate aging conditions of incoming, post-industrial prepregs.

In the process of the thermal analysis, it was observed that, with aging of the prepregs, an endothermic peak evolved for only OA-RT-4 and NA-16. Therefore, further study was performed to investigate the behavior and reasons for which the peak occurs.

3.3.3 Endothermic peak

The evolution of the endothermic peak can be helpful to categorize incoming prepreg. These peaks occur only in prepreg NA-16 and OA-RT-4 samples. These are shown by the red and black lines respectively in Figure 3.9. For comparison, the green line shows the heat flow curve for fresh prepreg. However, fresh prepreg does not show an endothermic peak. In addition, oven aged prepreg does not show this peak. Thus, the appearance of an endothermic peak represents the aged end of the scale from fresh to aged prepreg.

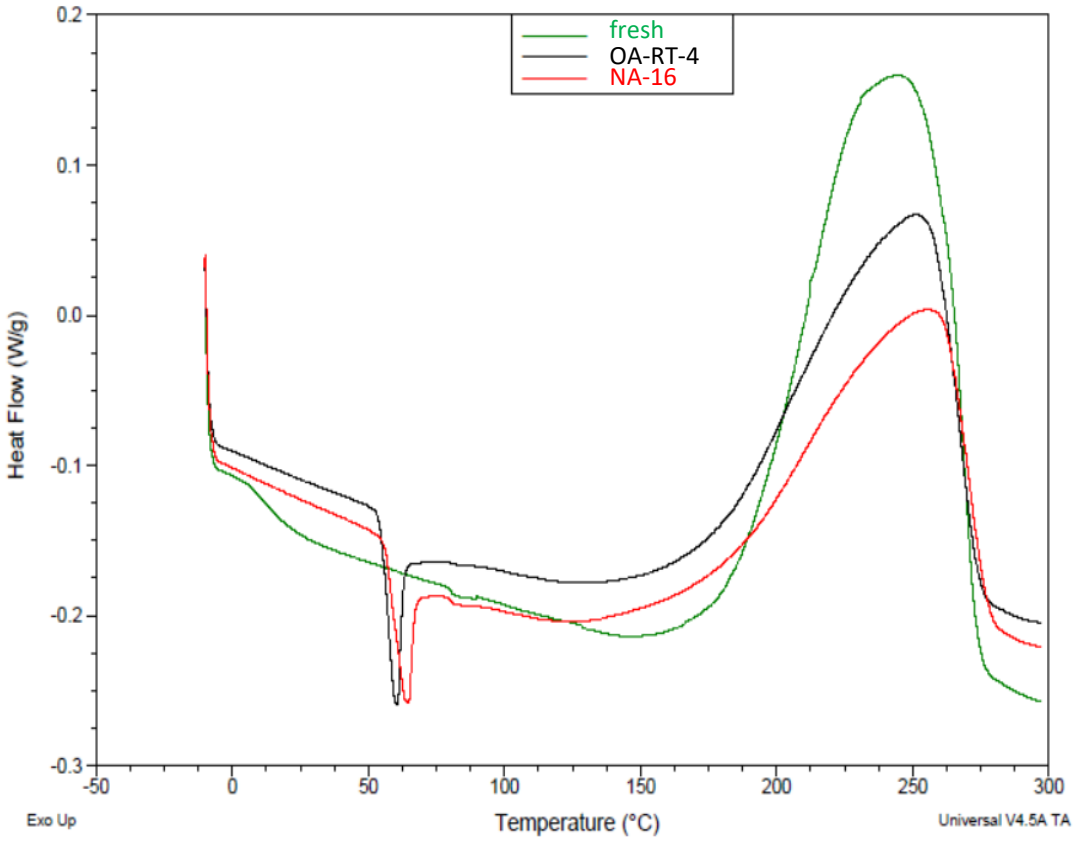

Figure 3.9: Occurrence of endothermic peak in the heat flow curve with RT aging

Further investigation via heat-cool-heat runs (Figure 3.10) show that the endothermic peaks are non-reversible. The heat-cool-heat run was performed in three stages: (1) heating from -40 to 300^{o}C; (2) cooling from 300 to -40^{o}C; and (3) heating from -40 to 80^{o}C. In the first stage heating, the endothermic peak could be observed. However, during second stage heating, the peak was not visible. Thermogravimetric analysis further clarified that this behavior was not influenced by moisture content (Figure B3.1). However, longer oven aging for nine days showed an endothermic peak at 100^{o}C (Figure B3.2). For comparison, all the heat flow curves for fresh to different aging conditions were plotted together (Figure B3.3).

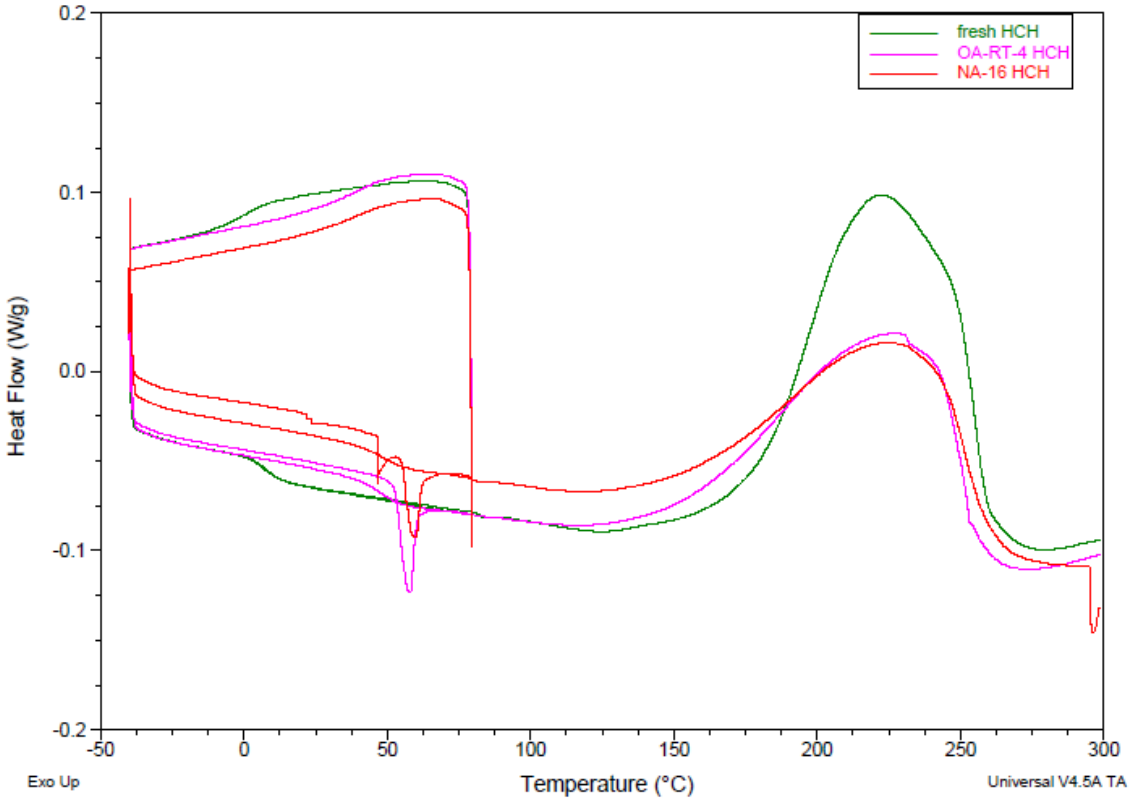

Figure 3.10: Heat cool heat cycle for fresh (green); oven aged at 70° C for 36 hours followed by 4 months RT aging (pink); and RT aging for 16 months (red) prepreg

According to the literature, the endothermic peak might occur from physical aging in epoxy resins [96]. Physical changes during aging occur from changes in molecular structure. This might result in changes in the free volume and configuration of the molecular network. The more time the polymer molecules get, the easier it becomes for them to reconfigure themselves to a lower energy configuration. It was also reported that longer aging time results in a decrease in specific volume. From a thermodynamic point of view, the specific enthalpy (h) can be written as h=u+pv, where u is specific energy, p is specific pressure, and v is specific volume. This enthalpy definition is more useful when considering the change from a reference point by dh=du+pdv+vdp. The aging was done at ambient pressure. So, the equation can be rewritten as dh=du+pdv. Thus, it might be said

that physical aging causes a decrease in enthalpy resulting from a decrease in free volume in the molecular network and in the internal energy of atoms due to reconfiguration with aging. Thus, endothermic peaks were observed after longer aging at room temperature, which was not visible for shorter RT aging. With longer aging, the resin molecules in the prepreg had enough time to reconfigure the molecular network such that the free volume as well as the change in internal energy were observable.

3.4 Conclusions

As the thermal history of incoming scrap prepreg is unknown, the study of its aging condition is crucial for recycling and its further use. Material behavior and performance can be controlled if it is known where the material falls along an aging scale of fresh to aged. The thermal analysis of incoming post-industrial prepreg demonstrated that cure kinetic values obtained from DSC dynamic runs, such as Thermal Transition 1(TT1), heat of reaction, degree of cure, activation energy, endothermic peak, are strong indicators of the ability to successfully cut the prepreg in a SMC line. TT1 and the degree of cure showed increasing trends with both oven aging and RT aging, whereas the heat of reaction showed a decreasing trend. This fact implies that aging results in the progression of the curing reaction with aging. The decrease in activation energy with longer RT aging supported this fact as well. Moreover, the advancement of the curing reaction results in non-tacky prepreg, which resolves the sticking issue in the SMC cutting head.

Based on the fact that the fresh (minimum out time) prepreg being aged at 70^{o}C for 36 hours or room temperature aged seven weeks was suitable to achieve a complete cut, the suggested TT1 is 16.5 ^{o}C or more whereas the degree of cure is of 27%. For the aged prepreg in a fresh to aged scale of prepreg, activation energy and endothermic peak may

be the identifying parameters. E_a of 50 KJ/mol might be used as the lower limit to attain a complete cut for aged prepreg. Endothermic peak could be observed only for OA-RT-4 and NA-16 prepreg. However, TT1 was not visible for these aged prepreg. The material could be cut completely in the SMC cutting head as well. Hence, it can be stated that a combination of kinetic parameters might be useful to identify the aging condition of the incoming prepreg more precisely and determine any further processing before feeding into the SMC cutting head for a complete cut without any mold releasing agent. A summary of the results is presented in Table 3.5.

Table 3. 5: Summary of cure kinetic parameters with aging, ability to cut and SMC sheet formability

	Fresh	**7 weeks RT aged**	**36 hours oven aged**	**48 hours oven aged**	**OA-RT-4**	**NA-16**
TT1 (^oC)	6.31	23	16.5	24.4	none	none
DOC (%)	16.4	27	27	35	48	45.8
Endothermic peak (^oC)	none	none	none	none	60	60
Activation energy (KJ/mol)	61.3	-	-	-	50.4	50.4
Cutting in the SMC cutting head	Sticking issue without MRA	Complete cut	Complete cut	Split along fiber length	Complete cut	Complete cut
SMC making	Good SMC sheet	Non-tacky and do not form SMC sheet				

Now that the aging condition has been optimized to obtain non-tacky prepreg that is readily cut on the SMC line, it is necessary to investigate the performance of the composites fabricated from aged prepreg compared to that of the fresh prepreg SMC

composites. The fabrication and performance of the aged prepreg composites will be discussed in chapter 4.

CHAPTER 4

MECHANICAL PERFORMANCE OF POST-INDUSTRIAL CARBON FIBER PREPREG SMC COMPOSITES

The aerospace industry produces a large quantity of carbon fiber/epoxy prepreg scrap that consists of high value resin and fiber. This chemically active, post-industrial material may be an inexpensive input to SMC fabrication because the aerospace industries must pay to dispose of it in a landfill [32]. This cheap scrap prepreg can be utilized in automotive industries to replace GF/epoxy SMC composites due mainly to their high strength to weight ratio [42]. This would be a positive solution for both aerospace and automotive industries.

Low manufacturing cost, high rate of production, ability to be molded in a complex shape, and reduction in overall part acquisition cost enable the use of SMC in the aerospace industry [75]. For example, the Boeing 787 uses Hexmc in its window frames. In a typical Hexmc, AS4/ Hexply 8552 unidirectional prepreg tape with dimensions of 50.8 mm by 8.4 mm is used. Consistent random distribution, which is needed for planar isotropy, has been reported in the Hexcel user guide for Hexmc. Another example of such a commercial material is Quantum Lytex 4149 [97]. It is noted that both Hexmc and Lytex prepreg tapes are not post-industrial scrap waste materials like the prepreg tapes used in this study.

A discontinuous fiber composite system made from Hexmc has been reported to have high tensile modulus. Feraboli et el. found tensile moduli of 20.68 GPa to 62.04 GPa with a high coefficient of variation of 19% for composites made of Hexmc [62]. They explained that this variation in the tensile modulus is due to the non-homogenous nature of

this material. Similar heterogeneity has been reported in randomly oriented strand systems of CF reinforced thermoplastic resin prepregs [66]. Tensile failure has been observed in thermoplastic composites, due to either strand (chip) breaking or disbanding of the strands, caused by interlaminar shear between the strands. In another study, four different failure modes were specified [98]: strand pullout, strand breaking, wedge pullout, and mixed mode failure. In most studies, impact properties were not investigated for randomly oriented prepreg chip composites. However, it is crucial to understand the behavior of the post-industrial prepreg SMC composite under impact loading, so as to show its applicability in automotive industries.

Fresh (unaged) prepreg composites showed promising mechanical performance compared to the conventional GF/epoxy composites as presented in chapter 2; but, as discussed, it is challenging to cut the fresh prepregs with a SMC line as they tend to stick to the cutting and support rolls. Hence, a methodology was developed to categorize the aging condition of the prepregs along with the ability to cut in the SMC cutting head discussed in Chapter 3 and summarized in Table 3.5. In this chapter, the fabrication of composites from aged prepreg chips and their mechanical performance will be studied. Then, comparison between the mechanical performance of test plaques fabricated from the fresh and aged prepregs will be presented. Finally, it will be determined if the mechanical properties of post-industrial prepreg composites are good enough for automotive applications, regardless of aging condition.

In this chapter, both uniaxial tension and Charpy impact tests were conducted to investigate the mechanical performance of post-industrial prepreg waste. Furthermore, the

failure modes of these composite materials were explored and provided an insight into their process-property relations.

4.1 Materials

Two different aging conditions were considered for aging prepreg for mechanical performance analysis: (1) 70^{o}C for 36 hours in an oven and (2) room temperature for about 16 months. These samples are termed oven aged and naturally aged (NA-16), respectively. The oven aging technique is faster, as the spools are heated at an elevated temperature to make the prepreg dry and crispy, therefore suitable for cutting in the SMC line. The prepreg tapes were cut on the SMC line into chips of two lengths: either 25.4 or 50.8 mm. The tapes were either 3.2, 6.35 or 12.7 mm in width.

4.2 Composite plate fabrication and characterization

The cure kinetics behavior of the tacky and aged material was discussed in chapter 3. In section 3.2, it was also discussed how aging may influence cutting in SMC cutting head. It is important to know how the mechanical performance is influenced by aging condition. Hence, the fabrication of composite test specimens is necessary to test its performance under tensile loading and impact loading. The procedure to fabricate composite plates was discussed in section 2.4. In the case of "dry" prepreg tapes, the SMC line was used as a chopper. The loose chips did not adhere to each other and were collected before they entered the compaction zone of the SMC line. These were stored at ambient conditions and were manually placed in the mold, which is shown in figure 4.1a, for compression molding. The total mass of the charge in case of the dry loose chips was 500g. More than 500g could not be used as the loose chips would not fit into the mold cavity and maintain a uniform layer thickness. The same curing cycle to prepare composite was

followed as discussed in section 2.4. The characterization techniques for mechanical performance analysis were discussed in section 2.5.

Figure 4.1: a. Loose dry chips manually sprinkled in the mold cavity, b. composite plate prepared from loose dry prepreg by compression molding

4.3 Results and discussions

4.3.1 Tensile properties

Uniaxial tension tests were conducted on the dog-bone samples cut from composite plates. Three types of load versus displacement curves were observed for these discontinuous fiber composite systems independent of whether the prepreg was fresh or aged, as shown in figure 4.2. For type A curves, the load increases linearly. Then it drops with one or more steps associated with failure followed by an increase to the ultimate tensile load. Finally, it drops drastically at failure. For type B curves, the load increases linearly to ultimate load followed by drastic drop at failure. For type C curves, the load increases linearly to the ultimate load followed by a gradual decrease in a stepped manner, which corresponds to failure of the fibers. Among the three types of curves, type B was

more dominant for both fresh and aged prepreg composites. However, types A and C were more common for fresh prepreg composites compared to the aged ones.

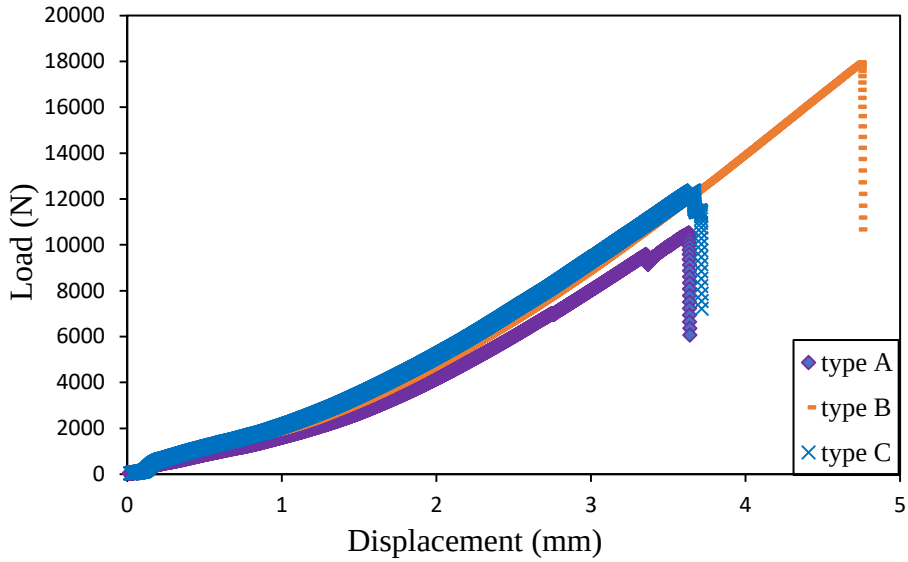

Figure 4.2: Typical load versus displacement curves for prepreg SMC composites

The drops in load-displacement curve may involve matrix cracking, chip-matrix debonding, fiber breakage within a chip. Load versus time curves follow are similar to the load-displacement curves. Chip-matrix debonding may be referred to as delamination. However, after failure, the two parts of samples maintained contact. Therefore, it is hard to define it as delamination. Moreover, for all the fresh and aged prepreg samples most of them did not break into two pieces.

In section 2.6.2, the tensile properties of fresh (minimum out-time) prepreg were discussed in detail. The pressure of the cure cycle was optimized based on the density and void content of the resulting composite plates. It was also shown that the effect of anisotropy significantly affects the properties of the composites due to through thickness fiber orientation. It is necessary to study the tensile properties for composites made of aged

prepreg. Table 4.1 lists the plates made from aged materials used to compare tensile and impact properties to those of the fresh samples listed in Table 2.3.

4.3.1.1 Effect of aspect ratio on tensile properties

To explore the effect of chip aspect ratio (AR), three different ARs of prepreg tapes were used. ARs were changed based on the dimensions of the chips as shown in the second column of Table 4.1. These dimensions were obtained by using tapes of different widths, which were provided by Boeing, and lengths, which were controlled by altering the spacing between the cutting blades in the SMC cutting head. The ARs are 2:1, 4:1, and 8:1. The initial mass of charge, curing cycle, and compression molding pressure were same for all the plates. The degree of cure (DOC) was calculated following the procedure presented in section 3.2.2. The DOC of plates made of NA-16 prepreg could not be calculated as squeezed out resin could not be collected from those plates.

Table 4. 1: Aspect ratio and aging conditions of prepreg chips for the mechanical performance analysis

Plate ID	**Chip dimension (mm)**	**Aspect ratio**	**Aging method**	**Mass of charge (g)**	**Molding Pressure (MPa)**	**DOC (%)**
P9.1	50.8 X 12.7	4:1	Naturally aged (NA-16)	500	2	-
P9.2	50.8 X 12.7					
P10.1	25.4 X 6.35	4:1	Oven aged			81±1
P10.2	25.4 X 6.35		NA-16			-
P11.1	25.4 X 3.2	8:1	Oven aged			80±1
P11.2	25.4 X 3.2					
P12.1	25.4 X 12.7	2:1	Oven aged			81±1
P12.2	25.4 X 12.7		NA-16			-

Figure 4.3 shows a trend of increasing strength with increasing AR. This trend is dominant for plates P12.2, P9.2, P10.2 and P12.1, P10.1, and P11.1. However, large standard deviations are seen for plates P9.1 and P9.2. A similar trend was been found in the literature [98]. The deviation might result from the nesting of the longer chips, which are more curled. Hence, it is difficult to maintain a randomness of chip orientation across the plates. This implies that longer chips may introduce preferred orientation resulting in planer anisotropy.

The tensile modulus did not show an effect from aspect ratio, for the tests performed in this thesis. Similar behavior was reported for discontinuous fiber composite systems [99]. The coefficient of variation (COV) of tensile properties increased with fiber length and was attributed to the size effect. The COV is defined as the ratio of standard deviation to the average for a set of data for a composite plate.

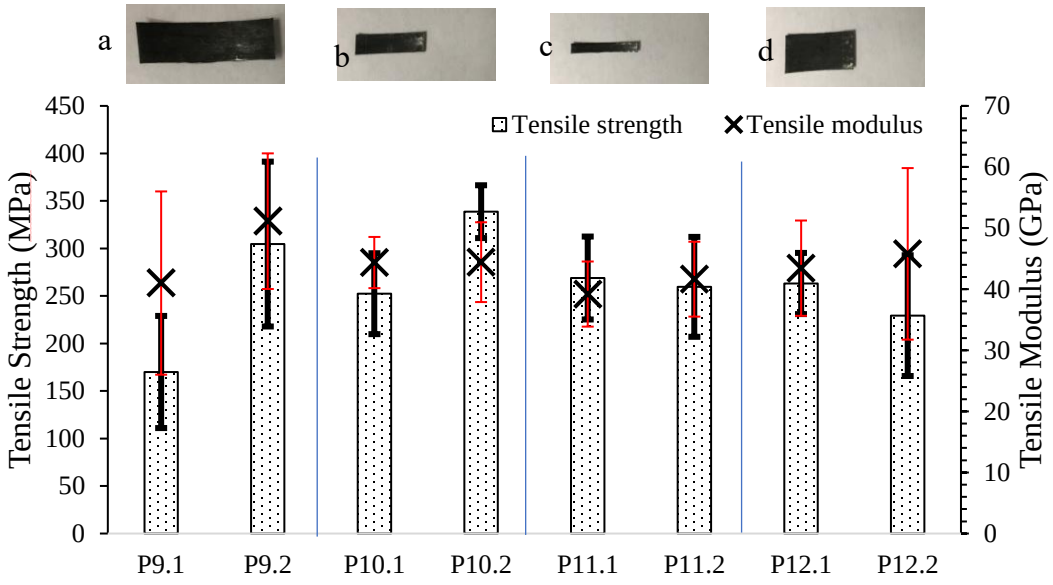

Figure 4.3: Effect of aspect ratio on tensile strength and modulus, on top: a. chip dimension of 50.8 mm X 12.7 mm; b. 25.4 mm X 6.35 mm; c. 25.4 mm X 3.2 mm; d. 25.4 mm X 12.7 mm

4.3.1.2 Effect of aging on tensile properties

The effect of aging on the tensile properties of the composite prepreg plates was studied. Both oven aged and naturally aged prepreg tapes were used for this study. The results were compared to those of fresh prepreg composites. Naturally aged prepreg plates had a greater standard deviation than the oven aged ones as seen in Figure 4.3. This may be the case because the resin flow is better for oven aged prepregs as compared to the naturally aged ones. Flowability of resin may be influenced by the viscosity and gel time of the resin with aging. The literature suggests that a gradual increase of viscosity and a decrease in gel time during storage time may result from the slow advancement of curing [86, 90]. This is evidenced by more resin squeeze out being observed for oven aged composites as compared to naturally aged ones. Figure 4.4 shows the tensile properties for plates made from three different prepregs with the same aspect ratio of 2:1 and the same compression molding conditions. Plates P12.1, P12.2 and P7.1 were fabricated from oven aged, naturally aged, and fresh prepregs, respectively. The plate fabricated from oven aged chips (P12.1) showed the highest average tensile strength. Oven aging causes advancement of cure, which might contribute to the higher tensile strength of the oven aged prepreg composites. Moreover, both oven aged and room temperature aged prepreg composites showed lower average void contents than the fresh prepreg composites (Figure C4.2). The overall strength as well as the modulus are similar for all three plates. In terms of cutting and SMC formation, the fresh ones could not easily be cut but adhered to each other and form a continuous SMC. The oven aged and room temperature aged ones did not stick while cutting. However, the aged prepreg chips were dry and loose and did not form a sheet. Composite plates were prepared from aged chips by manual sprinkling into the mold.

Based on cutting results, fresh prepreg is recommended for use because all three types of prepreg result in composites that exhibit similar tensile and impact properties and fresh prepreg are more readily and scale-ably processed into parts by compression molding. This also implies that aged prepregs can be utilized to prepare high quality composites, thereby saving energy from not requiring refrigerated storage.

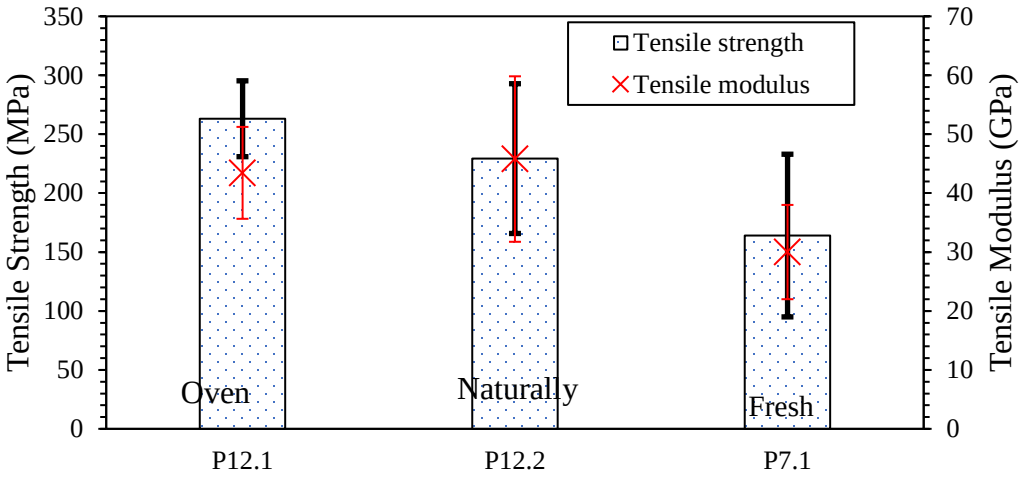

Figure 4.4: Effect of aging of prepreg on tensile strength and modulus

4.3.1.3 Effect of mold release agent on tensile properties

As mentioned in section 2.4, a mold release agent (MRA) was used to prepare the SMC from fresh prepreg tape. This might affect the final composites' properties and result in lower strengths and moduli. It has been reported that the molecules of the MRA are smaller than the epoxy molecules. Hence, they might migrate into the polymer and alter the properties of the cured polymer [77]. Figure 4.3 shows that the standard deviation is the smallest for an aspect ratio of 8:1. Hence, two plates were prepared with 25.4 mm by

3.2 mm prepreg chips with an aspect ratio of 8:1 to evaluate the effect of MRA. This prepreg was oven aged at 70^{o}C for 36 hours. During the fabrication of the plate, MRA was applied after sprinkling each layer of the oven aged chips in the mold cavity. The other plate was prepared without MRA. The two plates were identified as "With MRA" and "Without MRA" in Figure 4.5. It is observed that the MRA effect was not significant for this composite system in terms of tensile strength and modulus. In this discontinuous fiber composite system, the fiber dominates the performance of the final product. Hence, the through thickness orientation of the fibers might mask the effect of MRA. One-way analyses of variance (ANOVA) were performed on tensile modulus and tensile strength to determine a significant influence of MRA. The results suggest that the differences in the properties were statistically insignificant.

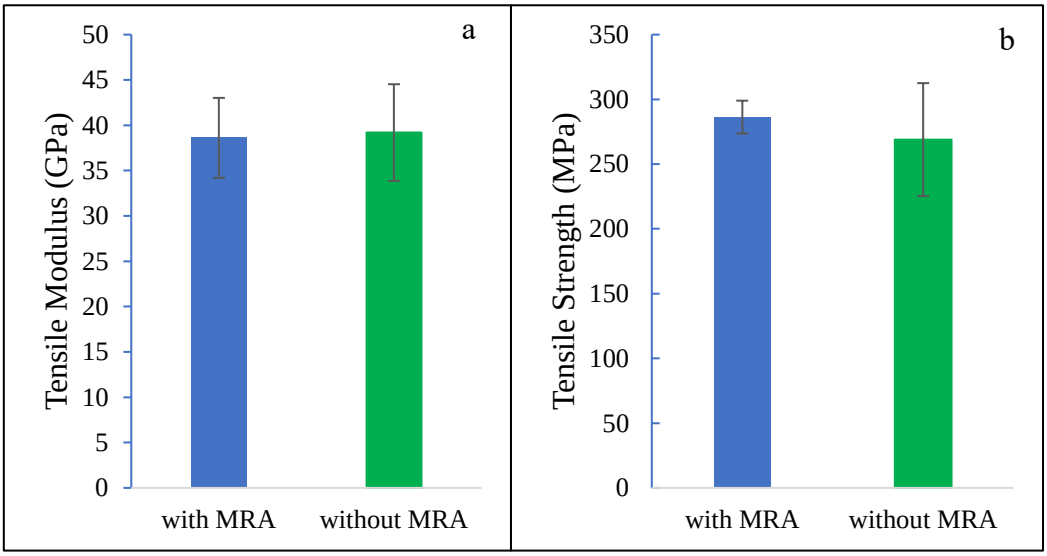

Figure 4.5: Effect of MRA on: a. tensile modulus and b. tensile strength.

The overall average tensile strengths and moduli of aged prepreg composites were comparable to those of fresh prepreg SMC composites. The overall strength of the CF

composites was 14% lower, whereas the modulus was more than two times higher than the conventional GF60/epoxy composite [54]. Conventional GF/epoxy composite was reported to be 70 wt.%.

4.3.2 Mechanism for tensile failure

After the tensile tests were completed, the fracture mechanisms were observed in the test samples at both macroscopic and microscopic levels. Discontinuous fiber composites prepared from chopped tape prepreg had four main modes of macroscopic fracture as shown in Figure 4.6: wedge pullout, strand pullout, strand breaking and mixed. In a single fracture surface, one or combination of any of the four modes could be observed. Fracture generally followed a tortuous path of least resistance. It is expected that the least resistance might occur at voids and resin rich areas, or where the fiber orientation is such that the fibers can barely take the load. Strand breaking, and pullout takes energy, and hence results in higher tensile strength. Interestingly, upon failure, most of the samples retained a large portion of their apparent integrity. Similar failure modes were observed by the B.C. Jin group [98] who studied composites made from reused prepreg scrap. Comparable behavior was found in thermoplastics resin based randomly oriented strand composites [66]. The literature suggests that a non-uniform strain field under tensile load may cause such failure [62, 66, 98]. Localized strain results from heterogeneity and little damage was found remote from the weak spot. Selezneva explained such failure as matrix dominated where fewer fibers are oriented in the loading direction [66]. Crack initiation occurs at the edge. As the chip length is reduced during cutting of the sample near the edges

of the sample, the edges become weaker than the mid-section of a sample composed of chips of nominal length.

Figure 4.6 helps to explain the macroscopic fracture modes. In Figures 4.6a and 4.6c, the two surfaces (X and Y distinguished by blue line) slightly slide against one another (Y moved left in reference to X), which can be observed in the front views of two fractured samples. Strand pullout and wedge pullout are shown in 4.6b and 4.6d, respectively. A wedge results from multiple strands pulling out together.

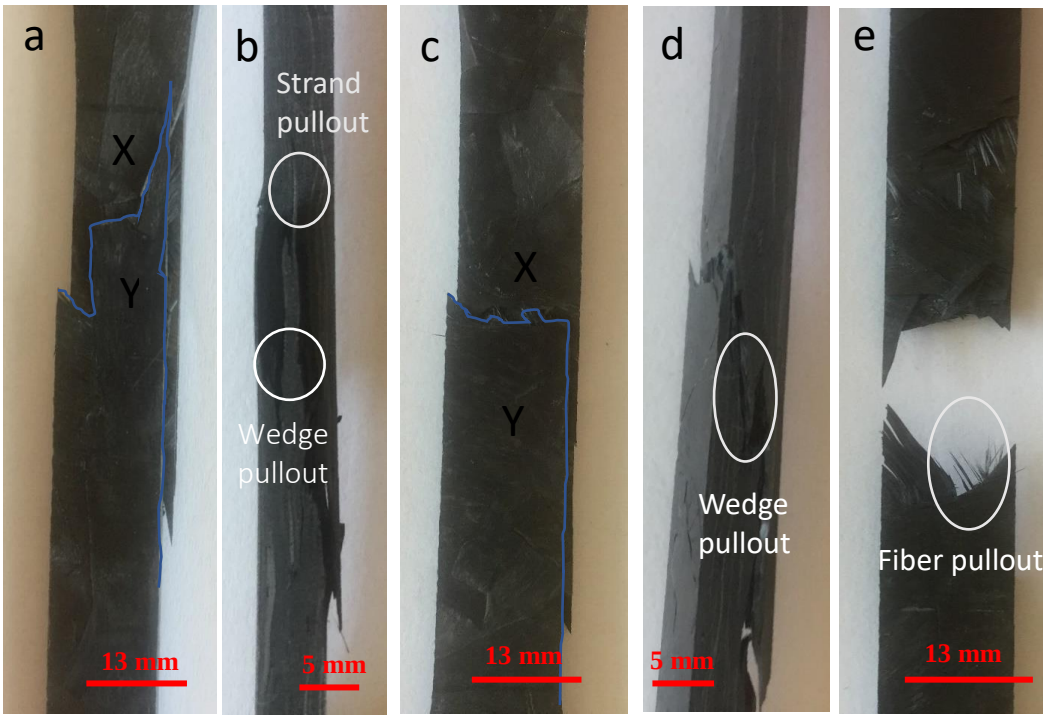

Figure 4.6: Macroscopic failure modes of the composites: a. front view of fracture surface; b. strand pullout and wedge pullout (mixed mode); c. relative sliding of fracture surfaces; d. wedge pullout; and e. fiber pullout

The resulting microscopic features of tensile fracture can be seen in figure 4.7. Figure 4.7a shows strand pullout of the composite prepreg. Fiber breakage can be seen as

well in figure 4.7b. Matrix cracking is also observed in figure 4.7c. The smooth surface results from fiber pullout; these are spots with low interfacial strength between fiber and matrix creating weak links. Overall, good adhesion between fiber and matrix is observed in figure 4.7d, and also shows resin residue on the fiber. This implies that the compression molding process utilize here results in good quality fiber and the matrix bonding.

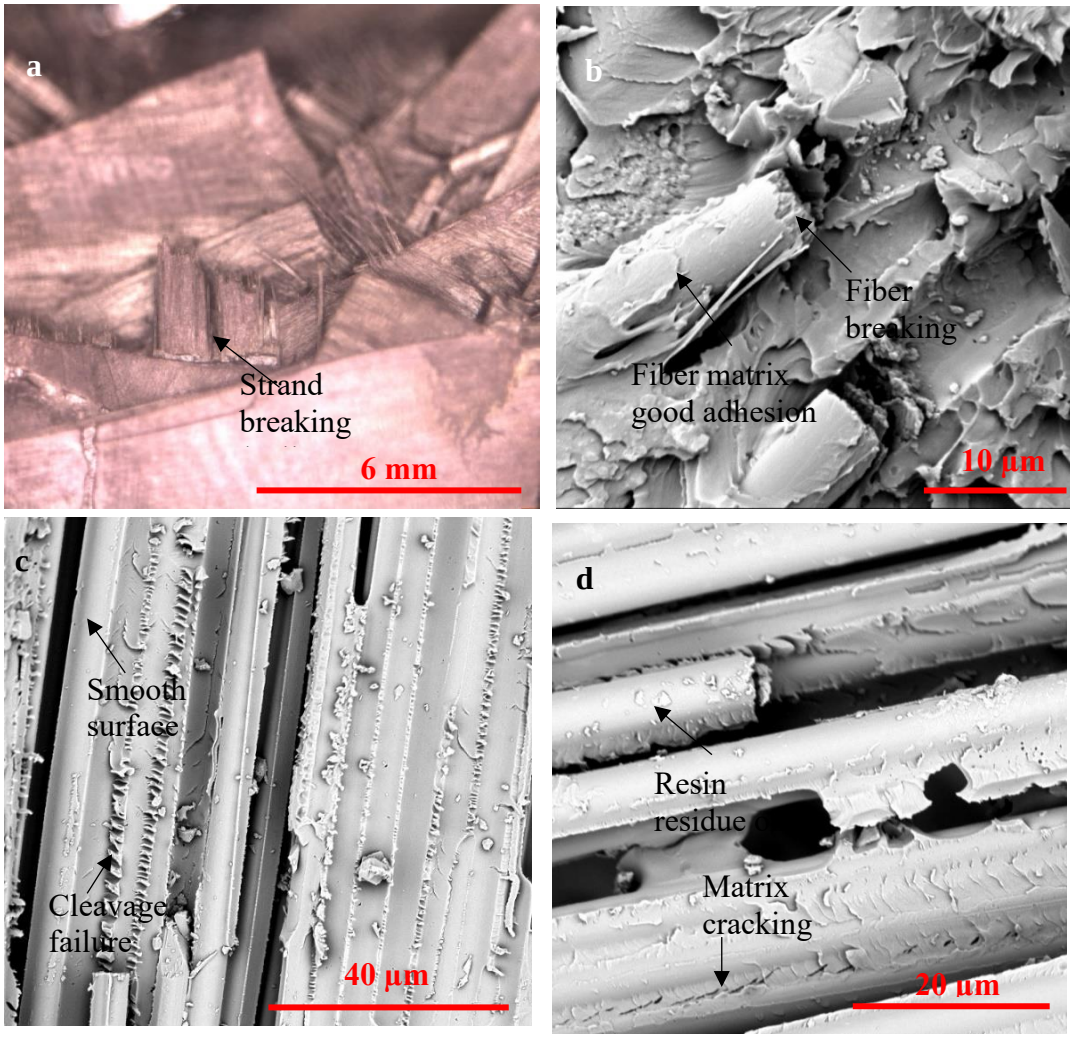

Figure 4.7: SEM micrographs showing fracture surface features: a. strand breaking or pullout; b. fiber breaking, fiber-matrix good adhesion; c. cleavage failure of matrix; d. good adhesion between fiber and matrix

4.3.3 Impact properties

4.3.3.1 Effect of aspect ratio of prepreg chip on impact strength

Impact strength was measured for composites plates made from the non-tacky, aged prepreg chips listed in Table 4.1. Aging was performed by either oven aging or RT aging. Their overall average strength is comparable to that of the fresh prepreg composites discussed in section 2.6.2. Their impact strength is 40% lower than the UD_L counterpart. The UD_L plate was prepared by hand layup from twenty-five layers of unidirectional prepreg ply. UD_L samples were cut from the plate along the fiber direction. However, it is 20% higher than that of GF70/epoxy composites [54]. The GF70/epoxy composite had a fiber content of 70 wt.%. GF70/epoxy composite was fabricated by compression molding at 100^{o}C for one hour followed by two hours of post curing at 120^{o}C under 430 kPa. Figure 4.8 shows that the effect of the aspect ratio is not significant on overall impact strength. However, plates P9.1 and P9.2 show higher standard deviations, which is a similar trend observed for the tensile strength. So, it can be concluded that the nesting of longer chip lengths causes preferred orientation.

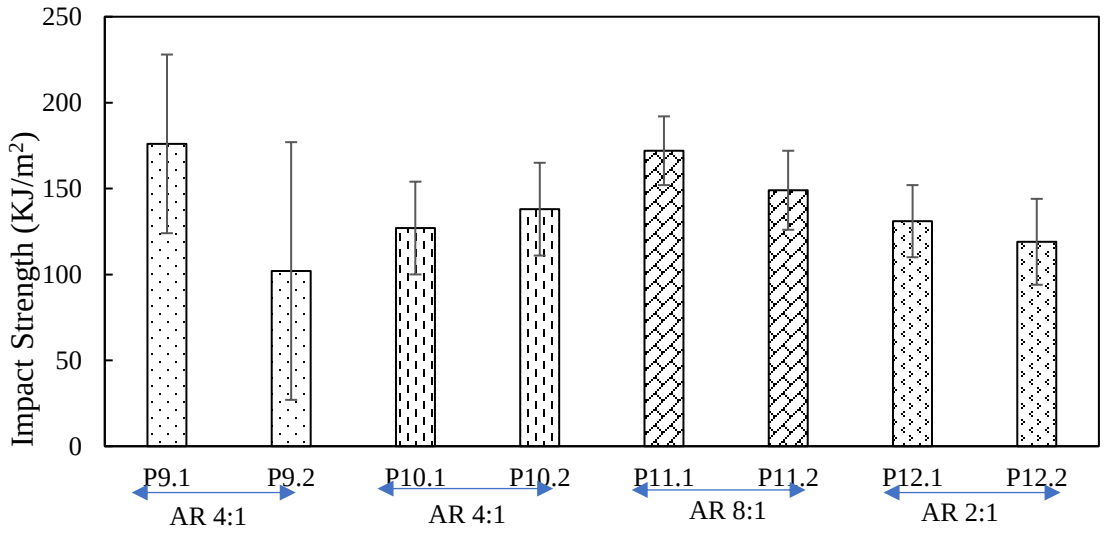

Figure 4.8: Effect of aspect ratio (AR) on impact strength of aged prepreg composites

4.3.3.2 Effect of aging of prepreg chip on impact strength

To study the effect of aging on impact strength, the results obtained for composites made of fresh, naturally aged, and oven aged prepregs were compared. Figure 4.9 exhibits negligible variations for plates P12.1, P 12.2 and P 7.1. So, it can be concluded that impact strength is similar for both aged and fresh prepregs.

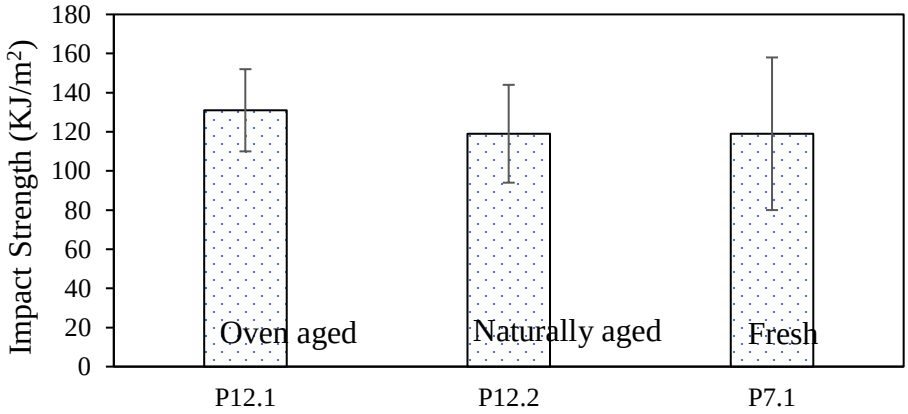

Figure 4.9: Effect of aging on the impact strength of prepreg composite

The effect of MRA was also investigated on composite panels made from 25.4 mm by 3.2 mm oven aged chips. Two plates were prepared with and without MRA. The MRA used here was Frekote® 700-NC. For both types of plates, the average impact strength was measured to be approximately 150 KJ/m^2. This implies that the effect of MRA is insignificant or masked by other effects.

4.3.4 Impact failure modes

Bader et al. explained fiber-matrix interface strength as the key factor to dictate the failure mode for unidirectional continuous CFRP composite [100].They observed brittle failure and little energy absorption with high interface strength, multiple delamination with disintegration of specimen for low interface strength while no disintegration of sample with high energy absorption for intermediate interface strength. Other studies on unidirectional continuous, unidirectional carbon fiber reinforced polymer composites suggested two main failure modes in Charpy impact tests [100-103]: (1) flexural failure by fiber fracture and pullout, and (2) shear failure by delamination. The flexural stress and the interlaminar shear stress (ILSS) developed during the dynamic impact loading are crucial for impact failure [104].

Fracture initiation energy increases with an increase in ILSS [105]. Fiber dominated brittle fracture shown in Figure 4.10 (a) implies that the ILSS is very high. This is a through thickness failure. Fiber breakage and fiber pull-out are also observed in figure 4.10(a). In this study, the chips are randomly orientated. Hence, disbanding occurs where there is the lowest ILSS, which is in between two chips or a block of chips. This is shown in figure 4.10(c). However, in most cases mixed mode failure is observed as shown in figure 4.10(b).

This implies that both fiber and resin take the load and that the ILSS is high. This also indicates a random distribution of the chips because such behavior has been observed in a quasi-isotropic laminate $[0/90/(\pm 45)_2]_s$ [106].

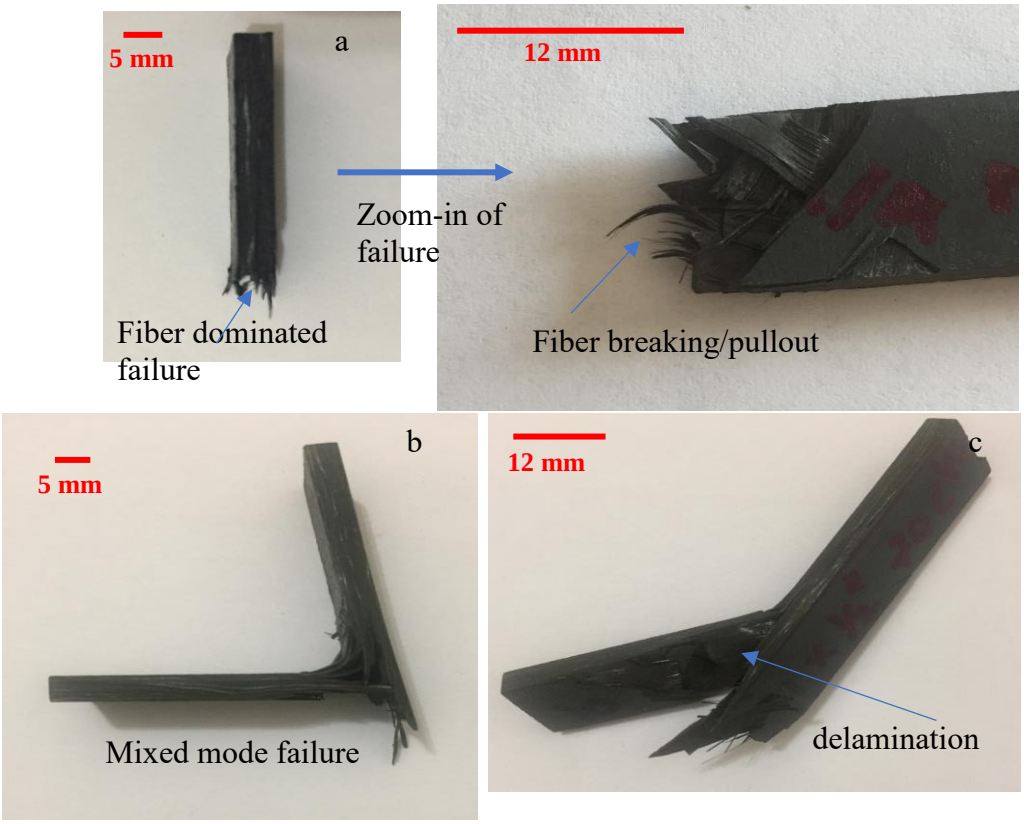

Figure 4.10: Failure modes of prepreg composite samples in Charpy impact test

Few samples showed complete delamination. This is significant as it indicates higher ILSS. The literature suggests that the value of ILSS is greatly influenced by the manufacturing process in addition to the fiber, matrix and interfacial properties [100, 105, 107, 108]. Thus, this result reinforces the fact that the manufacturing technique followed here helps to produce the high values of ILSS desired.

4.4 Conclusions

Composite plates were successfully fabricated from aged prepreg chips that were non-tacky. The average tensile and impact properties of this composite were comparable to fresh prepreg composites. Compared to 70 wt% GF- epoxy composites, aged prepreg composites were 8% lighter. The tensile modulus of the prepreg composites was more than two times higher while specific strength and impact strength were 10% and 30% lower, respectively. Composites fabricated from post-industrial prepreg might be suitable for light weight applications because they are 18% lighter than standard SMC [75]. An increasing trend of tensile strength with aspect ratio was observed. The enhancement in strength was about 7% between minimum (2:1) and maximum (8:1) aspect ratios. However, no trends for tensile modulus or impact were found with aspect ratio. The effect of mold release agent on the overall mechanical performance was also insignificant.

The results indicate that heterogeneity is an inherent property of this material system. The variation in tensile and impact properties might result from the local through thickness chip structure and orientation. During the SMC preparation, chips fall in a random manner. Thus, through thickness fiber orientation varies. From point to point, this may cause variations in properties.

As expected, tensile failure occurred due to high localized strain. Failure occurred along the shear plane of loading; specifically, along the ends of chips, resin rich area or the curved portions of chips. Cracks followed tortuous paths of least resistance. The integrity of the samples was maintained for most of the samples at locations remote from these weak points. Few samples broke into two pieces; failure was not catastrophic. For impact failure,

none of the samples showed complete delamination along their lengths. This implies good ILSS. Most of the failures were mixed mode due to the high flexural and shear strengths of the composites. This failure mode suggests that the compression molding utilizes the inherent properties of the high value fiber and the resin to create a final product with advantageous properties.

The mechanical performance of the carbon fiber composites fabricated from post-industrial prepreg chips suggests that they can be utilized in a SMC line regardless of their thermal history and have a tremendous potential in the automotive industry.

CHAPTER 5

CONCLUSIONS AND FUTURE WORK

5.1 Conclusions

The overall objective of this dissertation is to determine the potential of using post-industrial carbon fiber prepreg to fabricate a light weight composite as a solution to landfilling the chemically active prepreg waste, and to understand the corresponding process property relations of the composite material. In this chapter, the major findings observed in this dissertation will be summarized, and based on the conclusions, a few future research directions will be provided in the next section.

In Chapter 1, the key features of carbon fibers were explained followed by the importance of light weight composites and approaches to fabricate the composites such as fiber reinforced polymer composites. Carbon fiber (CF) reinforced polymers (CFRP) are used in aerospace industries for their high strength to weight ratios and the resulting increased fuel efficiency. It is predicted that the production of CF-prepreg will increase with time due to its booming commercial use. For instance, prepreg material can be utilized for fabricating lightweight composites for applications in automotive industries. However, a major challenge of using the carbon fibers in substantial industrial applications is their high cost. To overcome this challenge, recycling of CF-prepreg may be an alternative to replace the existing metals and GF/epoxy composites in automotive industries that have low specific properties and consequently save money and reduce environmental effects. This discussion led to replacing glass-fiber reinforced epoxy resin composites, which are

used in automotive applications. As an approach to find scalable and low-cost manufacturing method for recycling prepreg of arbitrary width, the SMC technique was proposed as a less labor intensive, low cost, and less scrap approach to recycle carbon fiber prepregs. With compression molding, composite fabrication becomes highly scalable. Further discussion revealed that the CF-SMC has the potential to replace GF-SMC and metals.

The challenges of recycling prepreg using SMC techniques and their pathways were addressed in Chapter 2. First, the SMC equipment was modified to develop a cutting protocol for the post-industrial CF prepreg tapes using the SMC technique. Initially, the SMC setup was designed for fabricating glass fiber system. As the properties of carbon fibers in CF-prepreg are very different than that of the GF, the SMC line could not be utilized to prepare SMC material from CF-prepreg. Hence, the existing SMC system was engineered to deal with the CF-prepreg wastes successfully; particularly, the blades and supporting sleeve were replaced with carbon steel blades and a harder PU sleeve. The cutting mechanics revealed that the fiber cutting is performed via flexural failure of the fiber, and the critical radius of curvature is crucial for cutting the fiber. Furthermore, it showed that the calculated critical radius of curvature for cutting the carbon fiber was higher than the actual measured critical radius of the blades.

To run the SMC smoothly and properly, various developments and modifications were performed on the existing setup such as the addition of guides to feed prepreg tapes while maintaining a certain angle with respect to the surface of spool, installation of end caps on the prepreg spools to reduce friction, and addition of a device to remove the back-up films of the prepreg tapes. Thickness uniformity of SMC sheet were attained by setting

guides to feed the prepreg tapes to the cutting head. Moreover, control of the speed of conveyor settings and of the number of spools being fed was crucial to produce a uniform thickness SMC sheet. Simultaneously, the cutting speed, cutting pressure, and the feed pressure were optimized to meet the motor capacity of the SMC setup. Composite plates were successfully fabricated, and tensile properties and impact strength were measured.

Statistical analysis of the average properties, such as tensile strength, tensile modulus, and impact strength was performed in JMP Pro. It was found as the compression molding pressure was increased that the impact strength and tensile modulus decreased while the tensile strength increased. However, it is hard to draw any firm conclusions because the prepregs did not have similar thermal histories. In addition, a decrease in void content with increasing compression molding pressure did not improve the tensile strength, modulus and impact strength, which emphasizes the dominant effect of through thickness heterogeneity.

Mechanical properties of the CF-prepreg composites were compared to the properties of GF/epoxy SMC composites with fiber content of 25 to 70 wt.% as reported in literature [54]. The results were also compared with that of commercial automotive SMC composites of 50 wt.% GF content as well. The overall comparison was presented in Table 2.9 of Chapter 2. Based on the overall comparison it was observed that CF-prepreg composite is about 8% lighter that the GF70/epoxy composite and 18% lighter than the standard SMC [54, 75].

The most significant point to note here is the tensile modulus. The average tensile modulus for the CF-prepreg composites was 40 GPa, while it was only 17 GPa for the

GF70/epoxy composites and 15 GPa for commercial GF SMC composite. The theoretical modulus was also calculated using a micro-mechanical model for short fiber reinforced composite which was 69 GPa. This is higher than the experimental value of 40 GPa. This discrepancy might result from manufacturing defects such as voids, resin rich areas, chip curl. These defects might result from the shorter cure cycle, flowability of resin, and lack of randomness of chips placement in the mold.

In addition to the high modulus, the high value of average specific tensile strength (98 kPa.m^3/kg: which is 70% higher than GF25/epoxy, 31% lower than GF70/epoxy SMC and 65% higher than commercial GF SMC) also suggests that CF prepreg SMC will be suitable for light-weighting in automotive applications. Surely, the recycling of CF prepreg is environmentally friendly and adds value to the economy, as an alternative to just throwing away the prepreg trim waste with the attendant landfill fees and environmental hazards. Therefore, it is necessary to utilize the post-industrial prepreg regardless of their age or thermal history.

Since the thermal history of incoming scrap prepreg is unknown, the study of the aging condition of the incoming prepreg is crucial for recycling and its further use in various applications such as automotive industries. Material behavior and performance can be controlled if it is known where the material falls along the aging scale of fresh to aged. The thermal analysis of incoming post-industrial prepreg demonstrated that cure kinetic values obtained from DSC dynamic runs such as thermal transition 1(TT1), heat of reaction, degree of cure, activation energy, endothermic peak are strong indicator of the ability to successfully cut the prepreg in the SMC line. TT1 and degree of cure showed increasing trend with both oven aging and RT aging while heat of reaction showed a

decreasing trend. This fact implies that aging results in progression of curing reaction with aging. The decrease in activation energy with longer RT aging supported this fact as well. Moreover, the progression of curing reaction results in non-tacky prepreg which resolves the sticking issue in the SMC cutting head.

Based on the fact that the fresh (minimum out time) prepreg being aged at 70^{o}C for 36 hours or room temperature aged seven weeks was suitable to achieve a complete cut. Therefore the suggested TT1 is 16.5^{o}C to 23^{o}C, whereas the degree of cure is of 27% to create complete cuts. For the aged prepreg in a fresh to aged scale of prepreg, activation energy and endothermic peak may be the identifying parameters. E_a of 50 KJ/mol might be used as the lower limit to attain a complete cut for aged prepreg. An endothermic peak could be observed only for OA-RT-4 (oven aged at 70 oC for 36 hours followed by 4 months of RT aging) and NA-16 (room temperature aging for 16 months) prepreg. However, TT1 was not visible for these aged prepregs. In addition, both of the aged materials could be cut completely in the SMC cutting head. Hence, it can be stated that a combination of kinetic parameters might be useful to identify the aging condition of the incoming prepreg more precisely and determine any further processing before feeding into the SMC cutting head for a complete cut without using any mold releasing agent.

After understanding the behavior of post-industrial CF prepreg with aging, it is necessary to investigate the performance of the aged prepreg. Aged non-tacky prepreg chips could be used successfully to fabricate composite plates. The average tensile and impact properties of this composite were comparable to fresh prepreg composites. Compared to the 70 wt.% GF- epoxy composites, the aged prepreg composites were 8% lighter. The tensile modulus of the prepreg composites was more than two times higher

while specific strength and impact strength were 10% and 30% lower, respectively. The post-industrial prepreg composites might be suitable for light weight application since it is 18% lighter than the standard SMC [75]. An increasing trend of tensile strength with aspect ratio (AR) was observed. The enhancement in strength was about 7% between minimum (AR 2:1) and maximum (AR 8:1) aspect ratio. However, no trend for tensile modulus or impact strength was found with aspect ratio. The effect of mold release agent on the mechanical performance under tensile loading was also found to be statistically insignificant based on ANOVA results.

The mechanical performance of the CF prepreg composites indicate that heterogeneity is an inherent property of this material system. The variation in tensile and impact properties might result from the local through thickness chip structure and orientation. During the SMC preparation, chips fall in a random manner. Thus, through thickness fiber orientation varies. From point to point, this may cause variations in properties.

As expected, tensile failure occurred due to high localized strain. Failure occurred along the shear plane of loading (approximately 45^{o} to the plane of loading); specifically, along the ends of chips, resin rich area or the swirled portions of chips (Swirled portion of the fibers are generally curved, not straight which might result from resin flow). The crack followed a tortuous path of least resistance. The integrity of the samples was maintained for most of the samples away from this weak spot. They hardly broke into two pieces. So, the failure was not catastrophic. For impact failure, none of the samples showed complete delamination along their length. This implies good ILSS. Most of the failure was mixed mode due to flexural and shear stresses. This failure mode suggests that the composite

manufacturing process utilizes the inherent properties of the high value fiber and the resin to create a final product with advantageous properties.

The mechanical performance of the carbon fiber composites fabricated from post-industrial prepreg chips suggests that the post-industrial prepreg can be utilized in the SMC regardless of their thermal history and has a tremendous potential in automotive industry.

In conclusion, modification on the SMC setup was successfully performed to run the line smoothly with the CF-prepreg. Fresh prepreg could be utilized to prepare composites with high specific tensile strengths and moduli as well as the impact strength. Thermal analysis of the prepregs revealed that the aging resolves the sticking issue in the cutting head as well as helps to provide a complete cut for aged non-tacky prepreg. It further clarifies that cure kinetic parameters, such as thermal transition 1 (TT1) and degree of cure, are found to be the best indicators to attain a complete cut of the aged prepreg, while activation energy and endothermic peaks are suitable for identifying aging condition for long-term aged prepreg. The aged prepreg showed comparable tensile and impact properties with fresh prepreg composites. Both fresh and aged prepreg composites are lighter than conventional GF SMCs. Although heterogeneity was observed to be inherent, the mechanical performance of the CF prepreg composites suggests that the post-industrial prepreg can be utilized in the SMC irrespective of their thermal history and has a great potential in lightweight composites for automotive industry.

5.2 Future work

The scientific findings of this research can form the basis of future studies that will further elucidate the process-property relationship in composites made by utilizing CF

prepreg trim waste and enable their manufacture of high value low cost materials via scalable and economically viable methods. Specifically, a number of technical issues are described below.

First the effect of the mold release agent on the overall performance of the composites needs to be determined. As mentioned in section 2.3.1, MRA was used to cut fresh tacky prepreg so that the prepreg does not stick to the cutting roller or the supporting sleeve. However, the application of MRA is not desirable as literature suggests that smaller MRA molecules may be absorbed by the resin. Thus, MRA might have a deleterious effect on the overall properties of the composites [77]. A. J. Shields et al. studied the influence of MRA on epoxy resin [77]. The cured epoxy samples were subjected to different stresses such as electrical, thermal, radiation and flexural. They observed significant effect only for electrical stress applied via a discharge mechanism. There were surface cracks observed on the sample which was electrically stressed. The effects of mechanical loading and handling, cleaning, and environmental exposure on the cured resin may be investigated by applying chemical stress by immersing the sample into distilled water, acetone, methanol, and a 10% solution of hydrogen peroxide and suspending samples in nitric acid fumes. Samples may also be tested under flexural loading, thermal loading and electrical discharge.

In another study, influence of MRA was investigated on the adhesion between the molded resin and the mold surface [109]. The authors explained that MRAs create a low surface energy coating on the mold surface that causes the reduction or elimination of adhesion to the surface of the mold. Less adhesion is also desired for automated manufacturing processes. However, adhesion is influenced by chemistry of both the resin

and the MRA, as well as the amount of the MRA. In most cases the chemistry is unknown. Hence, the adhesion between the molded composite and the mold surface needs to be tested experimentally. The study suggested a method of using an Instron 5567 with two platens made of the mold material. Both platens can have heating elements and temperature controllers and can be used as mold surfaces. The composite will thus be cured between the two platens. The force to separate the composite from the mold surfaces will thus provide an estimate of adhesion. Using similar principle, adhesion between two layers of prepreg may be tested with and without the Frekote ® 700-NC to identify how the inherent adhesion of the prepreg may be influenced by the MRA.

To make the recycling of CF-prepreg more efficient, finding an alternative to MRA would be beneficial to resolve the sticking issue. Zinc stearate powder might be useful to resolve the sticking problem. Zinc stearate is a widely used internal mold release agent in plastic industries. This powder might be introduced into the prepreg tapes before feeding to the cutting head or sprinkled over the cutting head. However, it should be applied in a limited weight% such that it will not affect the properties of the SMC composite. Another approach to resolve the sticking issue might be to cut the tape in a frozen state, because frozen tapes are less tacky. After cutting the tapes, they do not stick rather stay separate from each other, which facilitates their being cut on the SMC line relatively easily. However, prepreg tapes are very thin, so they may behave as fins and absorb heat from environment very quickly, eventually becoming tacky. Hence, a chilling system or cold air gun might be useful to set the cutting head of the SMC line in a chilled chamber to keep the prepreg tape non-tacky. Moreover, the chilled chamber would facilitate keeping the cutting head chilled. So, there will be no heat source for the frozen tape inside the chamber.

Another approach to alleviate the sticking problem of the tacky prepregs is to find a more appropriate material for the cutting blades of the SMC cutting head, which is more compatible with the tacky prepregs. For example, titanium or titanium coated blades may cut the tacky prepreg more efficiently without sticking problems. It has been reported that titanium-fused stainless steel blades are used in scissors, which are non-sticky and wear resistant, for cutting adhesive tapes [110]. Furthermore, a titanium coating on the roller that holds the cutting blades might be helpful to prevent the sticking of the prepregs on the roller as well.

A second issue that needs to be further investigated is the steps needed to increase the efficiency of SMC cutting head and composite fabrication, hence the overall performance of the composite. As the cutting head of the SMC setup was designed for cutting glass fibers, cutting the CF-prepreg sometimes causes faster chipping of blades. Similarly, the supporting PU sleeve may be degraded while cutting CF-prepregs. Consequently, the conditions of the blades and the sleeve influence the cutting of the prepreg. Further study to modify the cutting head would enhance the cutting performance of the prepreg resulting in low downtime. Thus, the process will be more economic if the blades and sleeve are replaced less frequently.

Apart from the modification of the SMC setup, the performance of the composite might be improved by tuning the cure cycle. The cure cycle used in this study was heating for 30 minutes from RT to 195^{o}C, then heating at 195^{o}C for 15 minutes followed by cooling to room temperature in 15 minutes. A longer cure cycle might provide a higher degree of cure resulting in a different microstructure as well as mechanical performance that might be more suitable for different industrial applications.

To further advance the recycling of CF-prepreg it will be necessary to study the flowability of the resin with aging. In Chapter 4, the effect of aging on tensile properties was revealed such that the naturally aged prepreg for 16 months showed higher standard deviation compared to that of oven aged prepreg. Fabrication of composites also exhibited that more resin was squeezed out for oven aged prepreg. This leads to the fact that resin flowability is influenced by aging. Literature also suggests increase in viscosity and decrease in gel time with out-time/aging [90]. So, studying the rheology of the resin in CF-prepreg with aging will help to improve the recycling of CF-prepreg more efficiently.

A third point that needs to be addressed is to explore the mechanical performance of the CF-prepreg composite under both static and cyclic loading such as compression, flexural and fatigue loading. In this dissertation, the mechanical performance of the recycled CF-prepreg was determined under the uniaxial tension and impact loads. However, the performance under compression and flexural load would help for attaining a deeper understanding of the mechanical performance of the CF-prepreg SMC composites. The compression and flexural tests can be conducted following the ASTM D695 and ASTM D792 standards, respectively [79]. Moreover, the time dependent performance via fatigue testing would reveal the long-term performance of the recycled prepreg composite under service load. It is reported that the commercial discontinuous fiber composite system such as HexMc was more tolerant to cyclic loading when compared to that of continuous fiber composite [111]. As the previous chapters of this dissertation indicate that the heterogeneity is the inherent property of the CF-prepreg SMC composite, it will be interesting to observe how the heterogeneity of the material system might influence the performance under compression, flexural and fatigue loading.

Theoretical calculation method may provide an estimation of the modulus the SMC composite, Finite Element Analysis (FEA) may be a more appropriate tool to study and to predict the tensile modulus more accurately. Furthermore, FEA may help to develop a design tool in the form of a FEA model to predict the elastic modulus of this SMC composite for a wider design space.

Adequate representative volume elements (RVEs) might be created to ensure that the convergence occurs over multiple simulations. As discussed in Chapter 2 and 4, the fiber volume fraction and fiber orientation are the key features of a composite material, the fiber angle distribution can be manipulated in the RVE with various statistical distribution such as uniform, normal, logarithmic, etc. to better fit with the real fiber distribution of the composite. An APDL code can be used to import the RVE to ANSYS software. For conducting the FEA analysis in ANSYS, the loading can be applied within the elastic limit of the CF-prepreg SMC composite. The input parameters such as Poison's ratio, Young's modulus and density of the carbon fibers and the resin, can be provided to conduct the analysis. For further analysis, element selection and meshing can be performed in ANSYS. A mesh convergence analysis can be undertaken for the imported RVE and the loading to determine whether the stress concentration developed become unstable in refinement.

Besides using RVE for the FEA analysis, the elastic modulus of the CF-prepreg SMC composite also can be determined using the classical lamination theory by comparing quasi-isotropic discontinuous fiber plate with quasi-isotropic laminated plate of continuous fiber. The elastic modulus of two-dimensional randomly oriented short fiber plates can be predicted based on the quasi-isotropic laminates plate $[0/90/\pm45]_s$ of identical volume fraction and aspect ratio. Input properties such as Young's and shear moduli, Poison's ratio

of lamina, chip area, chip thickness, and chip orientation will be needed to generate an equivalent laminate for a randomization run. Multiple randomizations will be needed to generate multiple equivalent laminates of different ply distributions. Shell elements might be useful for this analysis of the laminated structure of the composite. Thus, elastic properties of the CF-prepreg SMC composite can be obtained by applying the classical lamination theory.

Future pathways of improving the recycling of CF-prepreg at different stages include resolution of sticking of fresh prepreg to cutting head rollers, coating of cutting blade and roller with titanium or titanium carbides or nitrides, tuning the cure cycle, a rheological behavior study with aging as the variable. Furthermore, a deeper understanding of the CF-prepreg SMC composites and the influence of heterogeneity on their mechanical performance can be attained by conducting compression, flexural, and fatigue tests. Finally, FEA analysis can serve as a design tool to predict the elastic modulus of the composite for a wider design space because this discontinuous fiber composites system is reported to have a tensile modulus as high as quasi-isotropic laminate composites.

APPENDIX A

A2.1 Calculation of theoretical modulus of CF-prepreg SMC composite

Calculation of fiber volume fraction using Equation 2.8,

$v_f=(w_f/\rho_f)/[(w_f/\rho_f)+(w_m/\rho_m)]= (65.4/1.8)/[(65.4/1.80+(35.5/1.3)]=56.7\%$

here, w_f and w_m are weight fraction of fiber and matrix in the composite

Using the corresponding values from Table 2.6 in Equation 2.6 and 2.7, η_L and η_T are calculated to be 0.0083 and 0.9661.

Using the corresponding values in Equation 2.4 and 2.5, the tensile modulus for unidirectional discontinuous fiber composite E_{11} and E_{22} are calculated to be 169 and 16 GPa.

Finally, using equation 2.6 the tensile modulus for randomly oriented chopped fiber composite, E_c is found to be 69 GPa.

A2.2 Statistical analysis of tensile strength, tensile modulus and impact strength by JMP Pro

To find correlation between mechanical properties such as tensile modulus, tensile strength, impact strength and process parameters such as age of SMC and pressure, statistical analysis was performed using JMP Pro. The Figures A2.1 to A2.3 reveal that correlation might exist between mechanical properties and age of SMC. However, R^2 values were found to be 0.5 or less (in red ellipse). Moreover, Table A2.1 shows that the

SMCs prepared for making plates P6.1 to P8.2 the thermal history was not similar for all prepreg tapes. Thus, it is hard to draw a conclusion about the existing correlation between the properties and age of SMC.

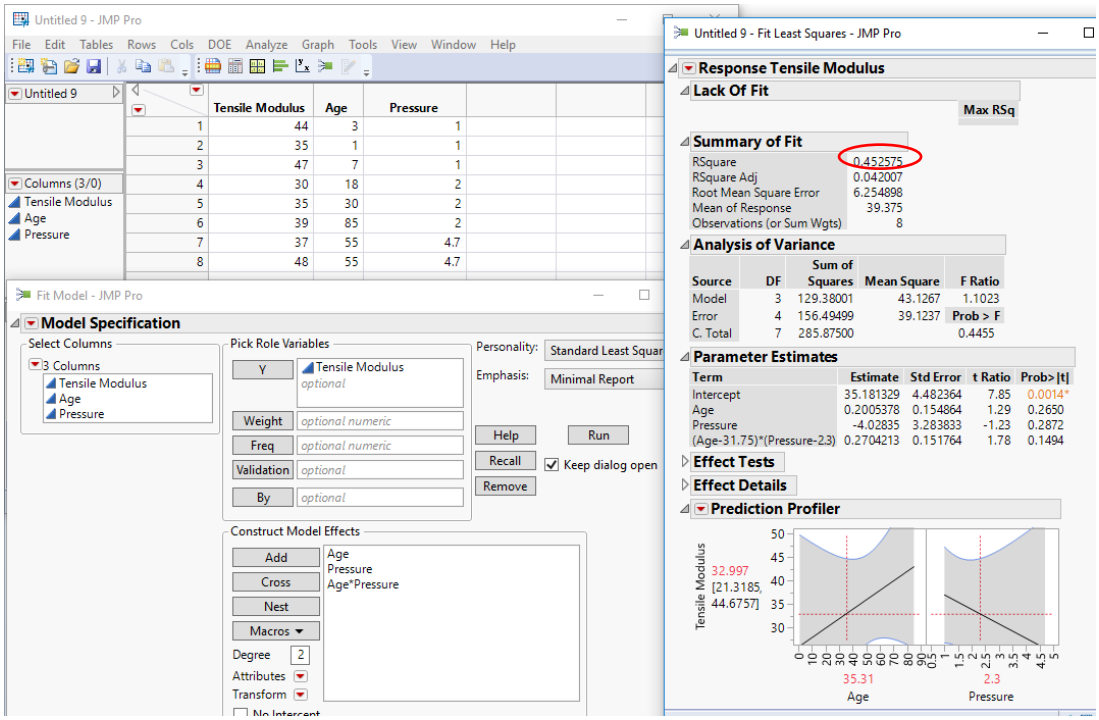

Figure A2.1: correlation between tensile modulus and age of SMC

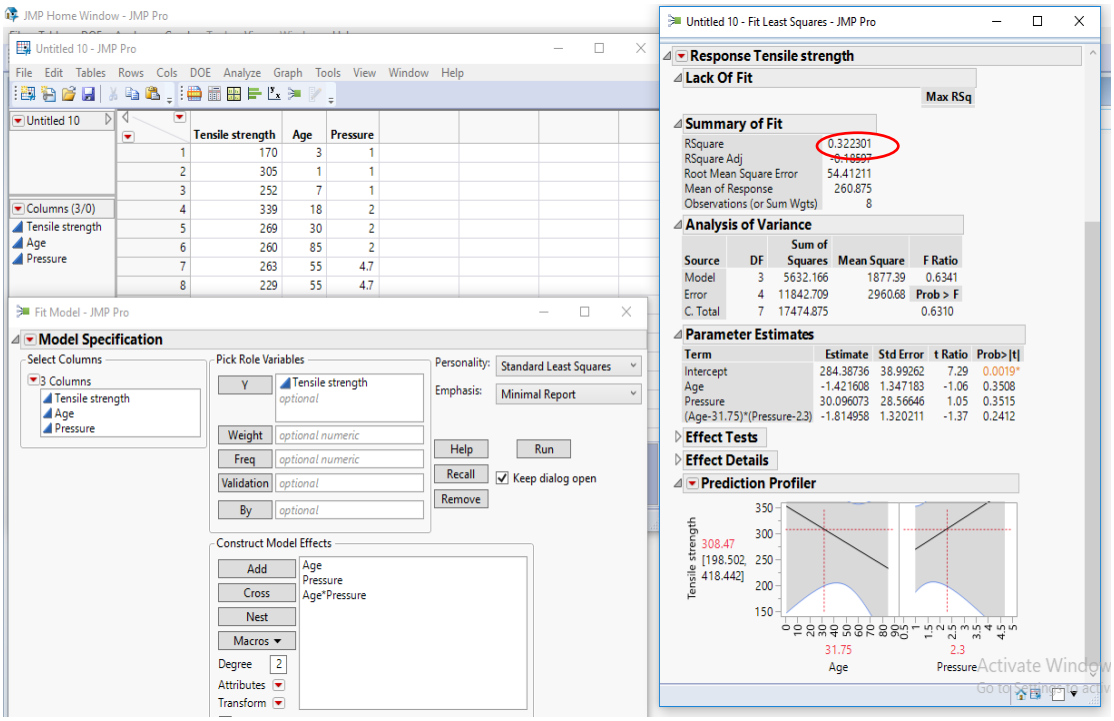

Figure A2.2: correlation between tensile strength and age of SMC

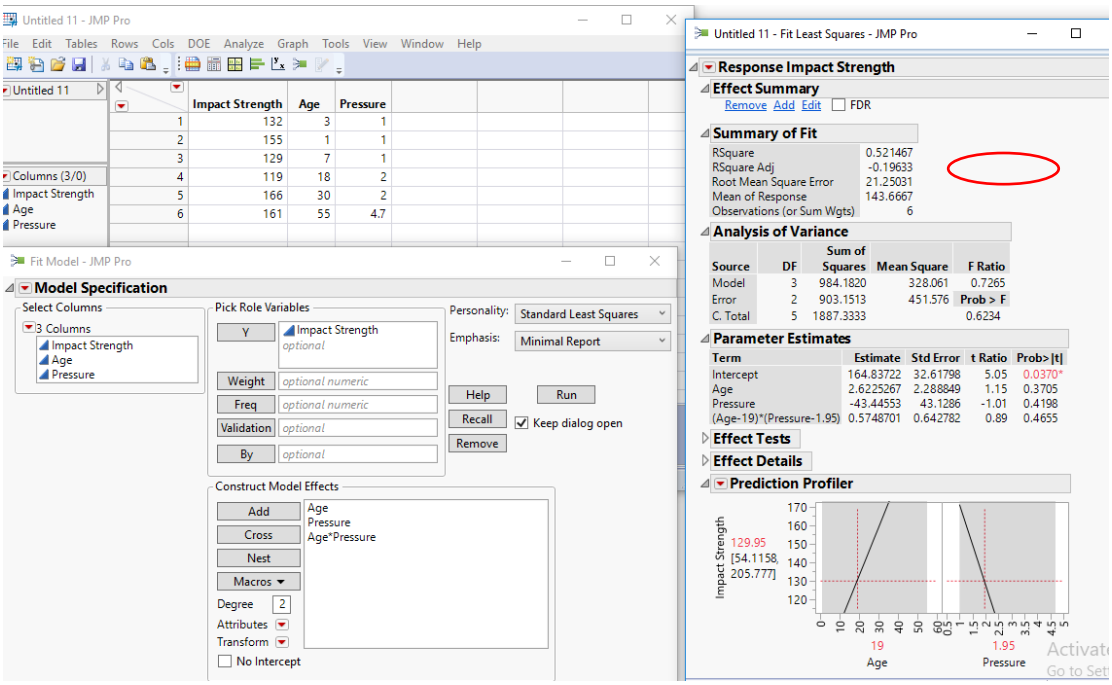

Figure A2.3: correlation between impact strength and age of SMC

Table A2.1 Detail information of SMC composites

Plate ID	**SMC detail**	**Age (days)**	**Pressure (MPa)**
6.1	prepreg received: 2/9/2017, SMC prepared: 28/2/2017, Hot pressed:3/3/2017 (under Vacuum)	3	1
6.2	Prepreg received: 4/3/2017, SMC prepared: 4/4/2017, Hot pressed: 4/4/2017 (under Vacuum)	1	1
6.3	Prepreg received:4/3/2017, SMC prepared: 4/4/2017, Hot pressed: 4/11/2017 (under Vacuum)	7	1
7.1	Prepreg received:4/3/2017, SMC prepared: 4/20/2017, Hot pressed: 5/8/2017 (under Vacuum)	18	2
7.2	Prepreg received: 4/3/2017, SMC prepared: 4/20/2017, Hot pressed: 5/20/2017 (under Vacuum)	30	2
7.3	Prepreg received: 2/9/2017,4/3/2017, SMC prepared: 2/28/2017, 5/20/2017, Hot pressed: 7/14/2017 (under Vacuum)	85	2
8.1	Prepreg received: 4/3/2017, SMC prepared: 4/20/2017, Hot pressed: 6/15/2017 (under Vacuum)	55	4.7
8.2		55	4.7

APPENDIX B

Endothermic peaks, as evolved after at least 4 months of RT aging, also help improve the cutting of the prepreg tapes because the tapes become non-tacky. As a result, the prepreg was kept in oven at 70 deg C for 9 days to observe whether any endothermic peak developed at higher temperature aging as compared to RT, as well as the location of endothermic peak. DSC was performed on prepreg that was oven aged for 9 days at 70^{o} C to determine if any endothermic peaks occur. Figure B3.1 shows an endothermic peak around 100^{o} C. However, the tapes become too brittle and the 9 days oven aged tapes split along the fibers during cutting.

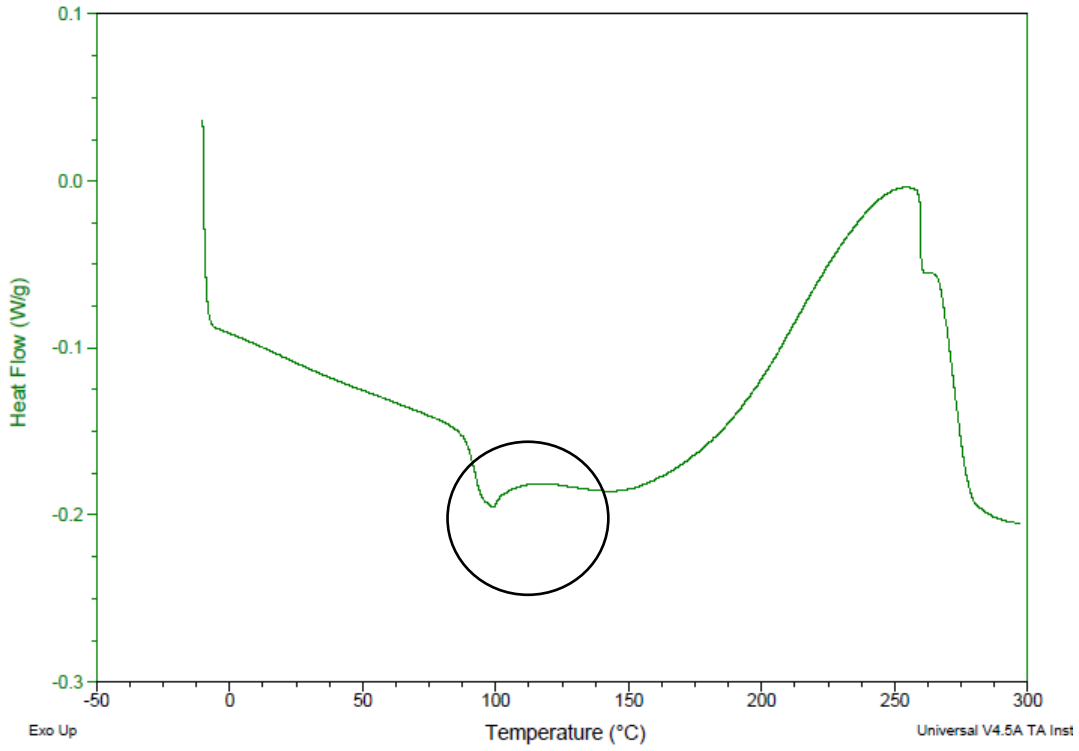

Figure B3.1: Endothermic peak observation on prepreg that is oven aged for 9 days

DSC thermograms of fresh, oven aged, and RT aged for 16 months prepreg are shown in Figure B 3.2. It can be observed that prepreg oven aged for 18 days also exhibits an endothermic peak. The endothermic peaks for 9- and 18-days oven aged prepregs are at 100^{o} C, as compared to that of longer RT aged prepreg at 60^{o} C. Figure B3.2 shows the comparison of location of endothermic peaks with aging, if any.

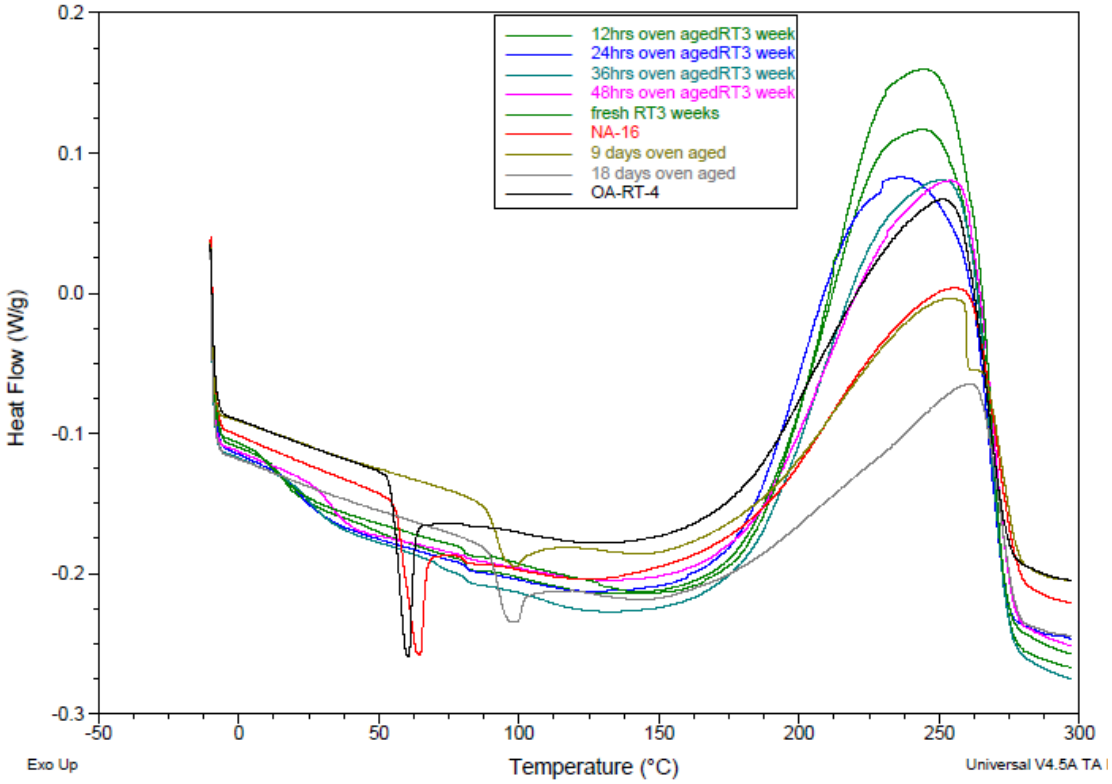

Figure B 3.2: Heat flow curves for fresh, oven aged and RT aged prepreg

Thermo-gravimetric analysis (TGA) is performed on fresh prepreg (green), 48 hours oven aged prepreg, 9 days oven aged prepreg, and NA-16 (RT aged for 16 months) prepreg to observe moisture content or other reactant which might be evaporating during the curing process. No such effect was observed in Figure B3.3.

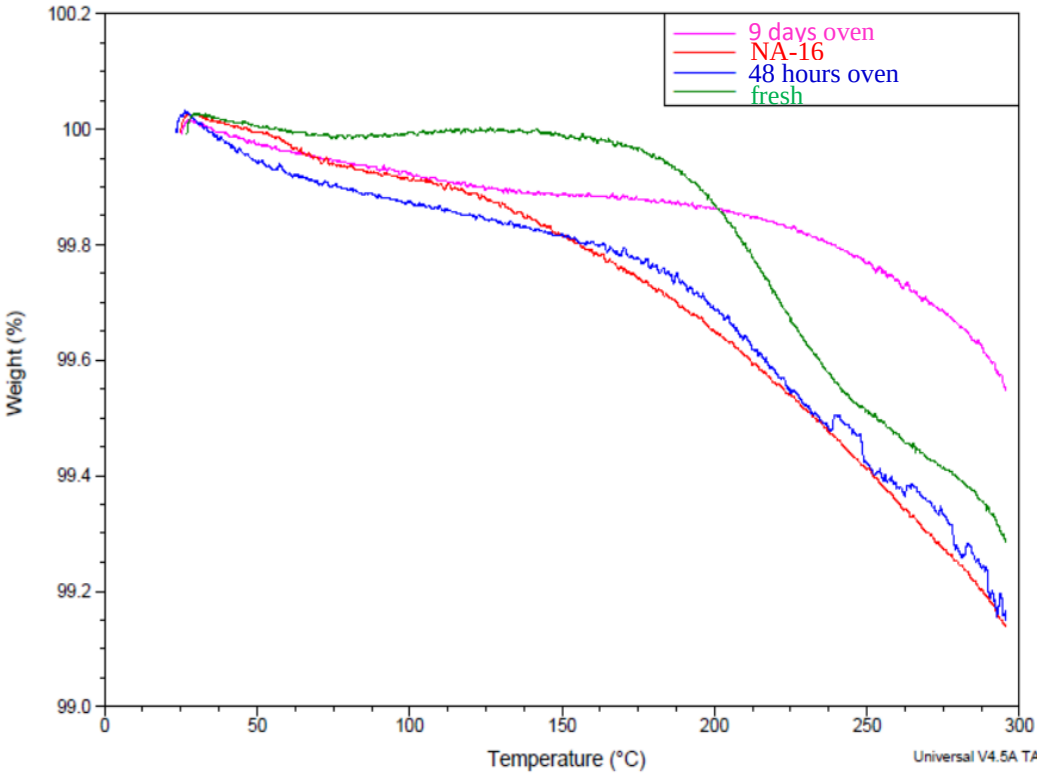

Figure B3.3: TGA on fresh and aged prepreg

APPENDIX C

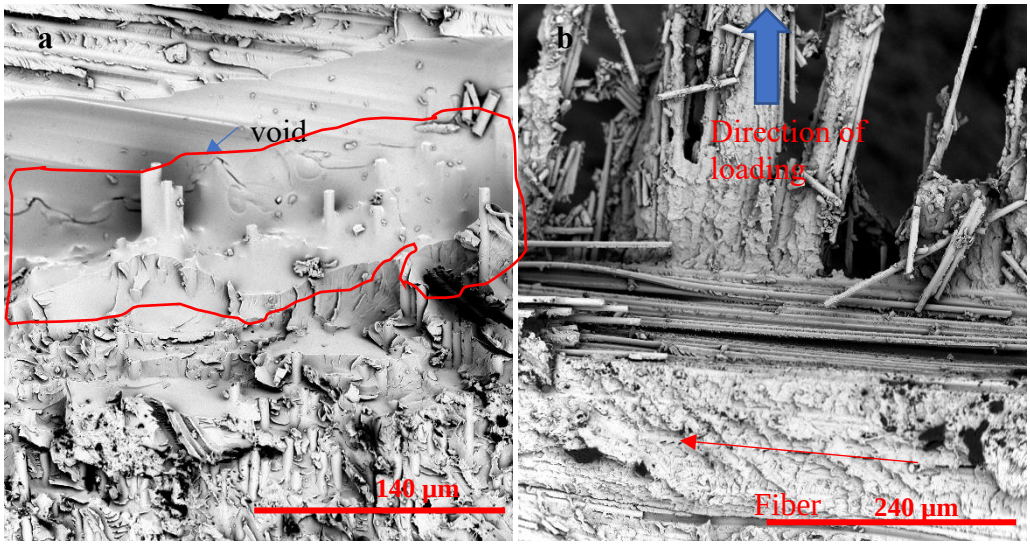

Figure C4.1: a. void can be seen (marked area) as it does not have trail of fibers; b. fibers normal to loading direction.

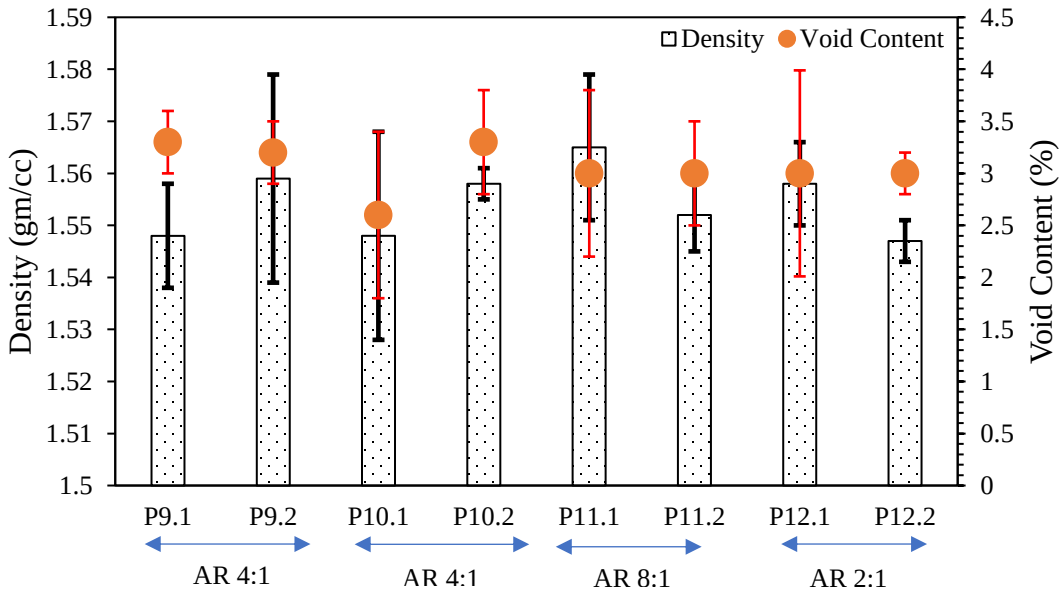

Figure C4.2: Effect of aspect ratio on the void content for aged prepreg composites

REFERENCES

[1] G. Oliveux, L.O. Dandy, G.A. Leeke, Current status of recycling of fibre reinforced polymers: Review of technologies, reuse and resulting properties, Progress in Materials Science 72 (2015) 61-99.

[2] K. Lu, The future of metals, science 328(5976) (2010) 319-320.

[3] K. Wood, Carbon fiber reclamation: going commercial, High Performance Composites 3 (2010) p1-2.

[4] L. Cheah, J. Heywood, Meeting US passenger vehicle fuel economy standards in 2016 and beyond, Energy Policy 39(1) (2011) 454-466.

[5] R. Stewart, Lightweighting the automotive market, Reinforced plastics 53(2) (2009) 14-21.

[6] P.K. Mallick, Fiber-reinforced composites: materials, manufacturing, and design, CRC press2007.

[7] E. Fitzer, Pan-based carbon fibers—present state and trend of the technology from the viewpoint of possibilities and limits to influence and to control the fiber properties by the process parameters, Carbon 27(5) (1989) 621-645.

[8] H.M. Ezekiel, R. Spain, Preparation of graphite fibers from polymeric fibers, Journal of Polymer Science Part C: Polymer Symposia, Wiley Online Library, 1967, pp. 249-265.

[9] R.G. Bourdeau, F.S. Galasso, High modulus carbon ribbon, American Ceramic Society Bulletin 55 (1976) 785-787.

[10] G. Bhat, R. Schwanke, Thermal properties of a polyimide fiber, Journal of Thermal Analysis and Calorimetry 49(1) (1997) 399-405.

[11] H. Ezekiel, Preprints ACS Div. ofOrg, Coatings, 1971.

[12] S. Chand, Review Carbon fibers for composites, Journal of Materials Science 35(6) (2000) 1303-1313.

[13] E. Boucher, R. Cooper, D. Everett, Preparation and structure of saran-carbon fibres, Carbon 8(5) (1970) 597-605.

[14] G.M. Jenkins, K. Kawamura, Polymeric carbons: carbon fibre, glass and char, Cambridge University Press1976.

[15] C. Warren, Carbon Fiber precursors and conversion, Oak Ridge National Laboratory, Tennessee,[abgerufen am: 9 (2017).

[16] D. Church, A revolution in low-cost carbon fiber production, Reinforced Plastics 62(1) (2018) 35-37.

[17] B. Smith, Engineered Materials Handbook, Vol. 1: composite, ASM International: Ohio, USA (1993) 786793.

[18] J.-B. Donnet, R.C. Bansal, Carbon fibers, CRC Press1998.

[19] N.R. Council, High Performance Synthetic Fibers for Composites, National Academies Press1992.

[20] A. Oliveira Nunes, R. Barna, Y. Soudais, Recycling of carbon fiber reinforced thermoplastic resin waste by steamthermolysis: thermo-gravimetric analysis and bench-scale studies, Proceedings of the 4th international carbon composites conference (4th IC3), 2014, pp. 12-14.

[21] L.O. Meyer, K. Schulte, E. Grove-Nielsen, CFRP-Recycling Following a Pyrolysis Route: Process Optimization and Potentials, Journal of Composite Materials 43(9) (2009) 1121-1132.

[22] S. Pimenta, S.T. Pinho, Recycling carbon fibre reinforced polymers for structural applications: Technology review and market outlook, Waste Management 31(2) (2011) 378-392.

[23] ELG carbon fibre. http://www.elgcf.com. 2015).

[24] S.J. Pickering, Recycling technologies for thermoset composite materials—current status, Composites Part A: Applied Science and Manufacturing 37(8) (2006) 1206-1215.
[25] E. Lester, S. Kingman, K.H. Wong, C. Rudd, S. Pickering, N. Hilal, Microwave heating as a means for carbon fibre recovery from polymer composites: a technical feasibility study, Materials Research Bulletin 39(10) (2004) 1549-1556.
[26] Eltron research and development. http://www.eltronresearch.com/. 2015).
[27] R. Piñero-Hernanz, J. García-Serna, C. Dodds, J. Hyde, M. Poliakoff, M.J. Cocero, S. Kingman, S. Pickering, E. Lester, Chemical recycling of carbon fibre composites using alcohols under subcritical and supercritical conditions, The Journal of Supercritical Fluids 46(1) (2008) 83-92.
[28] L. Yuyan, S. Guohua, M. Linghui, Recycling of carbon fibre reinforced composites using water in subcritical conditions, Materials Science and Engineering: A 520(1) (2009) 179-183.
[29] I. Okajima, K. Watanabe, T. Sako, Chemical recycling of carbon fiber reinforced plastic with supercritical alcohol, J Adv Res Phys 3(2) (2012) 1-4.
[30] G. Schinner, J. Brandt, H. Richter, Recycling Carbon-Fiber-Reinforced Thermoplastic Composites, Journal of Thermoplastic Composite Materials 9(3) (1996) 239-245.
[31] M. Roux, C. Dransfeld, N. Eguémann, L. Giger, Processing and recycling of a thermoplastic composite fibre/peek aerospace part, Proceedings of the 16th European conference on composite materials (ECCM 16), 2014, pp. 22-26.
[32] G. Nilakantan, S. Nutt, Reuse and upcycling of aerospace prepreg scrap and waste, Reinforced Plastics 59(1) (2015) 44-51.
[33] D.A. Baker, T.G. Rials, Recent advances in low-cost carbon fiber manufacture from lignin, Journal of Applied Polymer Science 130(2) (2013) 713-728.
[34] F. An, A. Sauer, Comparison of passenger vehicle fuel economy and greenhouse gas emission standards around the world, Pew Center on Global Climate Change 25 (2004).
[35] Quadrennial Technology Review: U.S. Department of Energy, 2011, p. 39.
[36] P.K. Mallick, Materials, design and manufacturing for lightweight vehicles, Elsevier2010.
[37] J. Remy, M. Voss, D. Blackwell, C. Di Natale, 2006 Corvette Z06 Carbon Fiber Fender-Engineering, Design, and Material Selection Considerations, SAE Technical Paper, 2005.
[38] M.-Y. Lyu, T.G. Choi, Research trends in polymer materials for use in lightweight vehicles, International journal of precision engineering and manufacturing 16(1) (2015) 213-220.
[39] M. Fisher, J. Kolb, S. Cole, Enhancing future automotive safety with plastics, 20th International Technical Conference on the Enhanced Safety of Vehicles (ESV) National Highway Traffic Safety Administration, 2007.
[40] A. Jacob, Carbon fibre and cars–2013 in review, Reinforced Plastics 58(1) (2014) 18-19.
[41] M. Verbrugge, T. Lee, P.E. Krajewski, A.K. Sachdev, C. Bjelkengren, R. Roth, R. Kirchain, Mass decompounding and vehicle lightweighting, Materials Science Forum, Trans Tech Publ, 2009, pp. 411-418.
[42] A. Asadi, M. Miller, A.V. Singh, R.J. Moon, K. Kalaitzidou, Lightweight sheet molding compound (SMC) composites containing cellulose nanocrystals, Composite Structures 160 (2017) 211-219.
[43] S. Erden, K. Sever, Y. Seki, M. Sarikanat, Enhancement of the mechanical properties of glass/polyester composites via matrix modification glass/polyester composite siloxane matrix modification, Fibers and Polymers 11(5) (2010) 732-737.
[44] C. Atas, D. Liu, Impact response of woven composites with small weaving angles, International journal of impact engineering 35(2) (2008) 80-97.
[45] B. Suresha, G. Chandramohan, J. Prakash, V. Balusamy, K. Sankaranarayanasamy, The role of fillers on friction and slide wear characteristics in glass-epoxy composite systems, Journal of Minerals and Materials Characterization and Engineering 5(01) (2006) 87.

[46] M. Aktaş, C. Atas, B.M. İçten, R. Karakuzu, An experimental investigation of the impact response of composite laminates, Composite Structures 87(4) (2009) 307-313.
[47] N. Mohan, S. Natarajan, S. KumareshBabu, Investigation on Sliding Wear Behaviour and Mechanical Properties of Jatropha Oil Cake-Filled Glass-Epoxy Composites, Journal of the American Oil Chemists' Society 88(1) (2011) 111-117.
[48] N. Gupta, B.S. Brar, E. Woldesenbet, Effect of filler addition on the compressive and impact properties of glass fibre reinforced epoxy, Bulletin of Materials Science 24(2) (2001) 219-223.
[49] N. Hameed, P. Sreekumar, B. Francis, W. Yang, S. Thomas, Morphology, dynamic mechanical and thermal studies on poly (styrene-co-acrylonitrile) modified epoxy resin/glass fibre composites, Composites Part A: Applied Science and Manufacturing 38(12) (2007) 2422-2432.
[50] H. Iba, T. Chang, Y. Kagawa, Optically transparent continuous glass fibre-reinforced epoxy matrix composite: fabrication, optical and mechanical properties, Composites Science and Technology 62(15) (2002) 2043-2052.
[51] A. Godara, D. Raabe, Influence of fiber orientation on global mechanical behavior and mesoscale strain localization in a short glass-fiber-reinforced epoxy polymer composite during tensile deformation investigated using digital image correlation, Composites Science and technology 67(11-12) (2007) 2417-2427.
[52] M.A. Torabizadeh, Tensile, compressive and shear properties of unidirectional glass/epoxy composites subjected to mechanical loading and low temperature services, (2013).
[53] A. Patnaik, A. Satapathy, S. Biswas, Investigations on three-body abrasive wear and mechanical properties of particulate filled glass epoxy composites, Malaysian Polymer Journal 5(2) (2010) 37-48.
[54] F. Baaij, Advances in sheet molding compounds for automotive applications, Mechanical Engineering, Georgia Institute of Technology, 2017.
[55] B. Yang, V. Kozey, S. Adanur, S. Kumar, Bending, compression, and shear behavior of woven glass fiber–epoxy composites, Composites Part B: Engineering 31(8) (2000) 715-721.
[56] B.M. Icten, C. Atas, M. Aktas, R. Karakuzu, Low temperature effect on impact response of quasi-isotropic glass/epoxy laminated plates, Composite Structures 91(3) (2009) 318-323.
[57] S. Kajorncheappunngam, R.K. Gupta, H.V. GangaRao, Effect of aging environment on degradation of glass-reinforced epoxy, Journal of composites for construction 6(1) (2002) 61-69.
[58] F. Ellyin, R. Maser, Environmental effects on the mechanical properties of glass-fiber epoxy composite tubular specimens, Composites Science and Technology 64(12) (2004) 1863-1874.
[59] T. Sathishkumar, S. Satheeshkumar, J. Naveen, Glass fiber-reinforced polymer composites–a review, Journal of Reinforced Plastics and Composites 33(13) (2014) 1258-1275.
[60] E. Ramzan, E. Ehsan, Effect of various forms of glass fiber reinforcements on tensile properties of polyester matrix composite, Fac. Eng. Technol 16 (2009) 33-39.
[61] A.C. Galeb, A.M. Khayoon, Optimum design of transmission towers subjected to wind and earthquake loading, Jordan Journal of Civil Engineering 7(1) (2013) 70-92.
[62] P. Feraboli, T. Cleveland, P. Stickler, J. Halpin, Stochastic laminate analogy for simulating the variability in modulus of discontinuous composite materials, Composites Part A: Applied Science and Manufacturing 41(4) (2010) 557-570.
[63] L. Orgéas, P.J. Dumont, Sheet molding compounds, Wiley Encyclopedia of Composites (2011) 1-36.
[64] R. Brooks, S.M. Shanmuga Ramanan, S. Arun, Composites in Automotive Applications: Design, Reference Module in Materials Science and Materials Engineering, Elsevier2017.
[65] G. Mahajan, V. Aher, Composite material: a review over current development and automotive application, International Journal of Scientific and Research Publications 2(11) (2012) 1-5.

[66] M. Selezneva, Experimental and Theoretical Investigations of Mechanical Properties of Randomly-Oriented Strand (ROS) Composites, McGill University Libraries, 2015.
[67] P. Feraboli, E. Peitso, T. Cleveland, P.B. Stickler, Modulus Measurement for Prepreg-based Discontinuous Carbon Fiber/Epoxy Systems, Journal of Composite Materials 43(19) (2009) 1947-1965.
[68] M.S. Tuttle, Tory; Boursier,Bruno, Simplifying certification of discontinuous composite material forms for primary aircraft structures, International SAMPE Symposium and Exhibition (Proceedings), Seattle, WA, 2010.
[69] J. Halpin, Stiffness and expansion estimates for oriented short fiber composites, Journal of Composite Materials 3(4) (1969) 732-734.
[70] J. Halpin, N. Pagano, The laminate approx. for randomly oriented short fiber composites, Polymer Engineering and Science 3 (1969) 720.
[71] J.C. Halpin, J.L. Karoos, Strength of discontinuous reinforced composites: I. Fiber reinforced composites, Polymer Engineering & Science 18(6) (1978) 496-504.
[72] J. Kardos, M. Michno, T. Duffy, Investigation of high performance short fiber reinforced plastics, Final report, Naval Air Systems Command, No, N00019-73-C-0358, 1974.
[73] Boeing 787 features composite window frames, Reinforced Plastics 51(3) (2007) 4.
[74] J. Porter, Moving closer to the goal of cost effective complex geometry carbon composite parts, HPC4HPC special session, proceedings of the 19th ASC technical conference, Atlanta, GA, 2004.
[75] J. Aubry, HexMC — bridging the gap between prepreg and SMC, Reinforced Plastics 45(6) (2001) 38-40.
[76] M.F.A. Adamovsky, The Effect of Cutting Blade Geometry and Material on Carbon Fiber Severing as Used in High-Volume Production of Composites, (2015).
[77] A. Shields, D. Hepburn, I. Kemp, J. Cooper, The absorption of mould release agent by epoxy resin, Polymer degradation and stability 70(2) (2000) 253-258.
[78] A. Evans, C. Qian, T. Turner, L. Harper, N. Warrior, Flow characteristics of carbon fibre moulding compounds, Composites Part A: Applied Science and Manufacturing 90 (2016) 1-12.
[79] P. Feraboli, E. Peitso, F. Deleo, T. Cleveland, P.B. Stickler, Characterization of Prepreg-Based Discontinuous Carbon Fiber/Epoxy Systems, Journal of Reinforced Plastics and Composites 28(10) (2008) 1191-1214.
[80] H. Cai, M.T. Bashar, J.J.C. Picot, Thermal and mechanical anisotropy in compression molded carbon fiber/resin composites, Polymer Composites 26(5) (2005) 684-688.
[81] T. CA, T800S carbon fiber, (2018).
[82] T. CA, 3900 prepreg system, (2018).
[83] H. Zhu, B. Wu, D. Li, D. Zhang, Y. Chen, Influence of voids on the tensile performance of carbon/epoxy fabric laminates, Journal of Materials Science & Technology 27(1) (2011) 69-73.
[84] P. Feraboli, T. Cleveland, M. Ciccu, P. Stickler, L. DeOto, Defect and damage analysis of advanced discontinuous carbon/epoxy composite materials, Composites Part A: Applied Science and Manufacturing 41(7) (2010) 888-901.
[85] S. Agius, K. Magniez, B. Fox, Cure behaviour and void development within rapidly cured out-of-autoclave composites, Composites Part B: Engineering 47 (2013) 230-237.
[86] Y. Yu, H. Su, W. Gan, Effects of storage aging on the properties of epoxy prepregs, Industrial & Engineering Chemistry Research 48(9) (2009) 4340-4345.
[87] S.G. Miller, J.K. Sutter, D.A. Scheiman, M. Maryanski, M. Schlea, Study of out-time on the processing and properties of IM7/977-3 composites, (2010).

[88] K. Cole, D. Noël, J.J. Hechler, P. Cielo, J.C. Krapez, A. Chouliotis, K. Overbury, Room-temperature aging of Narmco 5208 carbon-epoxy prepreg. Part II: Physical, mechanical, and nondestructive characterization, Polymer composites 12(3) (1991) 203-212.
[89] R.W. Jones, Y. Ng, J.F. McClelland, Monitoring ambient-temperature aging of a carbon-fiber/epoxy composite prepreg with photoacoustic spectroscopy, Composites Part A: Applied Science and Manufacturing 39(6) (2008) 965-971.
[90] M.H. Habibi, Effects of out-time on cure kinetics and rheological properties of out-of-autoclave and autoclave prepregs, Wichita State University, 2013.
[91] D.G. Lee, H.G. Kim, Non-isothermal in situ dielectric cure monitoring for thermosetting matrix composites, Journal of Composite Materials 38(12) (2004) 977-993.
[92] T. Ozawa, Kinetic analysis of derivative curves in thermal analysis, Journal of Thermal Analysis and Calorimetry 2(3) (1970) 301-324.
[93] J.H. Flynn, L.A. Wall, A quick, direct method for the determination of activation energy from thermogravimetric data, Journal of Polymer Science Part B: Polymer Letters 4(5) (1966) 323-328.
[94] N. Sbirrazzuoli, S. Vyazovkin, A. Mititelu, C. Sladic, L. Vincent, A Study of Epoxy-Amine Cure Kinetics by Combining Isoconversional Analysis with Temperature Modulated DSC and Dynamic Rheometry, Macromolecular Chemistry and Physics 204(15) (2003) 1815-1821.
[95] N. Sbirrazzuoli, S. Vyazovkin, Learning about epoxy cure mechanisms from isoconversional analysis of DSC data, Thermochimica Acta 388(1-2) (2002) 289-298.
[96] G. Odegard, A. Bandyopadhyay, Physical aging of epoxy polymers and their composites, Journal of Polymer Science Part B: Polymer Physics 49(24) (2011) 1695-1716.
[97] https://kevra.fi/wp-content/uploads/HexMC_User-Guide.pdf.
[98] B.C. Jin, X. Li, A. Jain, C. González, J. Llorca, S. Nutt, Optimization of microstructures and mechanical properties of composite oriented strand board from reused prepreg, Composite Structures 174 (2017) 389-398.
[99] A.D. Evans, C.C. Qian, T.A. Turner, L.T. Harper, N.A. Warrior, Flow characteristics of carbon fibre moulding compounds, Composites Part A: Applied Science and Manufacturing 90(Supplement C) (2016) 1-12.
[100] M. Bader, J. Bailey, I. Bell, The effect of fibre-matrix interface strength on the impact and fracture properties of carbon-fibre-reinforced epoxy resin composites, Journal of Physics D: Applied Physics 6(5) (1973) 572.
[101] M. Bader, R. Ellis, The effect of notches and specimen geometry on the pendulum impact strength of uniaxial CFRP, Composites 5(6) (1974) 253-258.
[102] H. Maikuma, J.W. Gillespie Jr, D.J. Wilkins, Mode II interlaminar fracture of the center notch flexural specimen under impact loading, Journal of composite materials 24(2) (1990) 124-149.
[103] D.F. Adams, J.L. Perry, Instrumented Charpy impact tests of several unidirectional composite materials, Fibre Science and Technology 8(4) (1975) 275-302.
[104] M. Wisnom, The role of delamination in failure of fibre-reinforced composites, Phil. Trans. R. Soc. A 370(1965) (2012) 1850-1870.
[105] P. Yeung, L.J. Broutman, The effect of glass-resin interface strength on the impact strength of fiber reinforced plastics, Polymer Engineering & Science 18(2) (1978) 62-72.
[106] M. Caminero, G. Rodríguez, V. Muñoz, Effect of stacking sequence on Charpy impact and flexural damage behavior of composite laminates, Composite Structures 136 (2016) 345-357.
[107] D.F. Adams, A.K. Miller, The influence of transverse shear on the static flexure and Charpy impact response of hybrid composite materials, Journal of Materials Science 11(9) (1976) 1697-1710.
[108] J. Tanks, S. Sharp, D. Harris, Charpy impact testing to assess the quality and durability of unidirectional CFRP rods, Polymer Testing 51 (2016) 63-68.

[109] R. Bjeković, K. Piotrowicz, Epoxy resin and release agents part I: Inflence of external and internal release agents on the adhesive properties of epoxy resin, Journal of Applied Engineering Science 13(1) (2015) 45-50.
[110] 3M.
[111] B. Boursier, A. Lopez, Failure initiation and effect of defects in structural discontinuous fiber composites, Hexcel Research and Technology (2010).